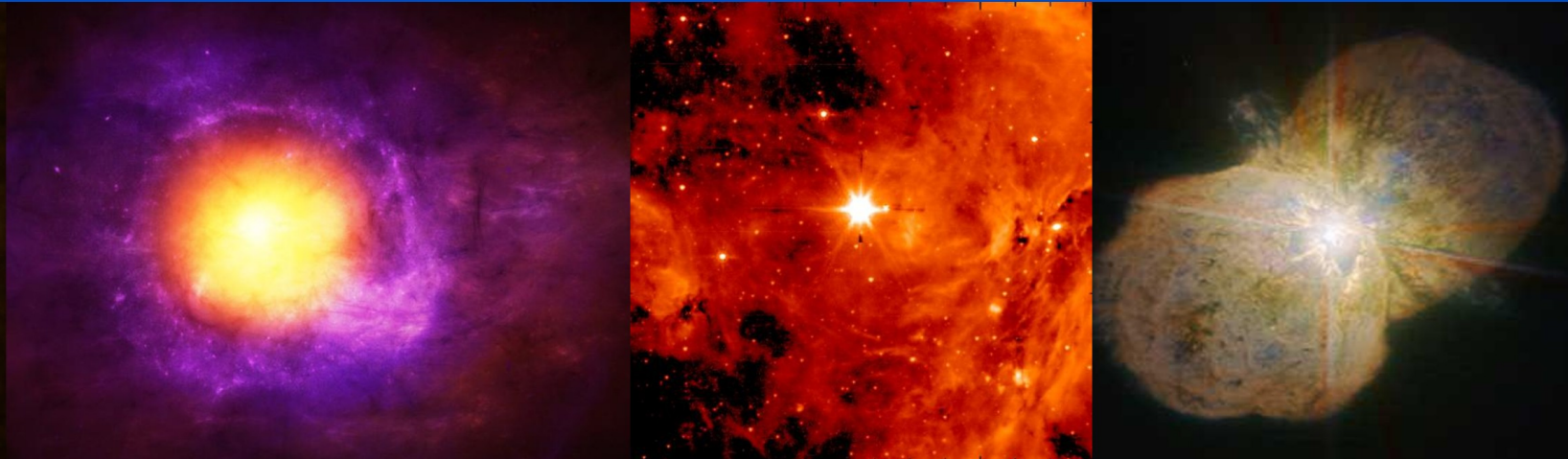


Winds of Luminous Blue Variables and Cool Hypergiants



Alex Lobel
Royal Observatory of Belgium, Brussels

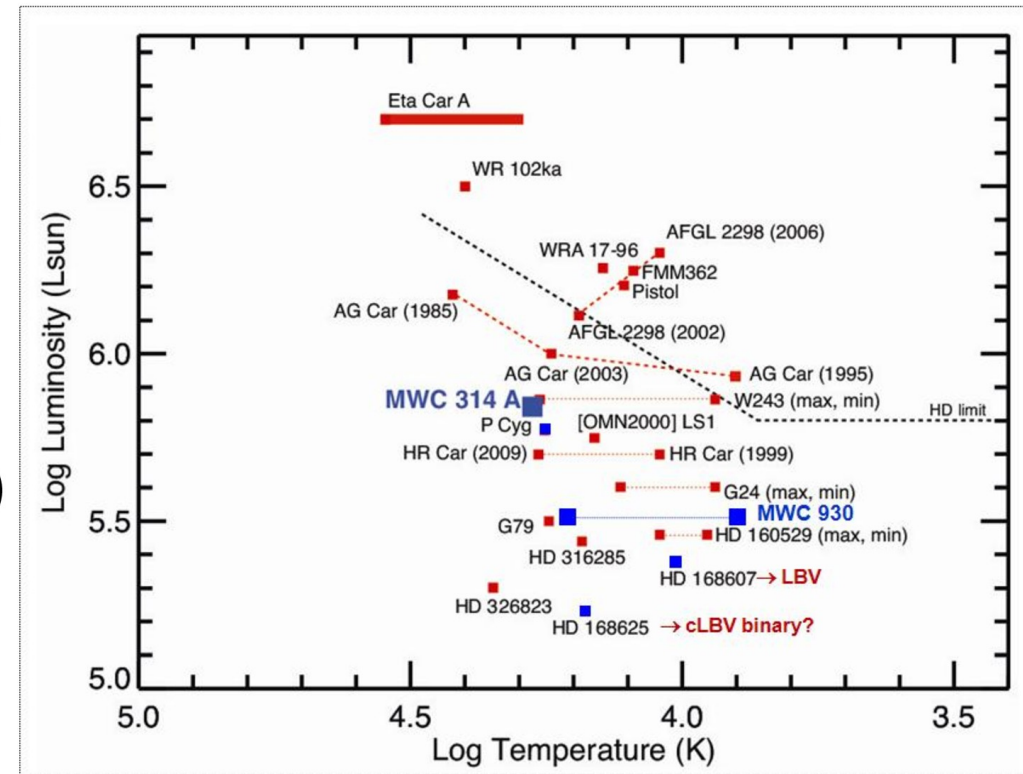


Outline

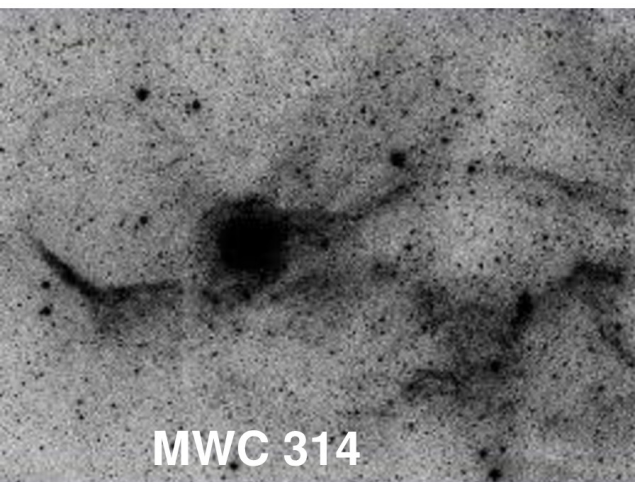
- What are Luminous Blue Variables (LBV) and Yellow Hypergiants (YHG)? Where do they live in the H-R diagram?
- What can long-term high-resolution spectroscopic monitoring of YHGs, LBVs, and candidate LBVs tell us about detailed spectroscopic variability of these rare massive stars close to the stellar luminosity limit?
- Investigations of the wind structure and atmospheric dynamics of LBVs and YHGs; e.g. pulsation properties, mass-loss rates, outburst events, etc. using long-term spectroscopy and photometry.
- Discuss some notorious LBVs: S Dor, P Cyg, MWC 314, and a few well-studied YHGs: Rho Cas, HR 5171, HR 8752.
- What can multi-D radiative transfer modelling of large-scale hydrodynamic wind structures in massive hot stars learn?

What are LVBs and candidate LBVs ?

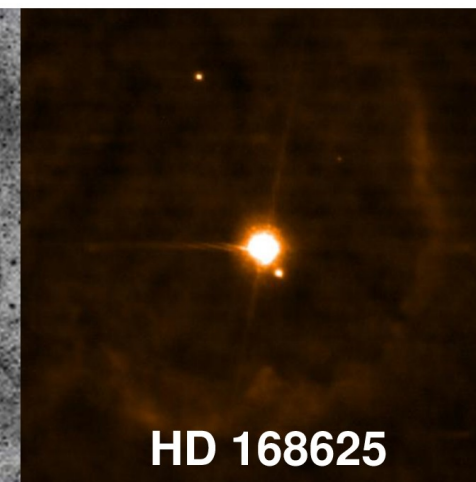
- LBV = luminous blue star showing S-Doradus cycles: irregular photometric and spectroscopic variability on time scales of ~10 yr
Entire spectrum changes dramatically between “quiescent” and “outburst” state
- cLBV = stellar parameters found in LBVs but without observed S-Dor cycle (“dormant LBV”)
- Galactic LBVs and cLBVs are often found in bi-polar or spherical circumstellar nebulae signaling past eruptive events



Mercator-HERMES high-resolution spectroscopic monitoring of LBVs and cLBVs



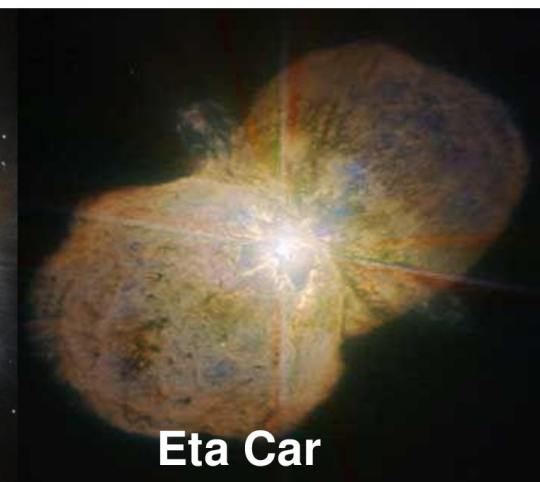
MWC 314



HD 168625



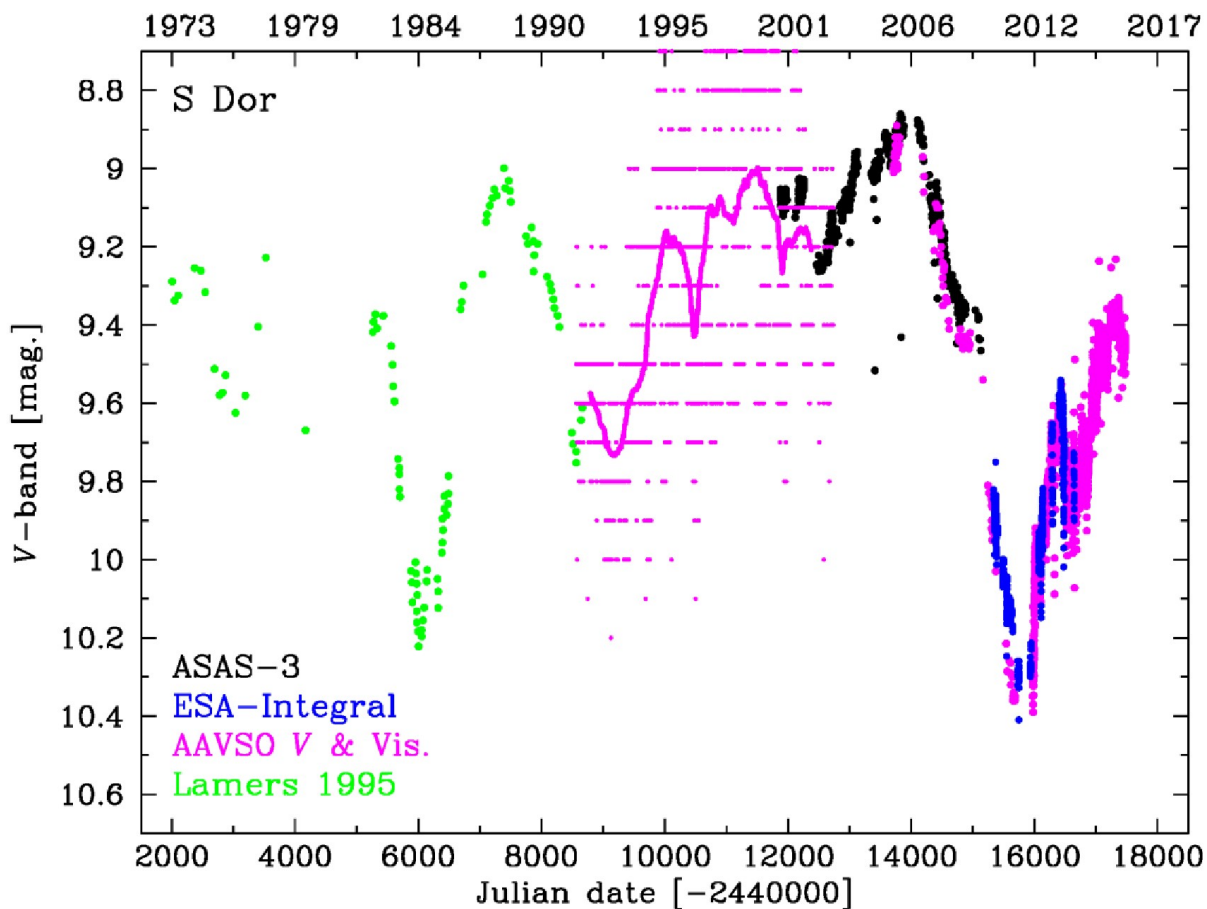
AG Car



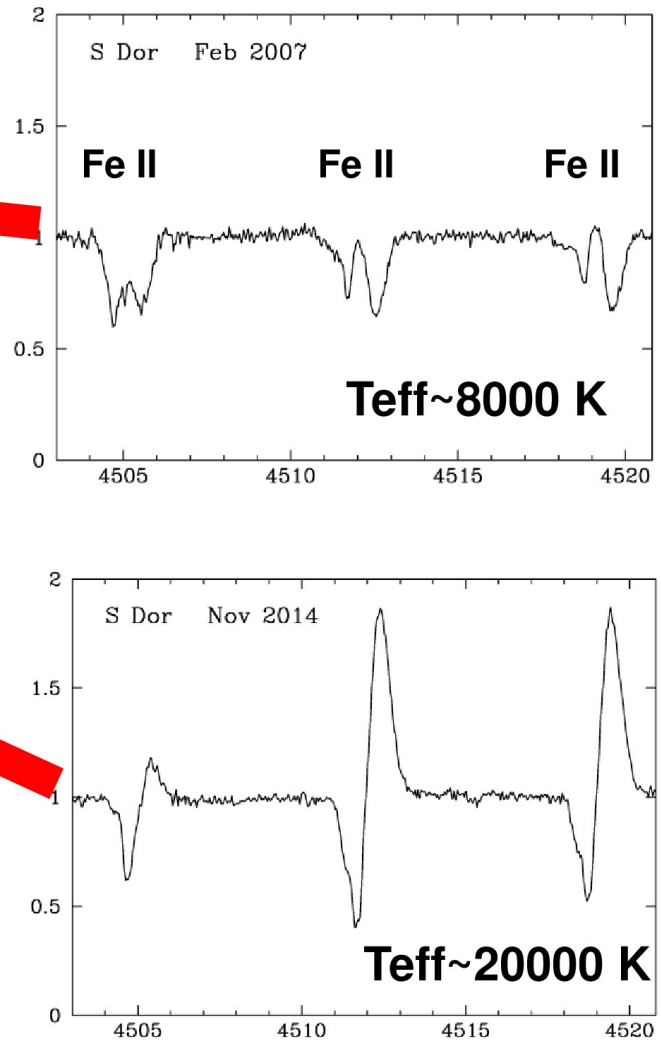
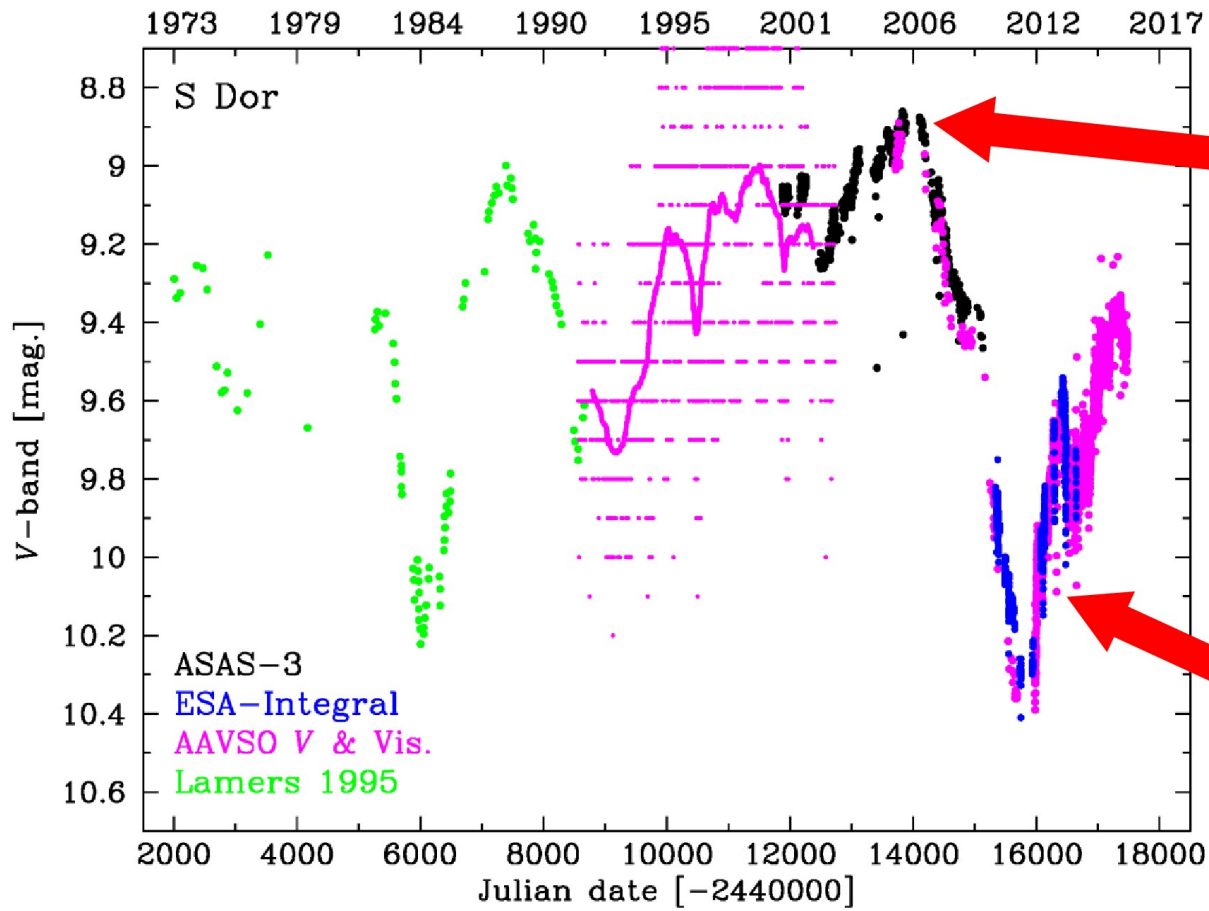
Eta Car

Long-term V brightness cycles of LBV S Dor

V brightness changes of $\sim 1^m.5$ over last 50 years

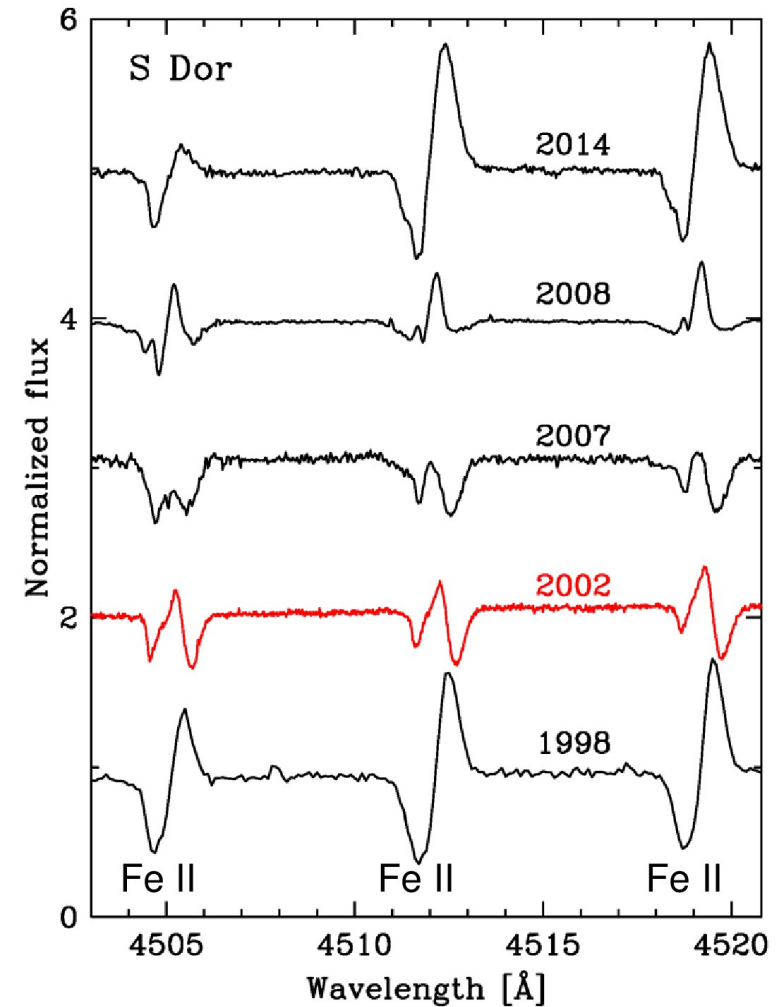
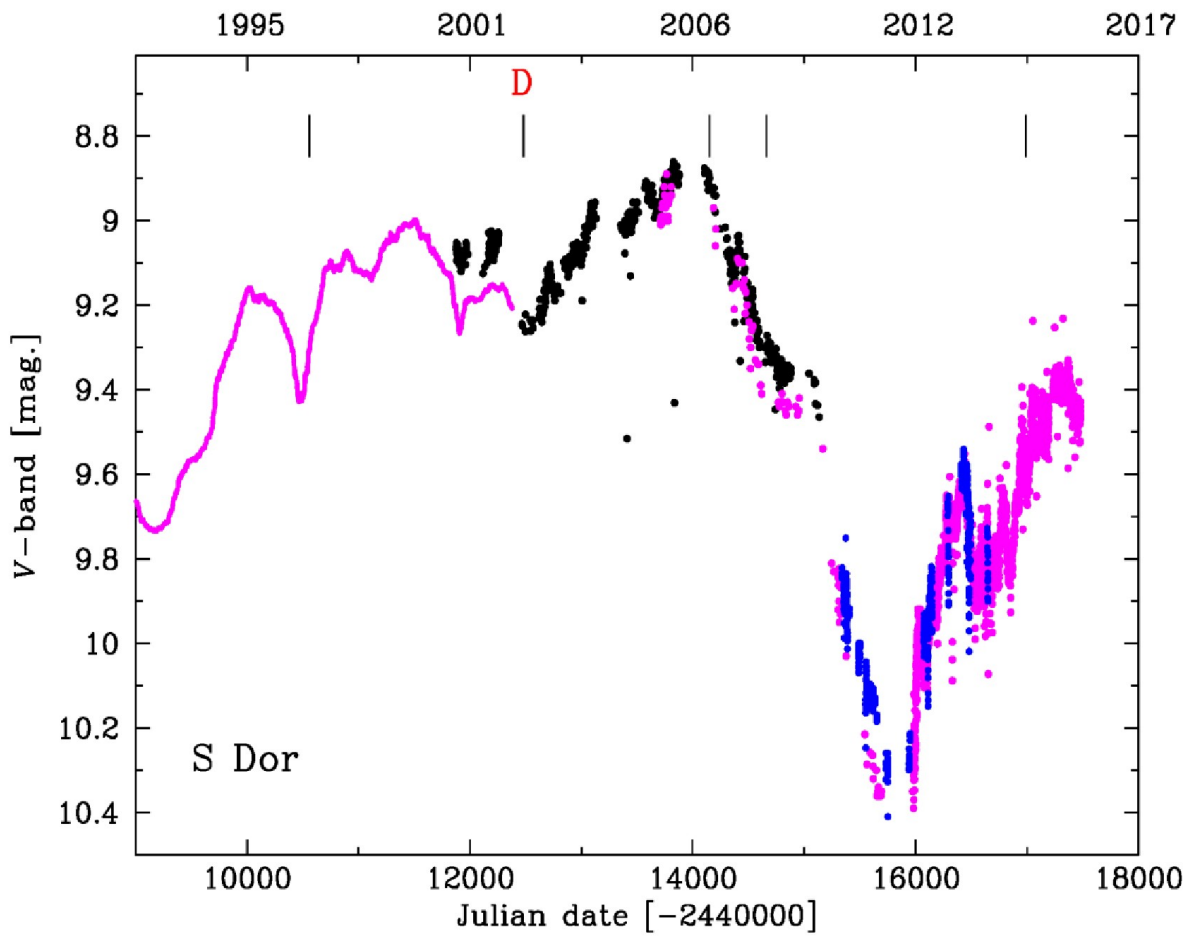


Spectroscopic variability of LBV S Dor



Strong P Cyg emission lines spectrum observed around minimum V brightness = “quiescent state”
 Metallic absorption line spectrum around maximum V brightness = “outburst phase”
 Increase of visible R_* from $100 R_\odot$ to $380 R_\odot$ in 1985-1989 and in 2006-2011 ? Or binary interaction?

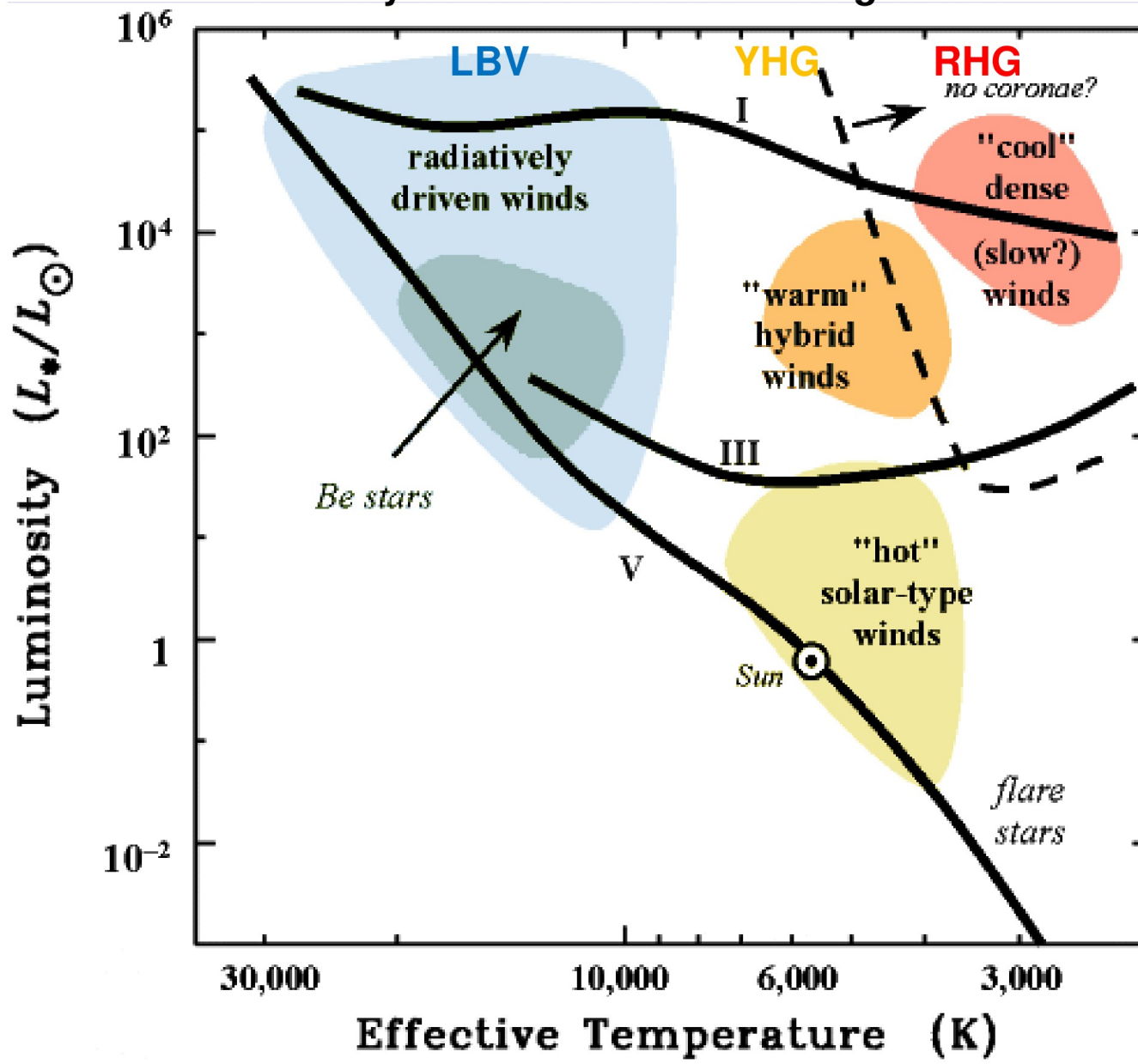
Line profile variability in LBV S Dor



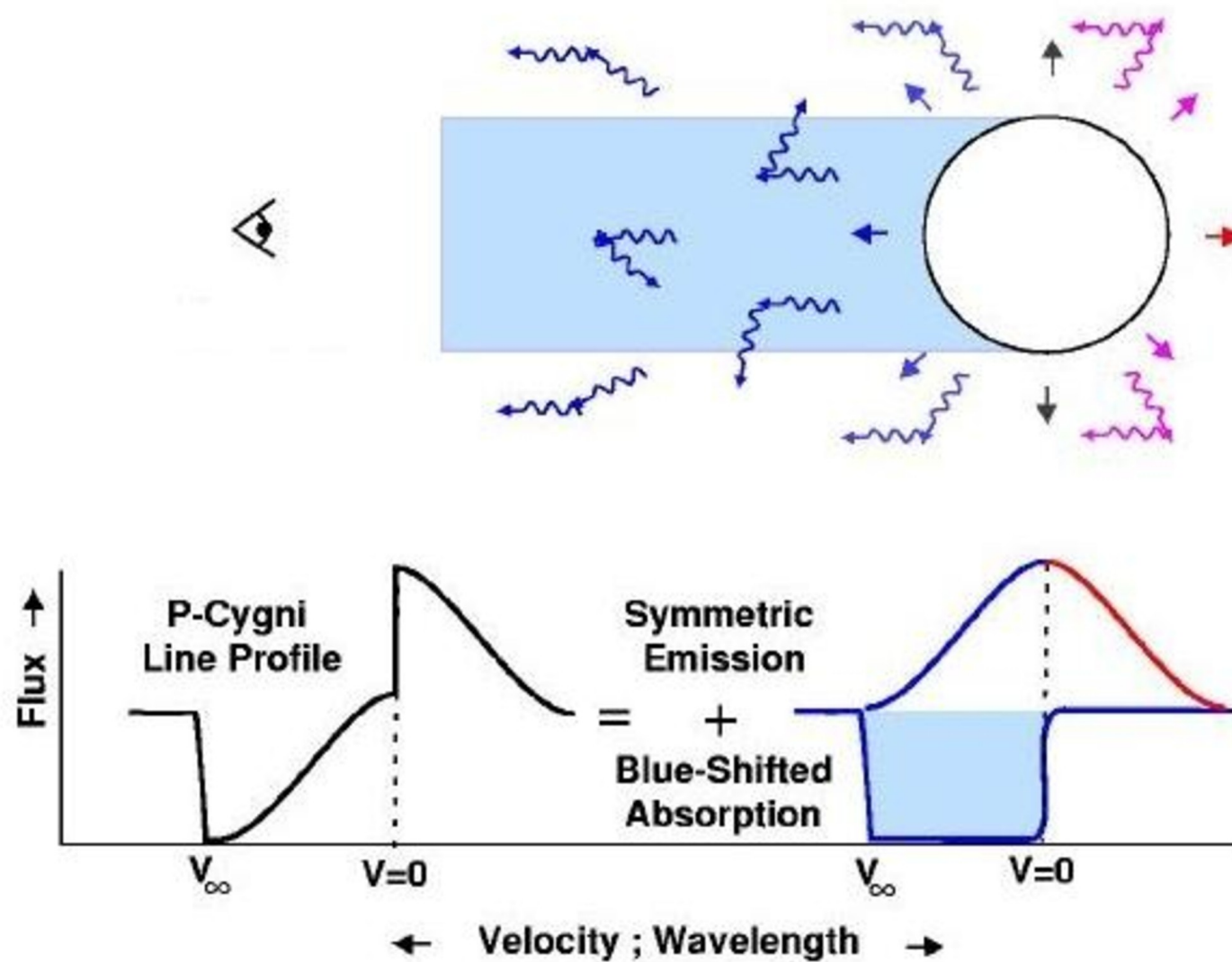
- During V -brightness increase before 2006 maximum, the Fe II P Cyg line profiles transform into split absorption lines with central emission cores.
- Is there a physical link with split metal lines observed in various YHG?

Luminous stars with radiatively driven winds

- LBV winds accelerate very fast
- very broad UV absorption wind lines in spectrum
- large mass-loss rates
- very extended line scattering winds

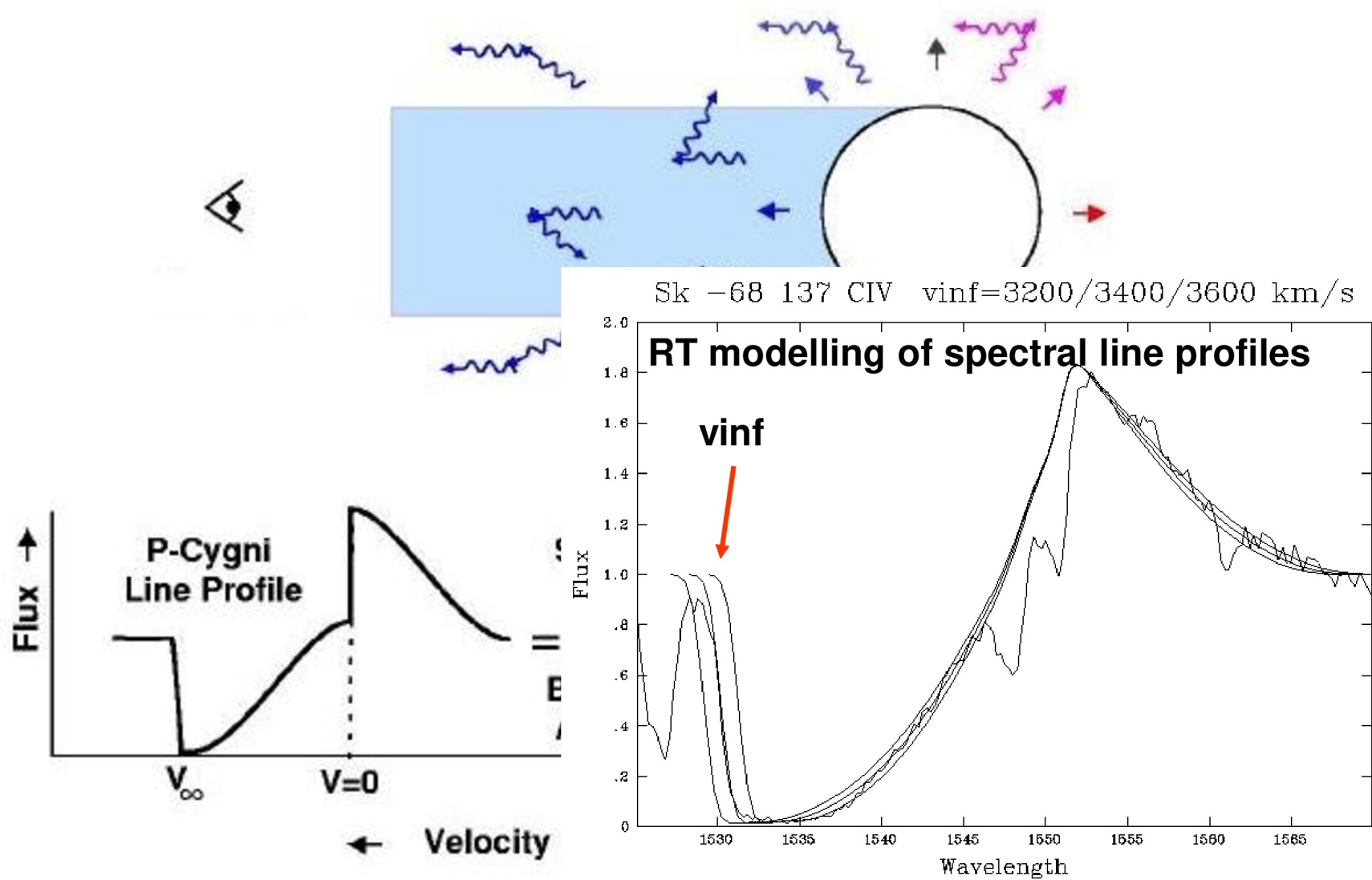


Formation of P Cyg wind line profile



Absorption portion samples wind opacity in front of the stellar disc.

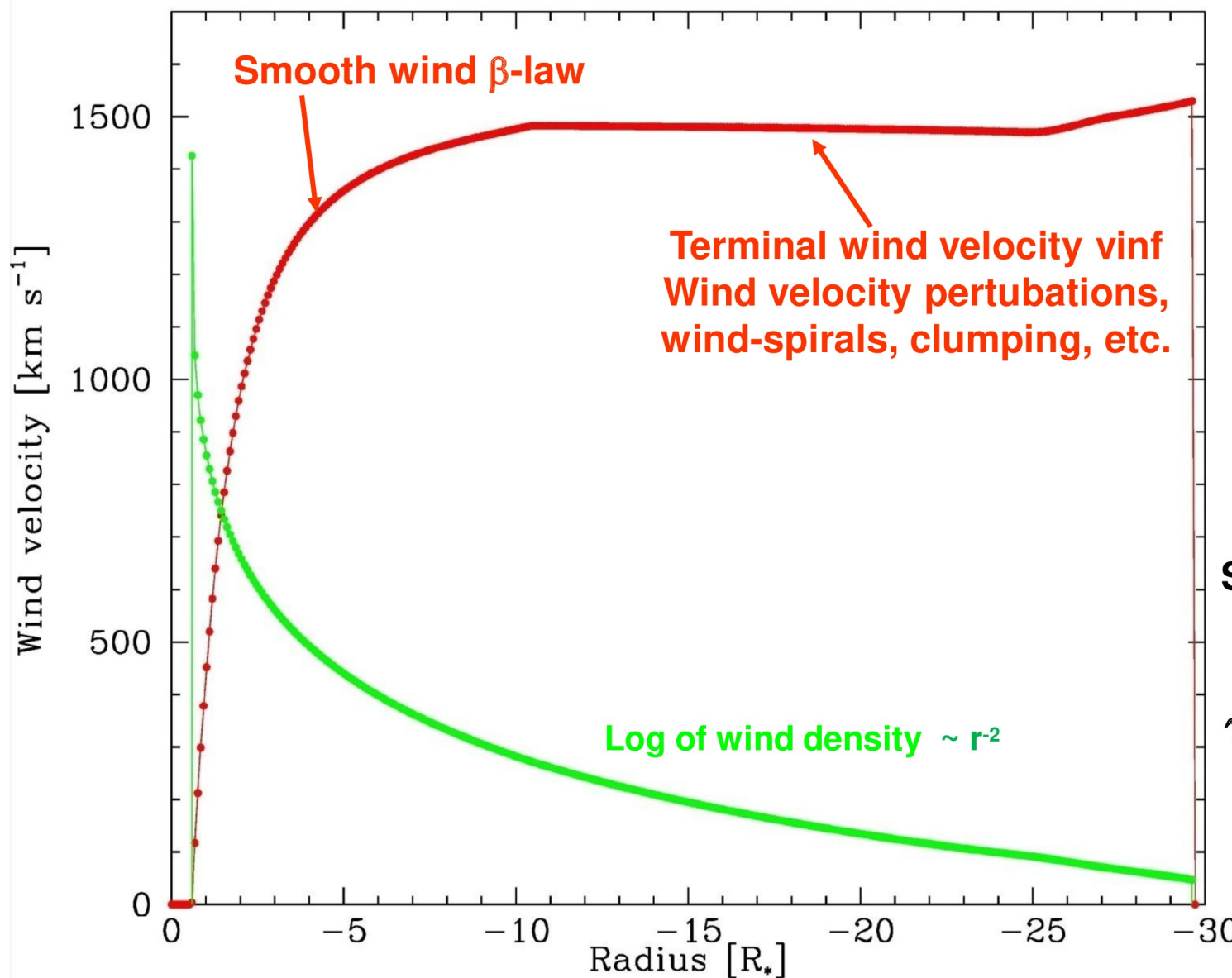
Formation of P Cyg wind line profile



Scattering of continuum photons in strong metal resonance lines causing momentum transfer from metal ions to bulk H/He plasma.

Radial wind velocity structure

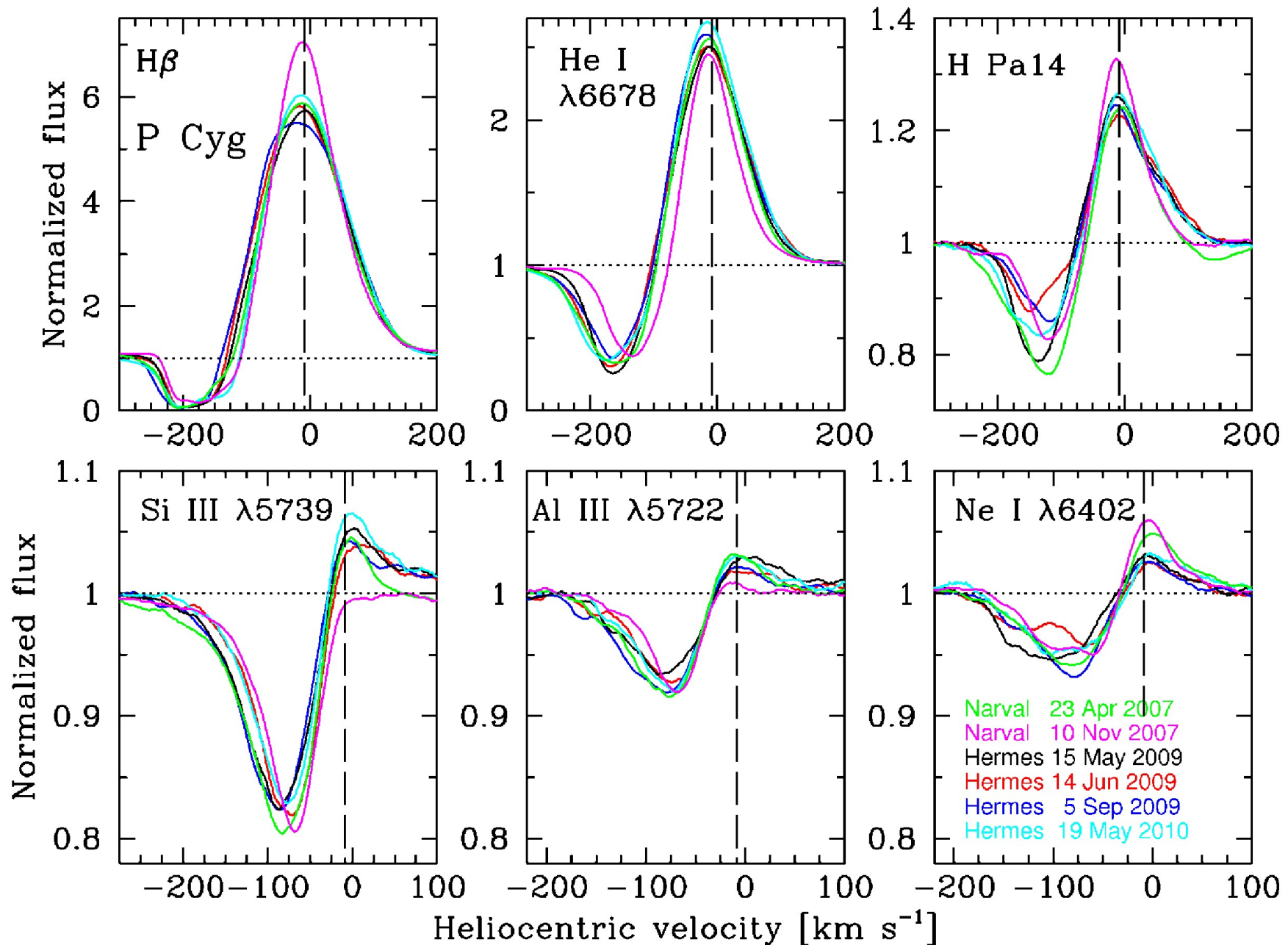
- Cross-section of LBV smooth wind structure calculated with hydro-code Zeus3D
- Radiatively accelerating (or ‘line-driven’) 1-D wind often approximated by ‘ β -law’



Sobolev optical depth:

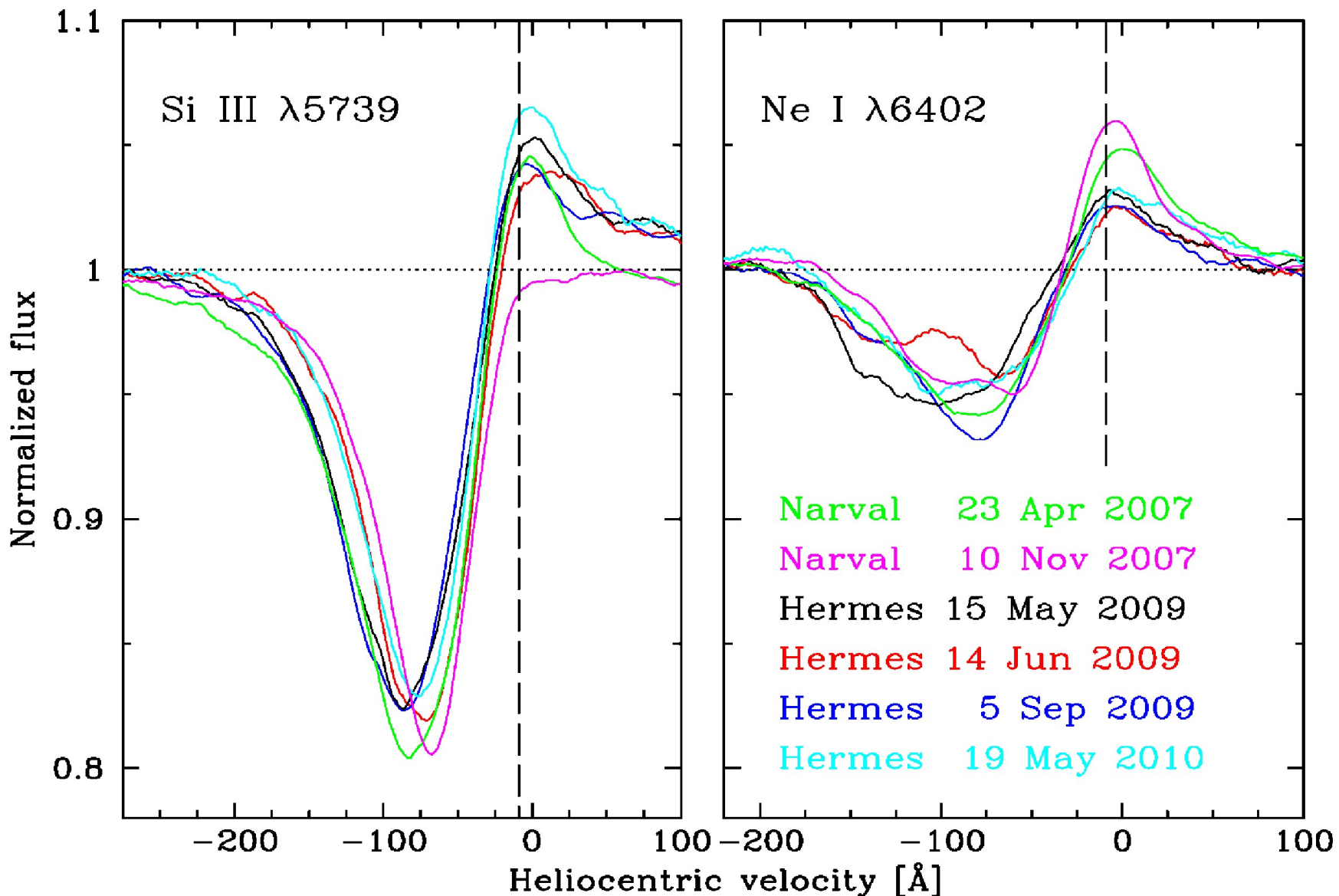
$$\tau/\tau_0 \propto \frac{\rho/\rho_0}{\left| \frac{dv}{dr} \right| / \left| \frac{dv}{dr} \right|_0}$$

Monitoring of ‘wind lines’ in P Cygni



Variability of ‘P Cyg-type’ line profiles due to temporal changes in wind structure/driving

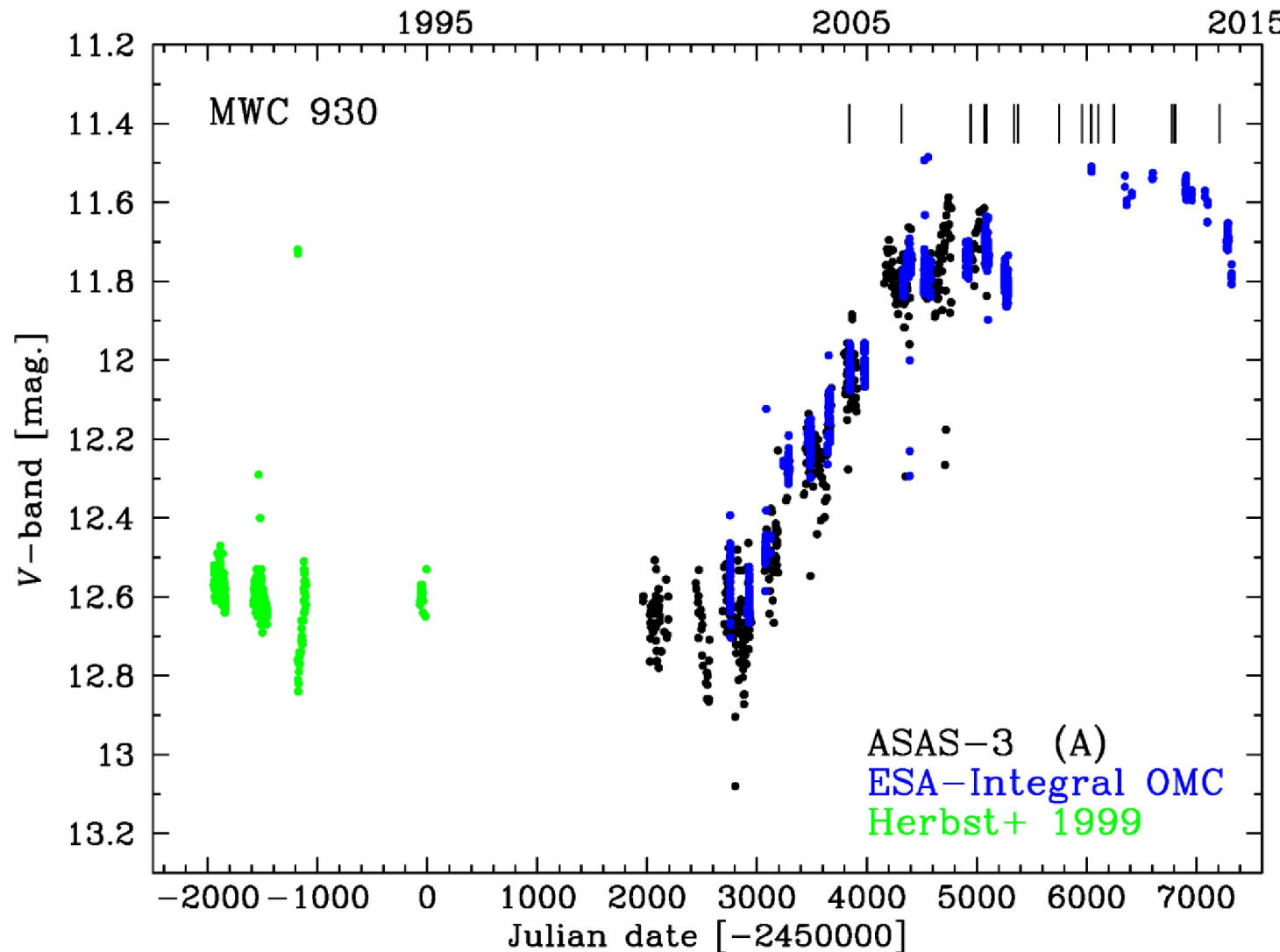
Monitoring of ‘wind lines’ in P Cygni



Use large spectral resolution spectrographs to investigate physical properties and variability of slow-wind regions close to the stellar surface from weak P Cyg profiles observed with large S/N ratios.

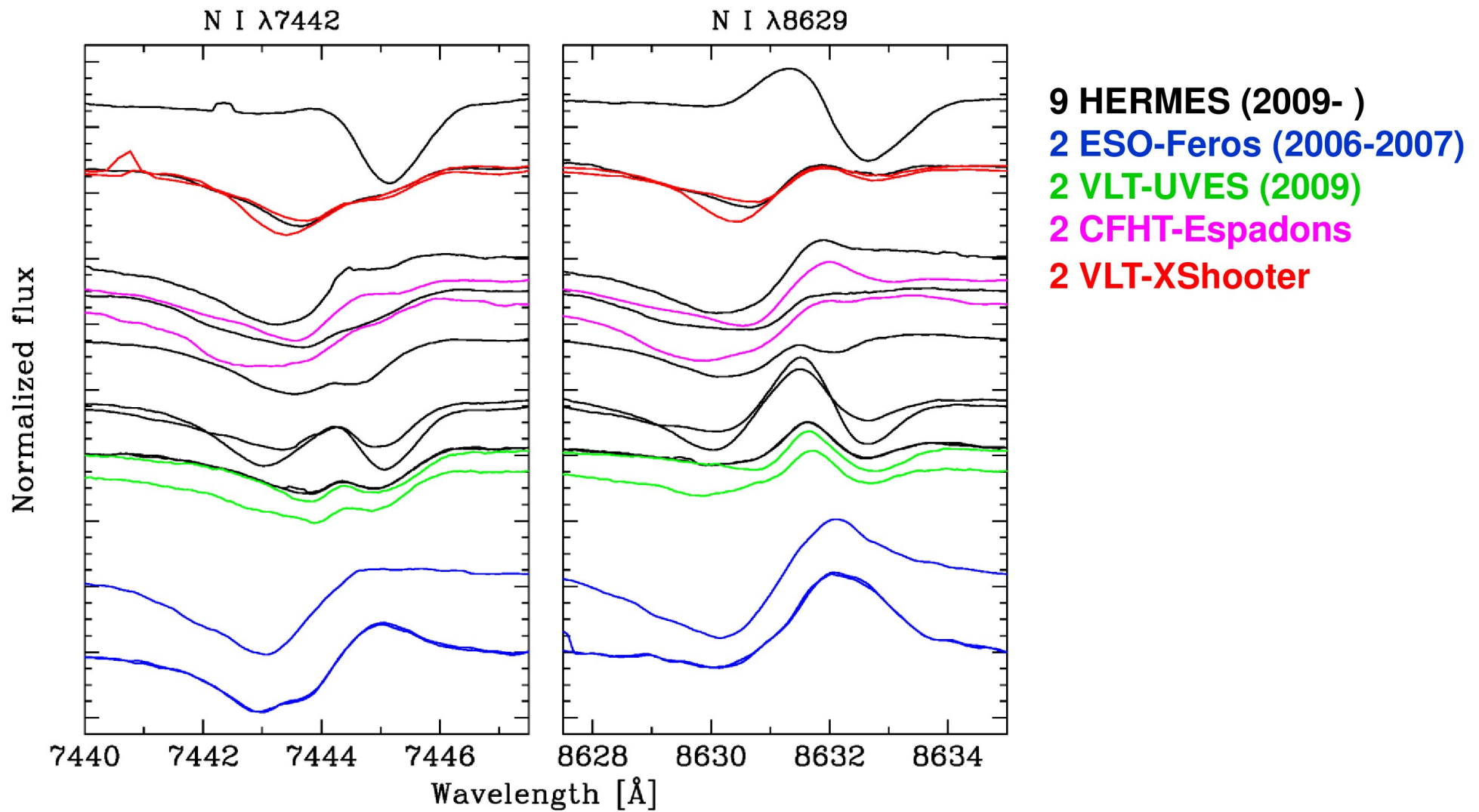
S Dor -like V brightness cycle of MWC 930

V brightness increase of $\sim 1^m.3$ between 2000 and 2014



High-resolution spectroscopic monitoring ongoing with Mercator-HERMES since 2009.

Spectroscopic monitoring of LBV MWC 930

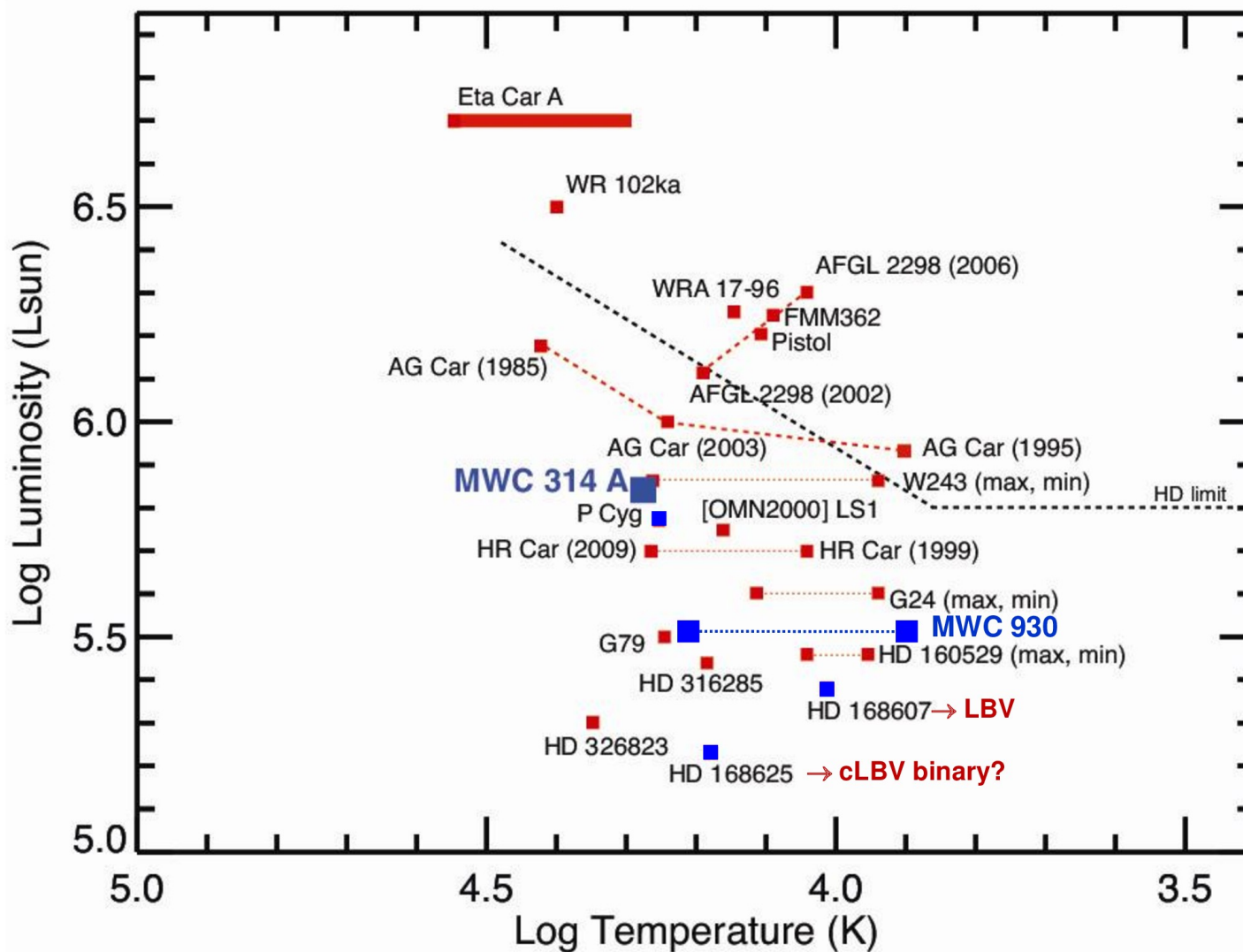


N I near-IR lines show remarkable shape transformations from P Cyg profiles to inverse P Cyg profiles over periods over several years, but without indications of binarity.

Wind expansion and contraction phases => **cyclic wind variability in massive stars**

HD 168625 and HD 168607 in the upper HRD

LBVs and candidate LBVs



HD 168607

LBV of S Dor-type

Teff = 9300 K.

$\log L_*/L_{\odot} = 5.4$

No nebula, but shows V micro-variability.

HD 168625

cLBV

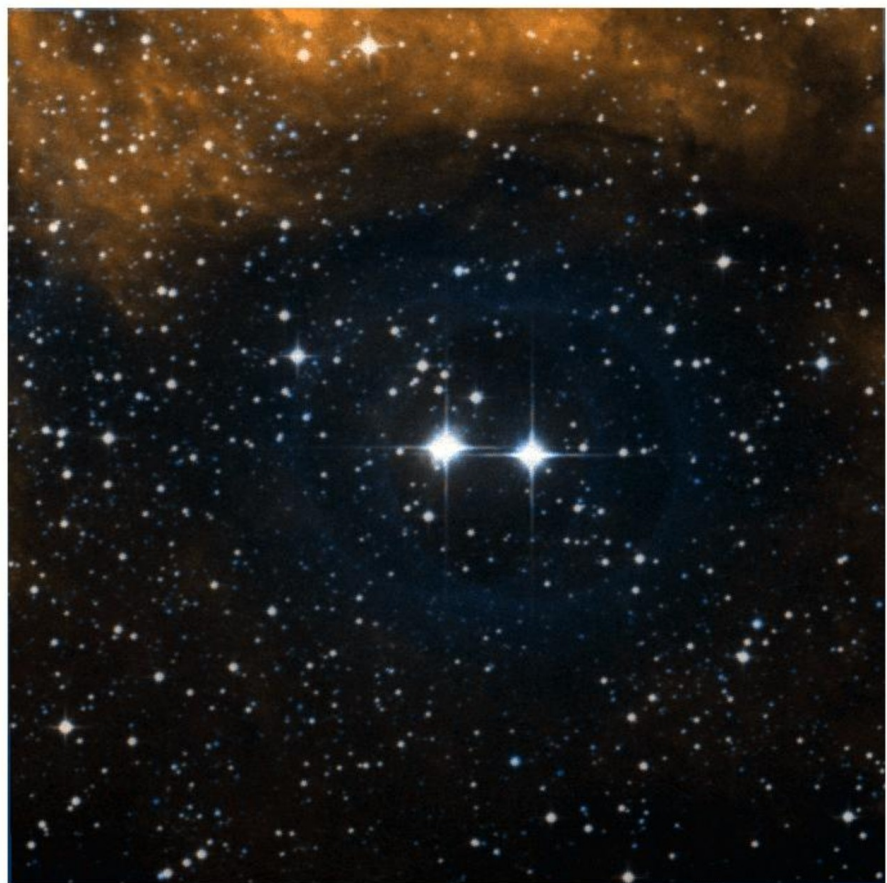
Teff = 13500 K.

$\log L_*/L_{\odot} = 5.1$

$\dot{M} = 1.4 \cdot 10^{-6} M_{\odot}/\text{yr}$

Loop-like inner and outer (bi-polar) nebulae.

LBV HD 168607 and cLBV HD 168625

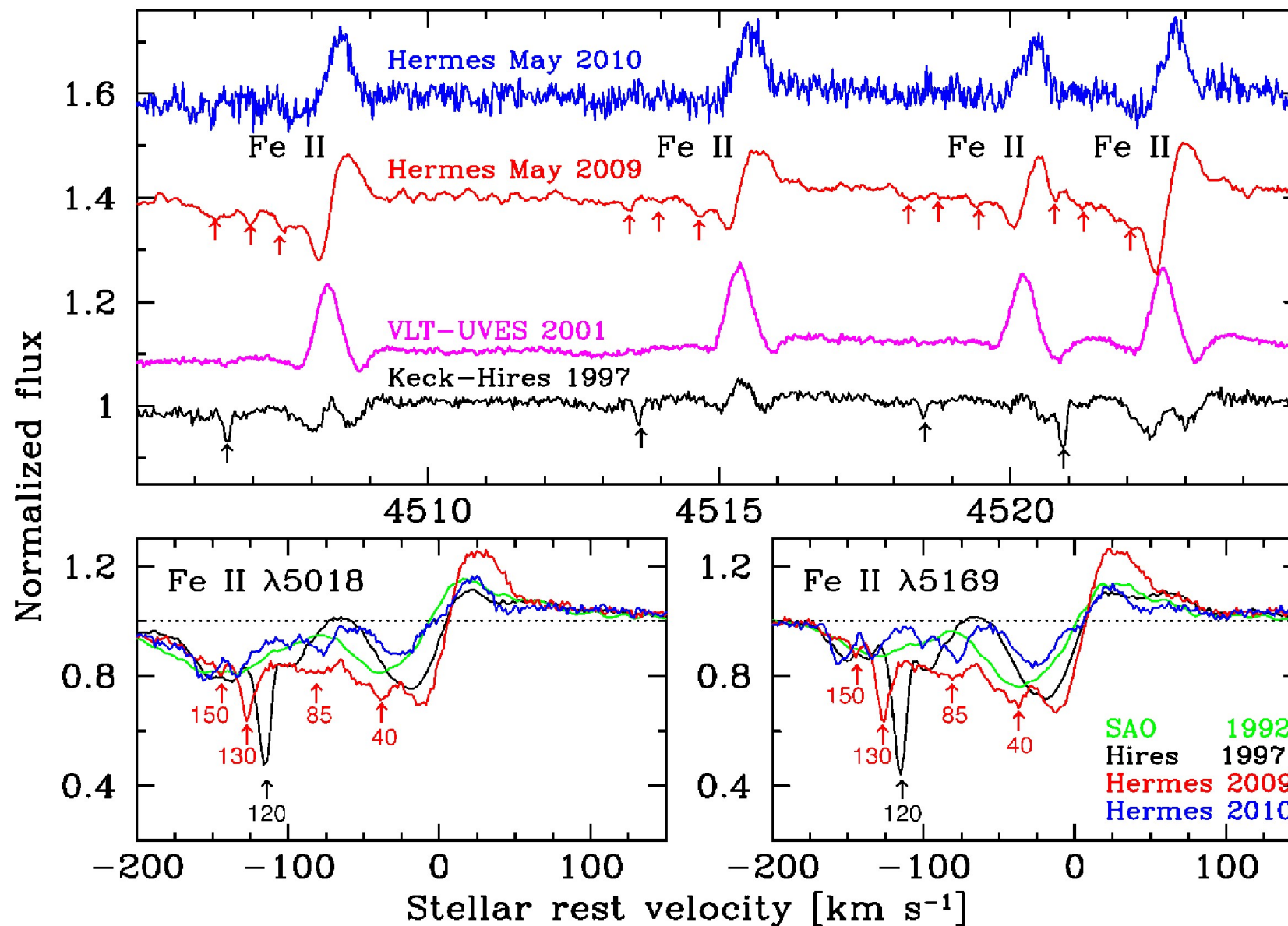


- Remarkable close pair. HD 168607 LBV without nebula & Teff = 9300 K B9.5 (van Genderen, A&A 2001)



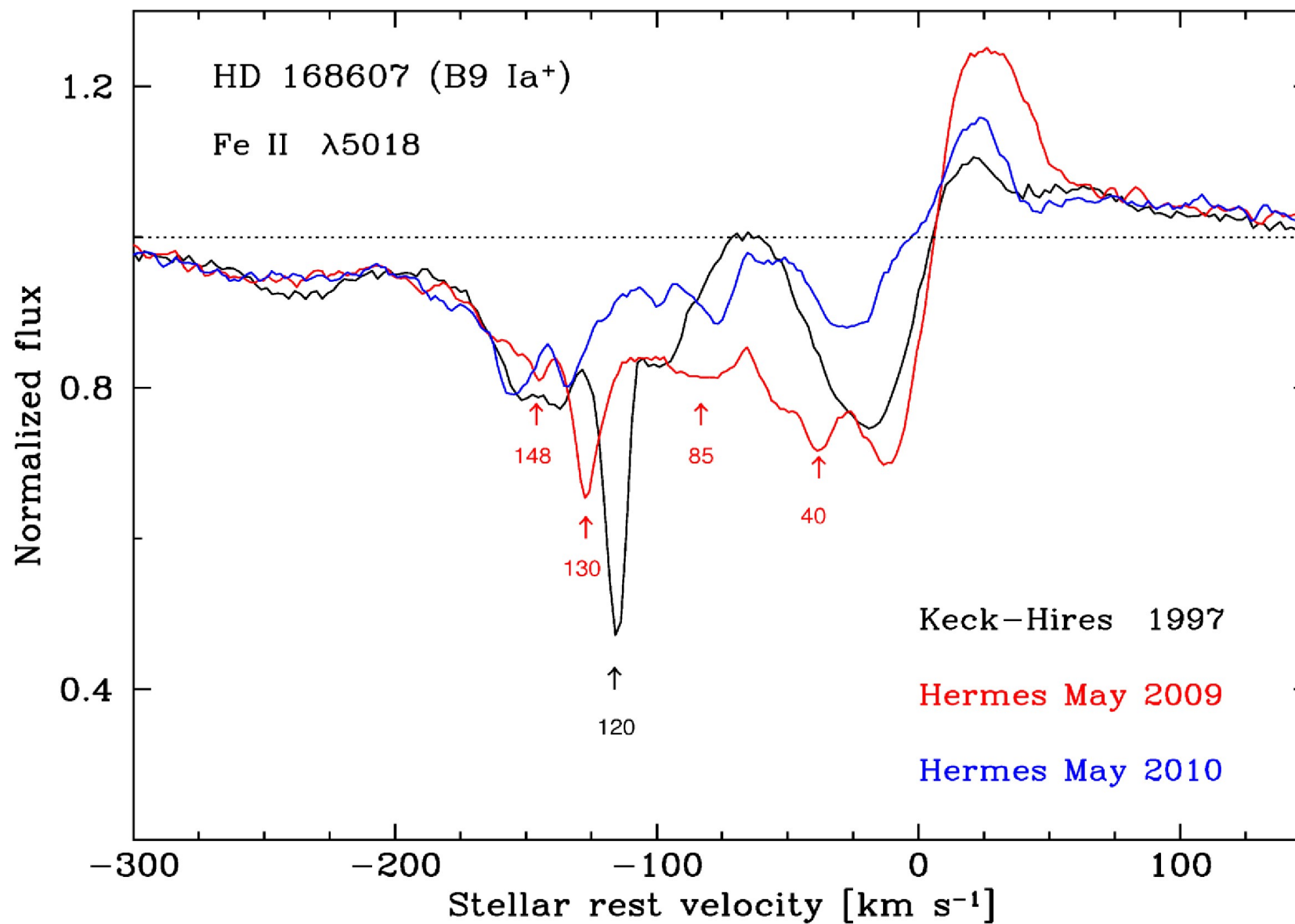
- HD 168625 (B5.5) dormant LBV?
Ring-like nebular structures observed
with IRAC-Spitzer (Smith+ 2007)

Discrete Absorption Components in LBV HD 168607



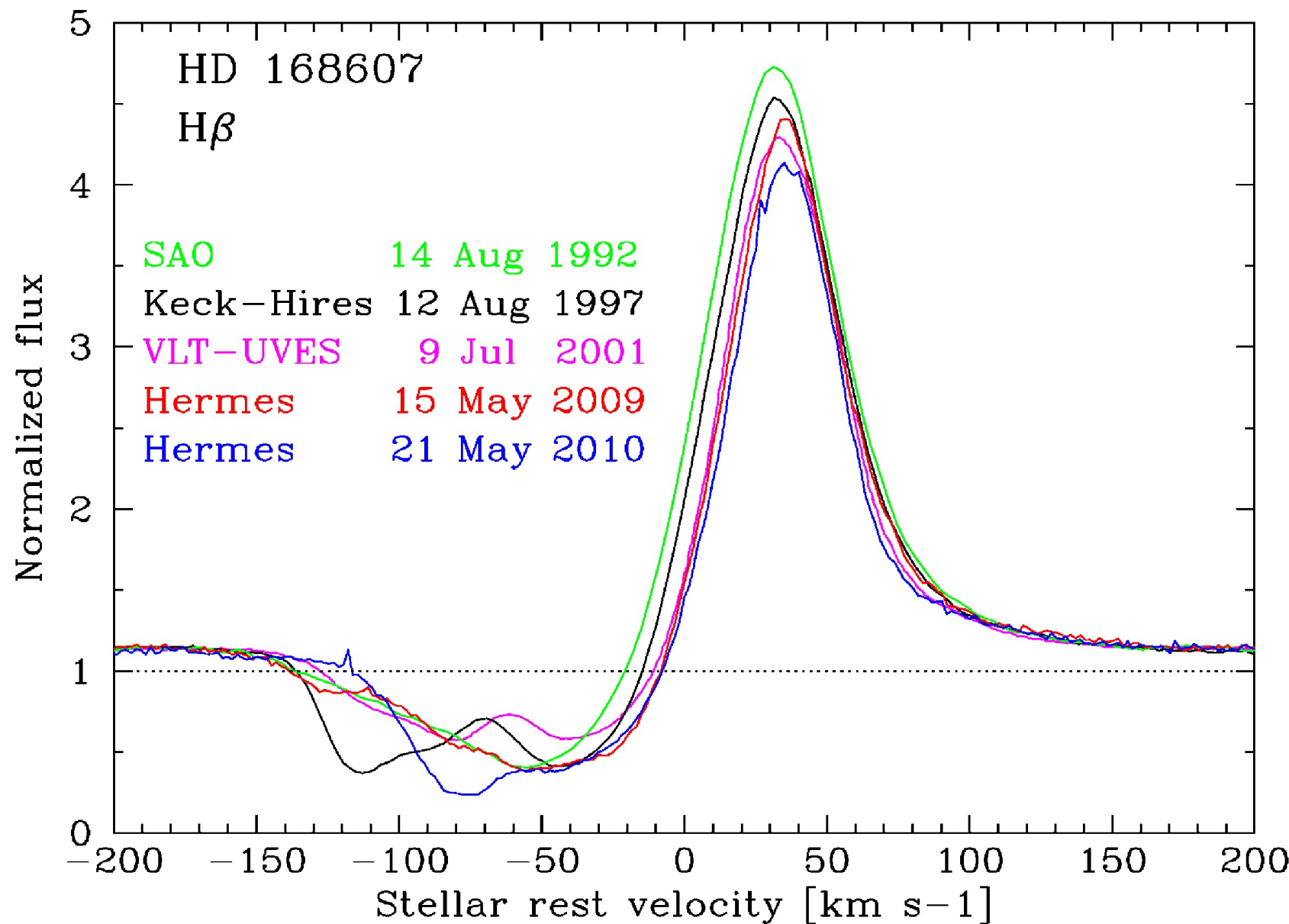
- DACs signal large-scale wind structures. DAC acceleration can help to constrain large-scale structured wind model (i.e. rotating wind interaction regions = CIRs).

Discrete Absorption Components in LBV HD 168607



Monitoring of DACs required for detailed 3-D RT wind modeling of DAC acceleration.

Discrete Absorption Components in LBV HD 168607

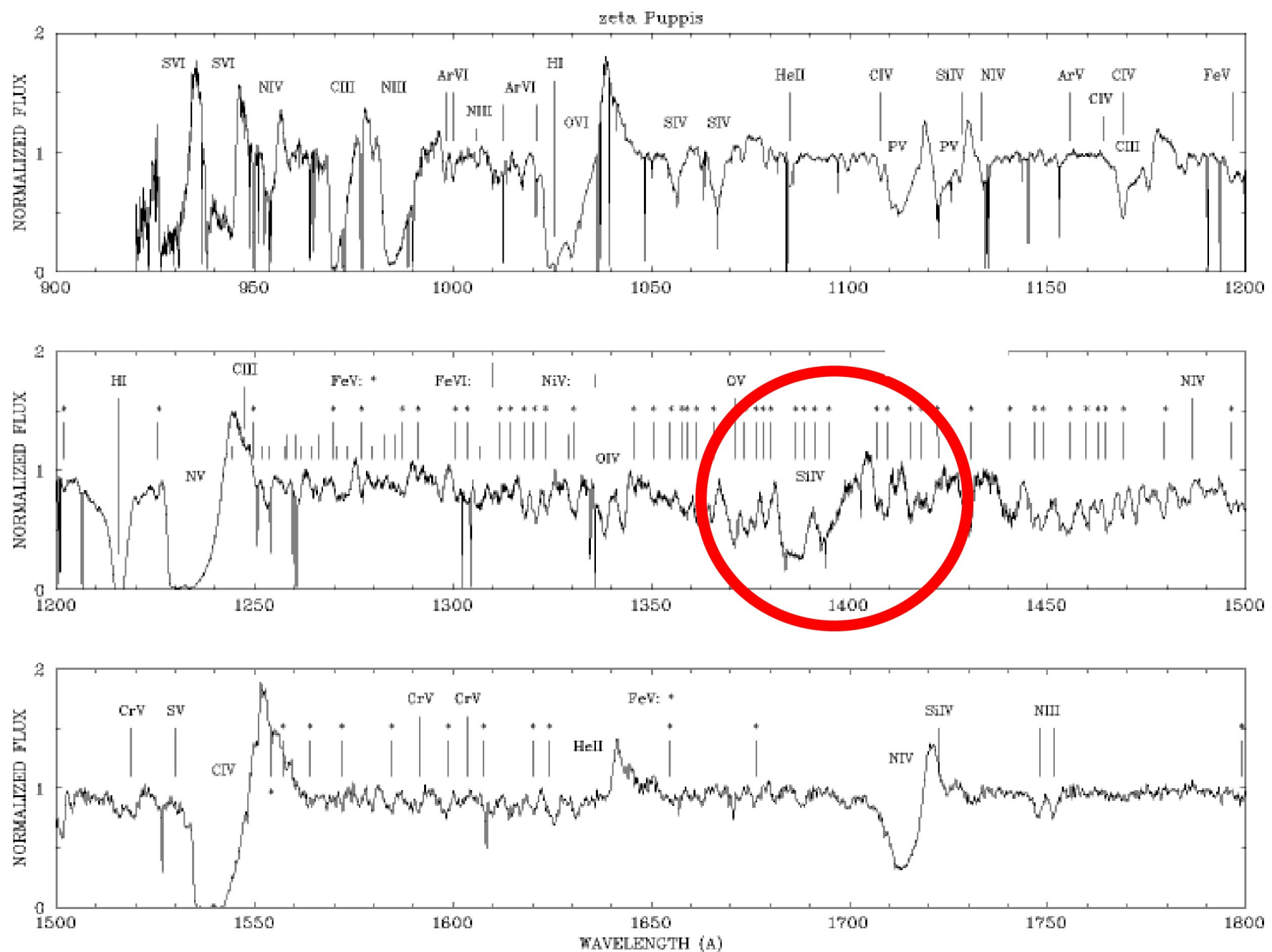


Strong variability of H β absorption observed with Mercator-HERMES, VLT-UVES, Keck-Hires (see also Chentsov+, A&A 2003).

Why study Winds of Massive Stars ?

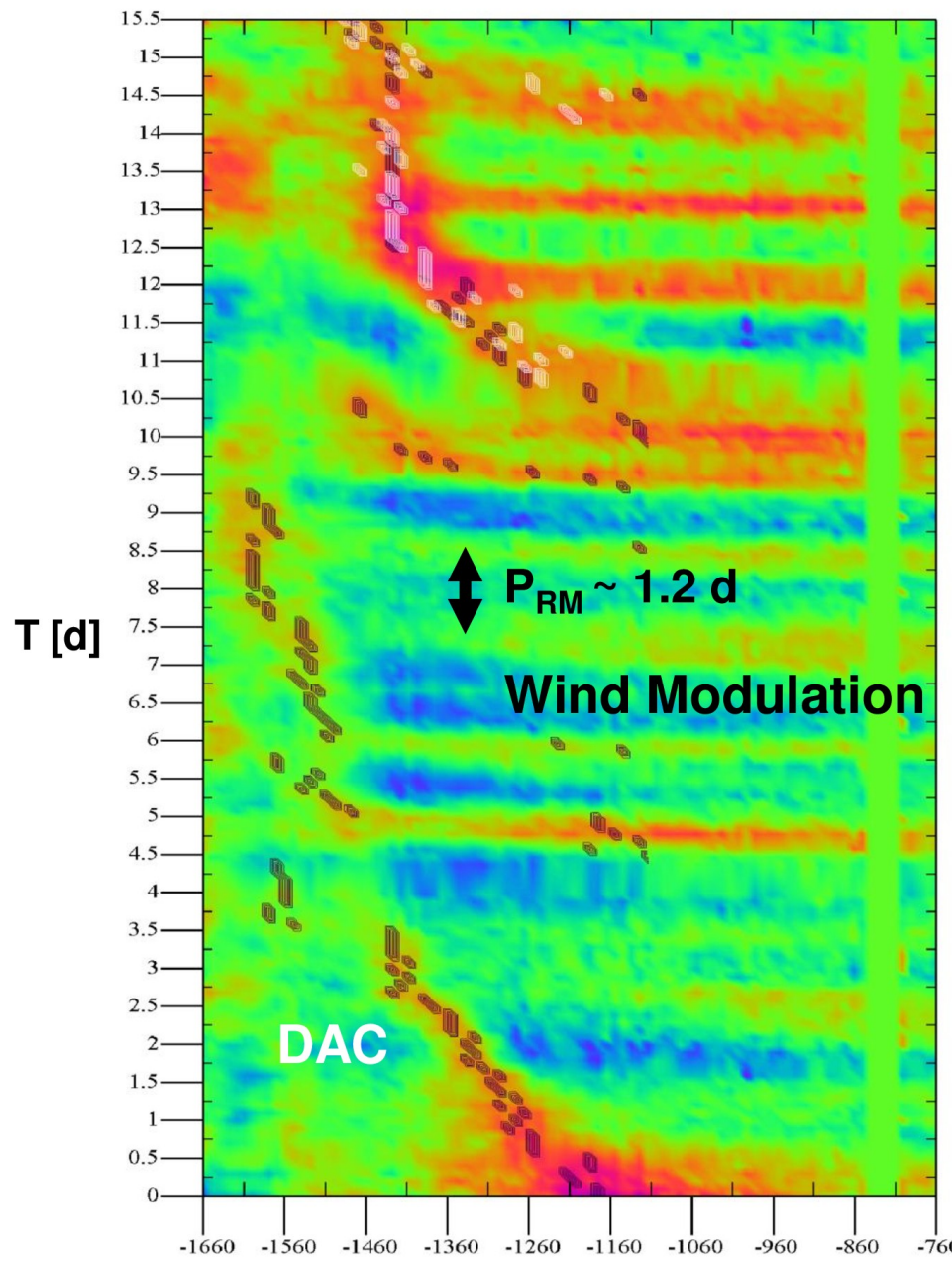
- Accurate mass-loss rate values are important to test evolutionary models of fast evolving luminous stars because mass-loss decreases stellar mass. Mass-loss rates are traditionally based on assumptions of spherically symmetric expanding wind models. Mass-loss rates of luminous hot stars overestimated by factor of 3 due to wind structures/clumping? What length scales are involved?
- Large mass-loss rates of massive stars dump substantial amounts of energy, momentum, and chemically enriched material into the local galactic environment thereby influencing dynamics of the interstellar medium and subsequent formation of stars.
- Ample evidence that outflows from massive stars are not spherically symmetric at all and must involve physical processes in their winds that shape their nebulae. E.g. hypergiants Eta Car, Pistol Star, MWC 314, P Cygni, etc.
- What physical mechanisms shape winds of stars across the H-R diagram? Spatial information about wind dynamics at several tens of stellar radii is required. Clear indicators of dynamics from optically thin wind regions are scarce and hard to model. 1-D modeling is useless.

IUE UV spectra with Si IV λ 1400 resonance doublet lines

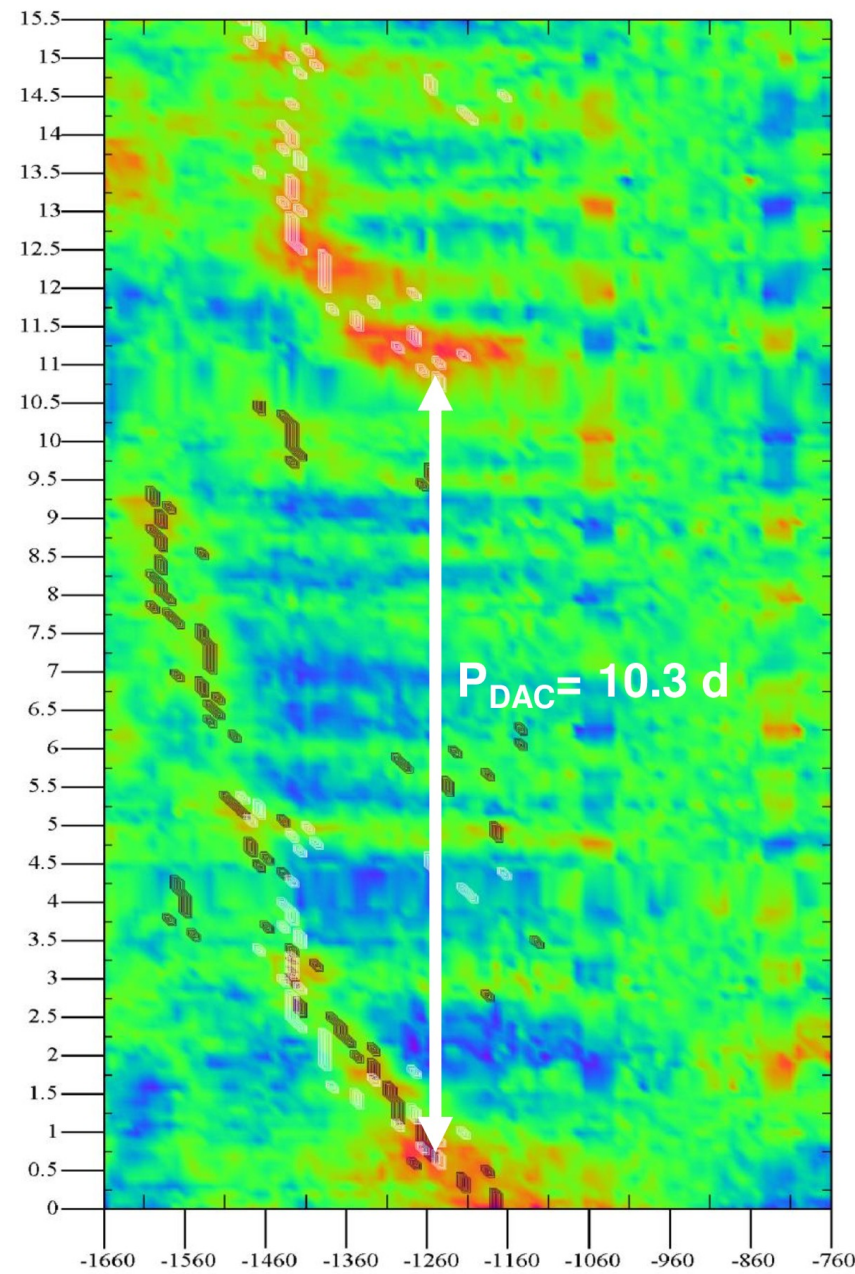


J Puppis observed Si IV λ 1394 line

Flux difference

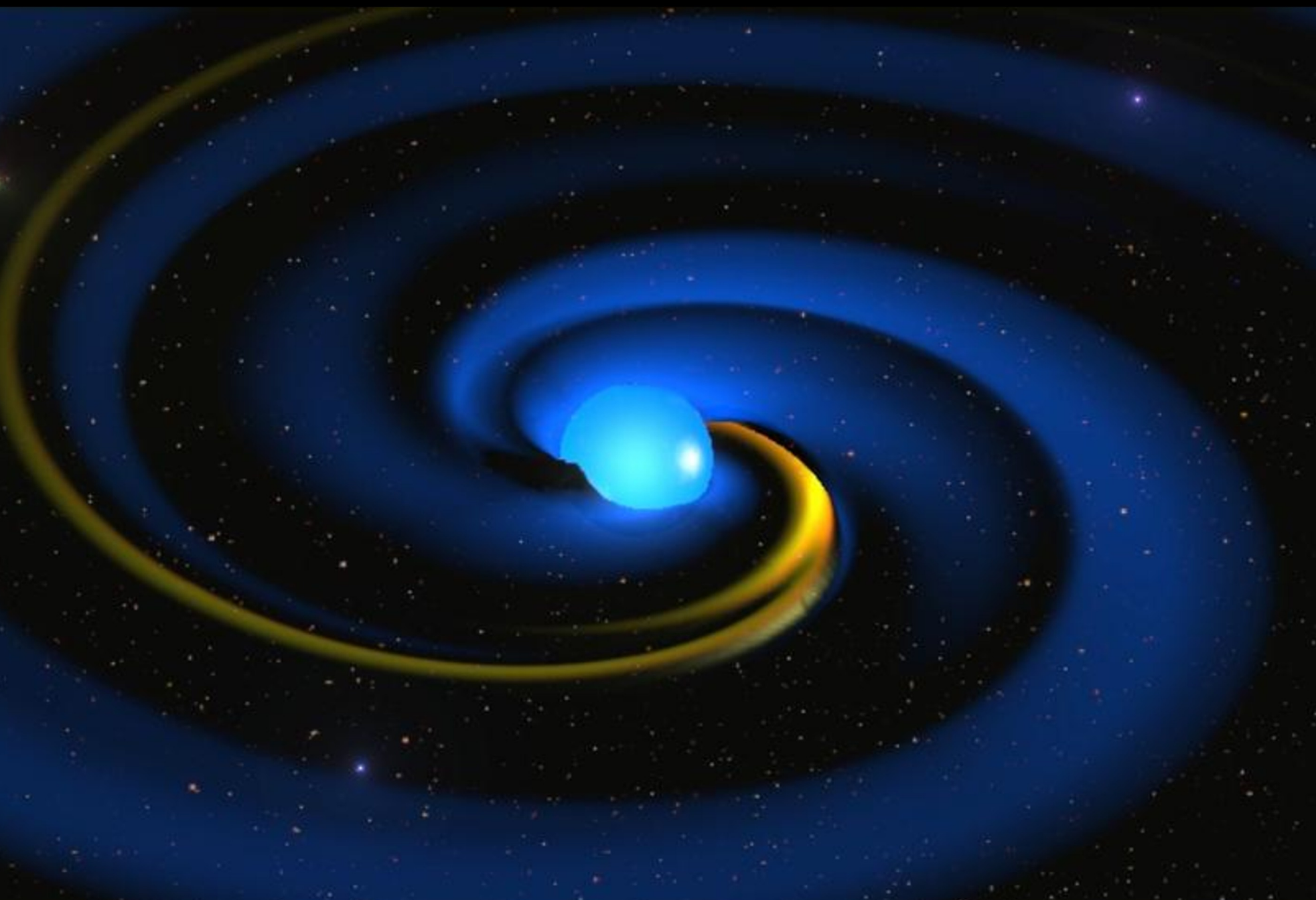


Flux filter modulations



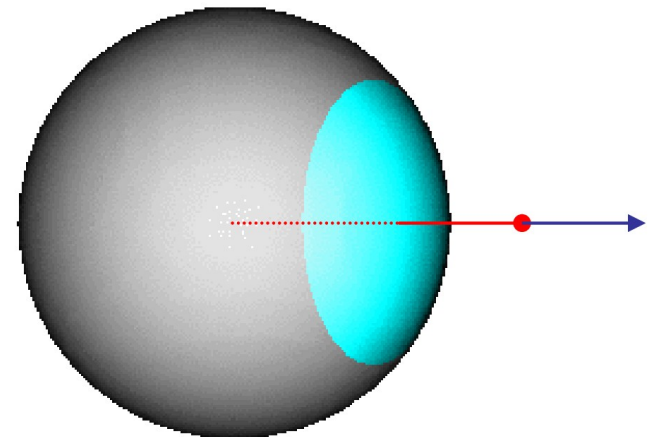
P_{DAC} = 10.3 0.5 d is period between 2 spots at base of wind causing wind structures that produce DACs.

**CIRs or Co-rotating Interaction Regions
are rotating density waves in the equatorial wind of massive hot stars**

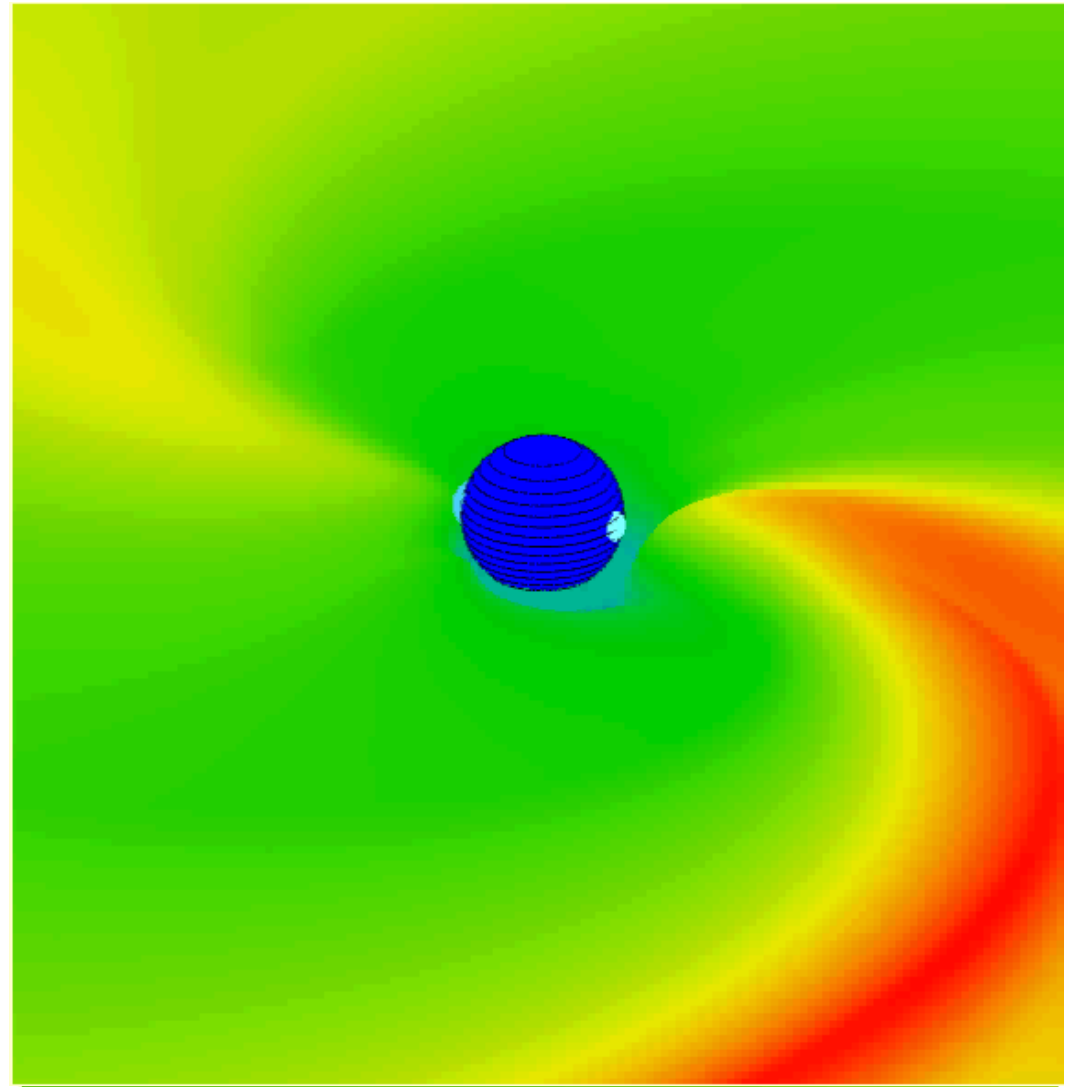
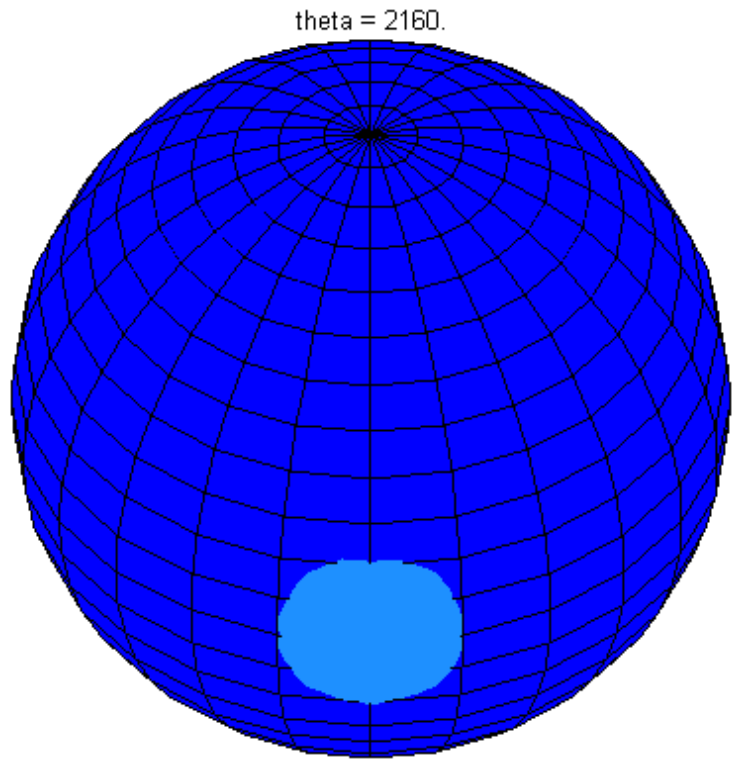


Multi-D hydrodynamic wind modelling

- **Zeus3D code**
 - Stone & Norman (1992)
 - Clarke (2007)
- **Used in 3-D RT by Lobel & Blomme (2007)**
 - 3-D hydro equations limited to equatorial plane
 - Rotation of the star and stellar wind
 - Acceleration by spectral lines included (CAK)
 - Spots on the stellar surface
 - Spots could result from NRP, magnetic fields ...



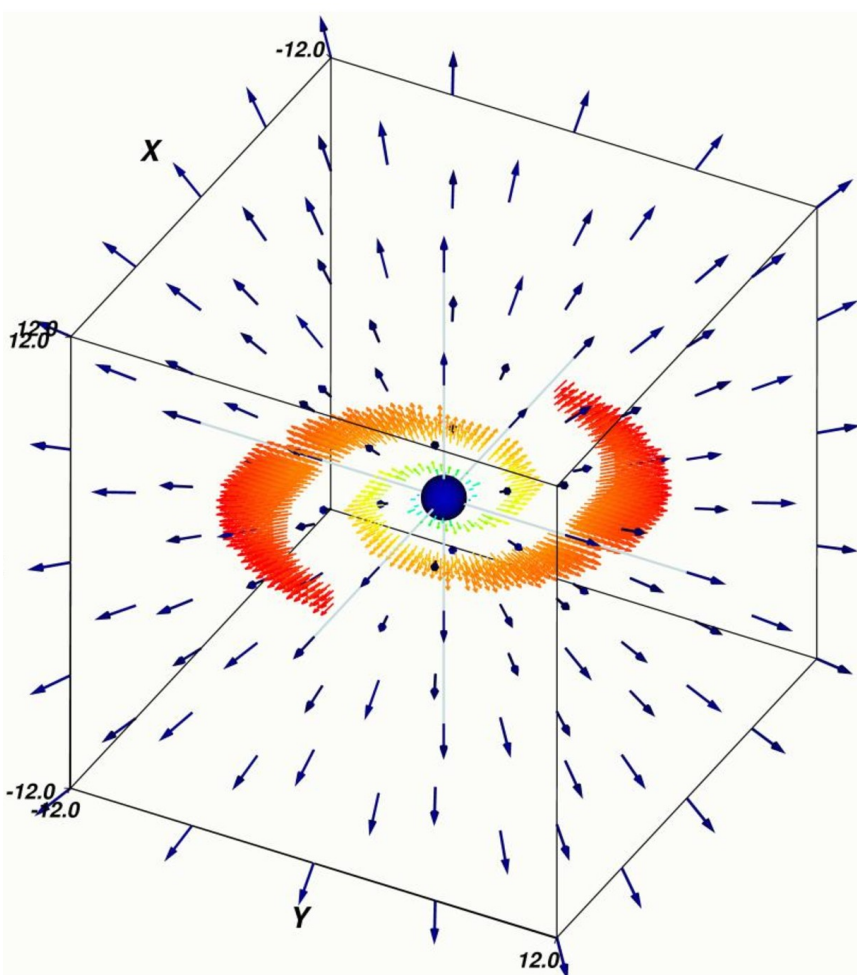
J Pup CIR model with Zeus3D hydrodynamics code



**CIRs caused by 2 unequally bright equatorial spots
that rotate 5 times slower than stellar surface rotation**

$$P_{\text{rot}} = 4.12 \text{ d} \quad P_{\text{spot}} = 20.6 \text{ d}$$

Development of 3-D radiation transport code Wind3D



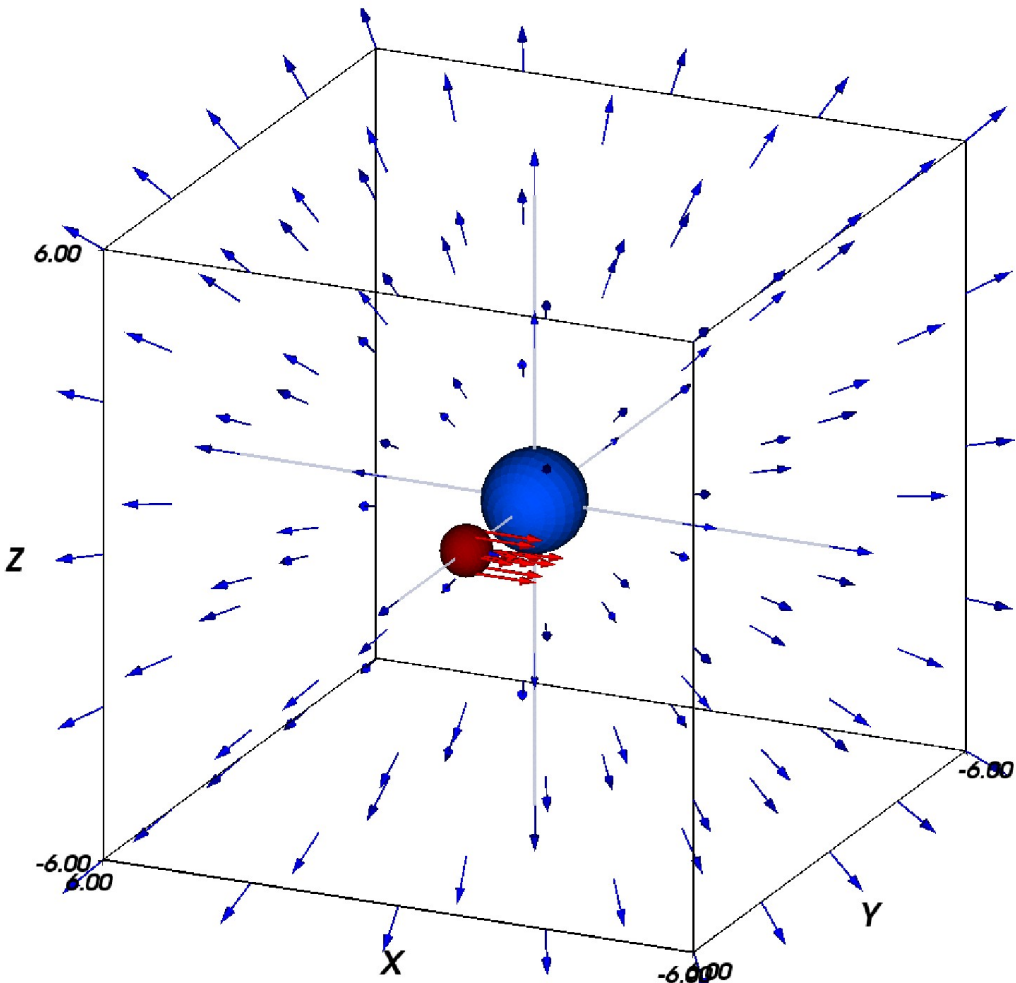
Hot star smooth wind with 'large scale' internal wind structures input for Wind3D

- implements **Cartesian** radiative transport scheme with short-characteristics method
- accepts **arbitrary 3-D wind-density and -velocity** structures
- exact **lambda iteration** of source function **starting from Sobolev approximation** in 3-D smooth wind model
- lambda iteration to **non-Sobolev** 3-D source function
- 100^3 source function points with 80^2 solid angles for 3-D intensity integral
- **non-LTE** radiative transfer equation is solved for density and velocity points with **3-D source function interpolation** technique
- **two-level atom** approx. for scattering dominated winds
- **fully parallelized** code with excellent load balancing
- 2010-2023: module implementation for parameterized structured wind models of radiatively-driven rotating winds. Also accepts hydrodynamic structured wind models computed with Zeus3D code.

⇒ Detailed modelling of DACs observed in UV P Cyg lines of J Pup (B0.5 Ib)

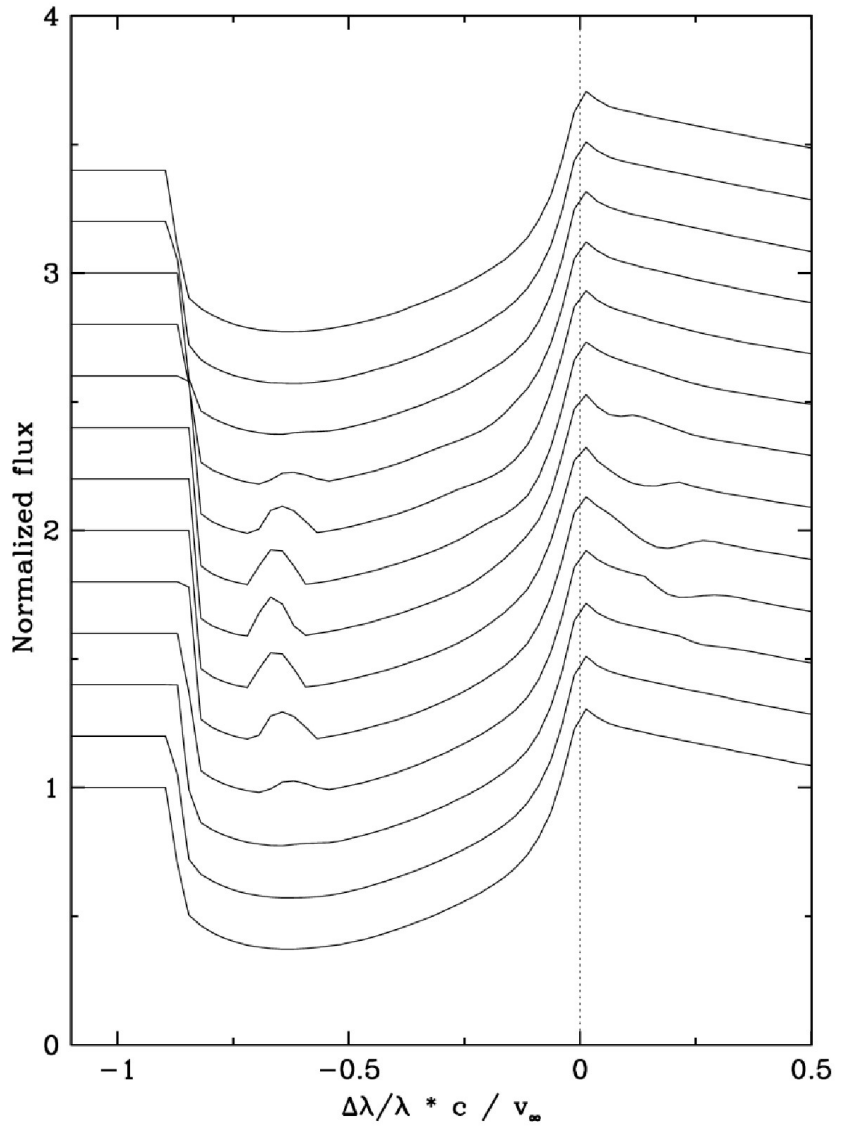
Testing 3D radiative transfer code Wind3D

Place clump of $\rho \times 10$ inside hot star wind model



Dense clump of $1/2 R_*$ moves perpendicular to the line of sight and partly obscures the stellar surface

Wind3D line profiles over 90° in eq. plane



3D radiative transfer produces decrease of scattering flux at wind velocity of blob position

Detailed best fit to DAC shapes using 2 unequal spots with 3D Radiative Transfer Wind3D

2-spot
hydrodynamic wind
model with

$$V_{\text{spot}} = V_{\text{rot}} / 5$$

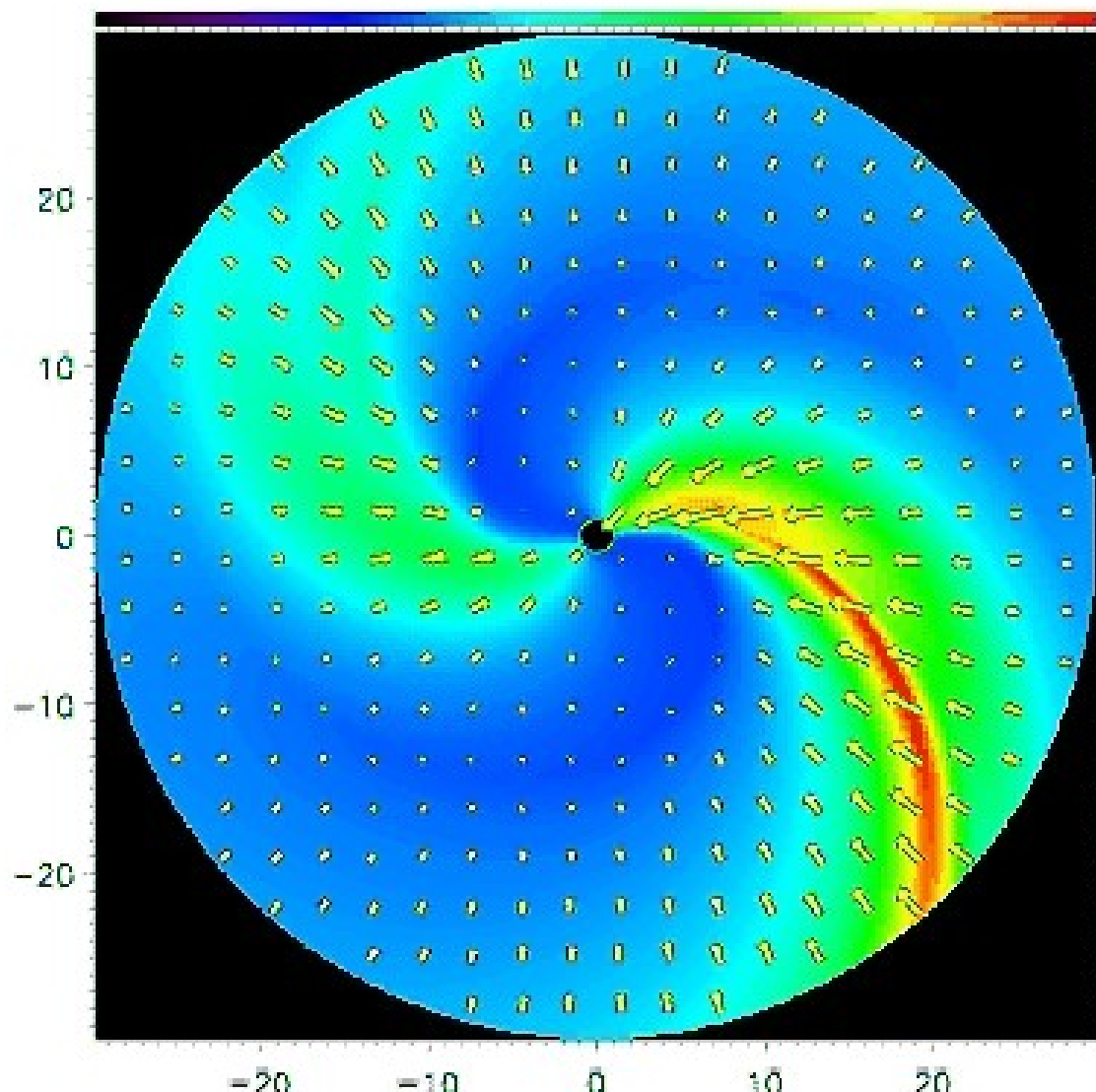
$$A_{\text{sp}} = 0.2 \quad \& \quad \Phi_{\text{sp}} = 20^\circ$$

$$A_{\text{sp}} = 0.08 \quad \& \quad \Phi_{\text{sp}} = 30^\circ$$

Density contrast:

minimum $\rho / \rho_0 = 0.87$

maximum $\rho / \rho_0 = 1.31$



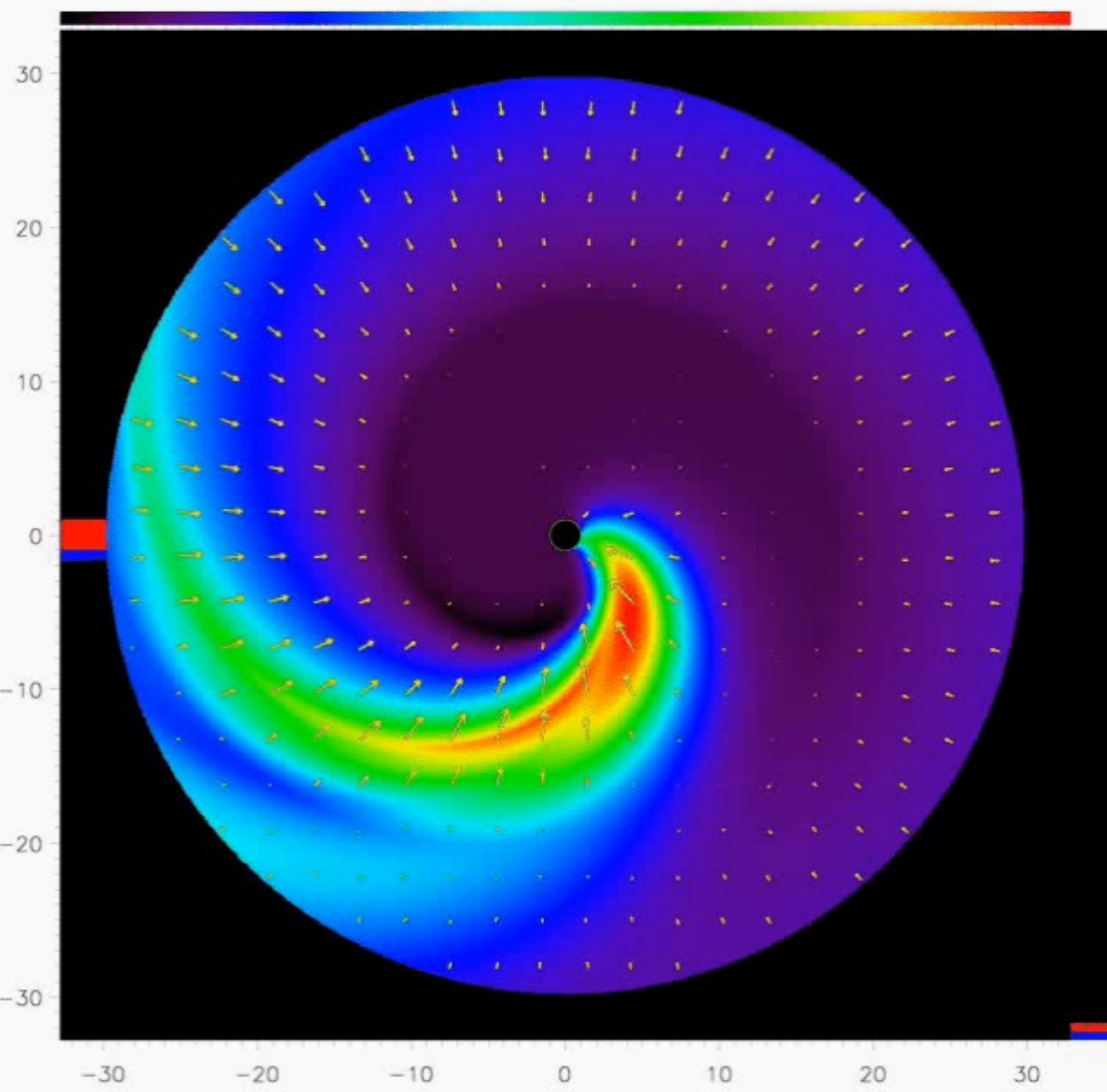
Hydrodynamic wind model with CIR lagging behind rotation of the stellar surface

Si IV $\lambda 1394$ computed with Wind3D

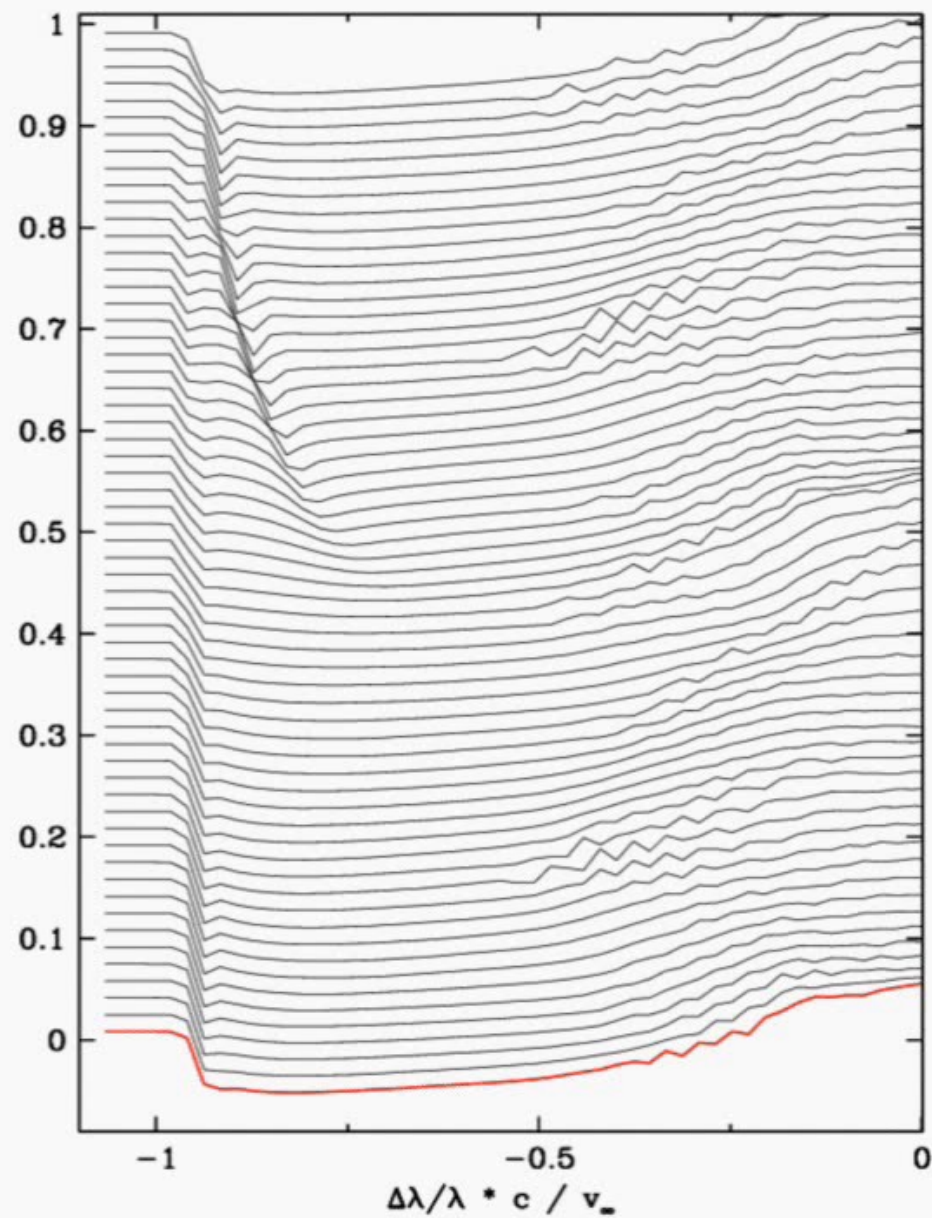
$\rho / \rho_0 = 0.985$ Density contrast

$\rho / \rho_0 = 1.2$

Normalized flux



$A_{\text{sp}}=0.1$ $\Phi_{\text{sp}}=50^\circ$ $V_{\text{spot}} < V_{\text{rot}}$



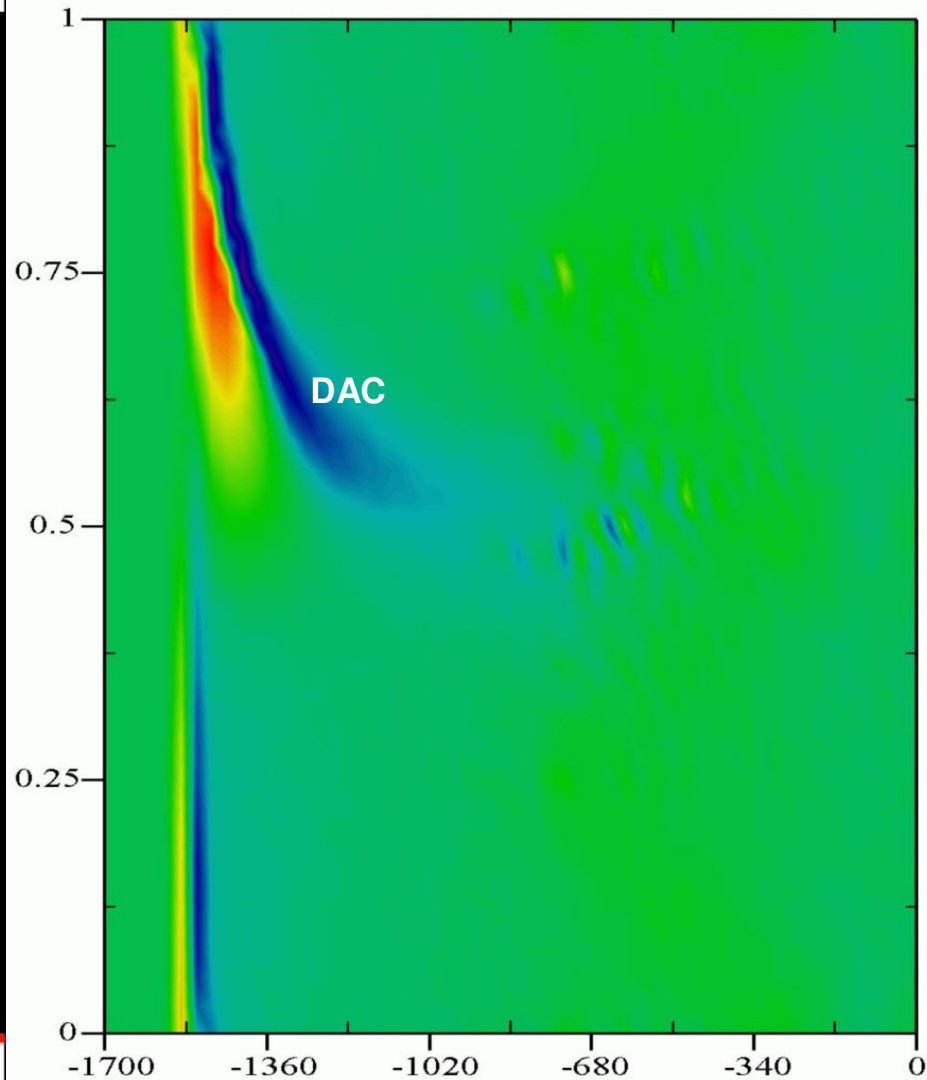
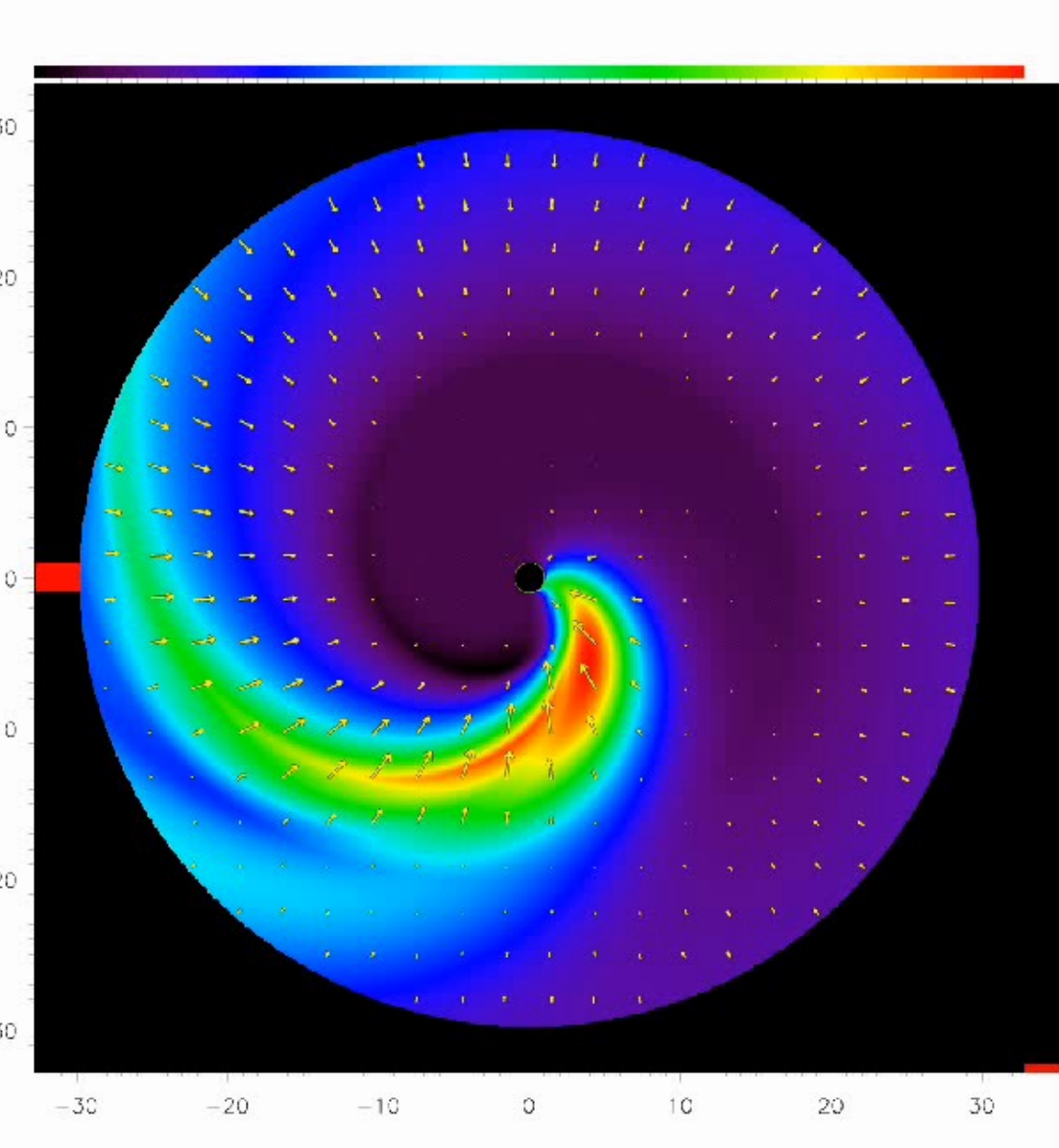
Hydrodynamic wind model with CIR lagging behind rotation of the stellar surface

Si IV $\lambda 1394$ computed with Wind3D

$\rho / \rho_0 = 0.985$ Density contrast

$\rho / \rho_0 = 1.2$

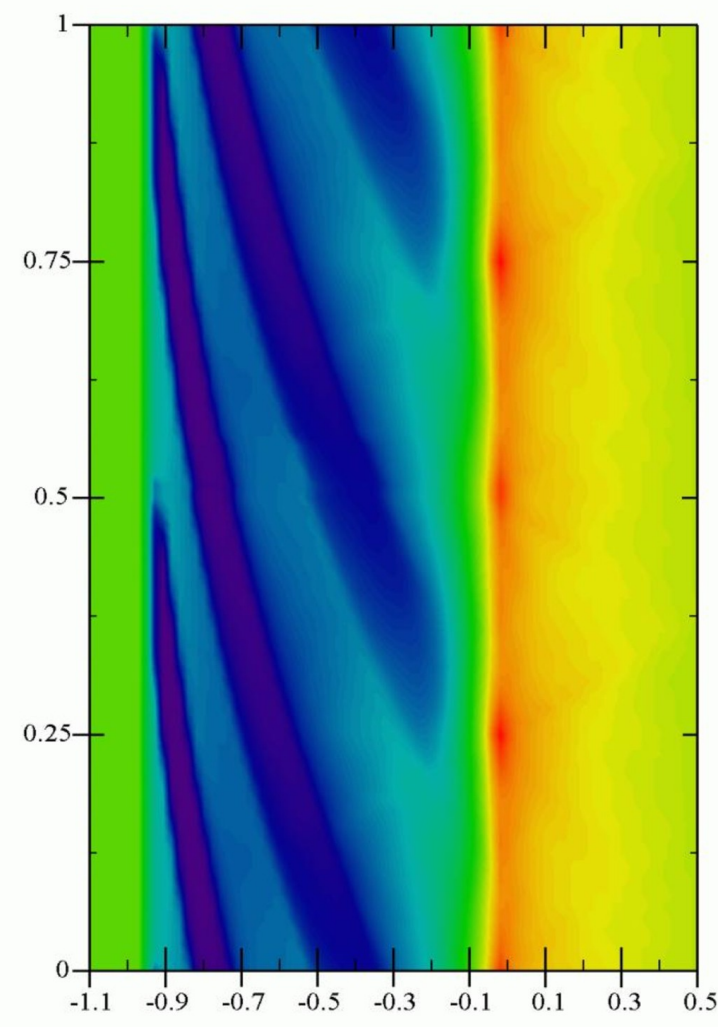
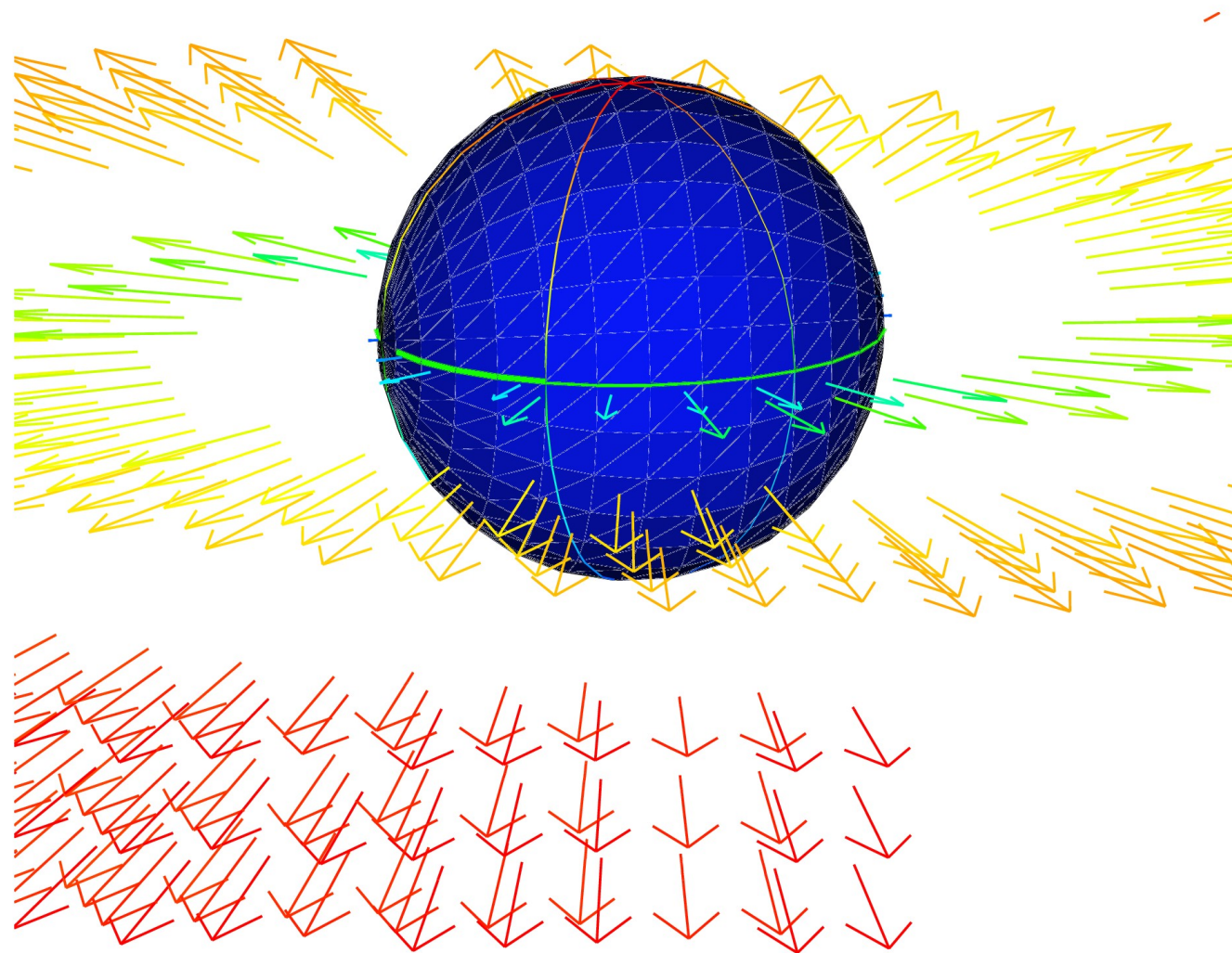
Flux difference



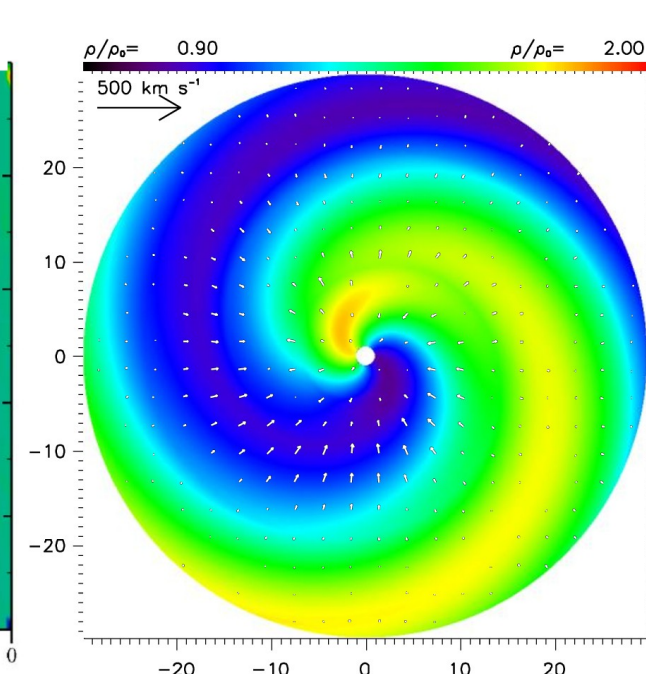
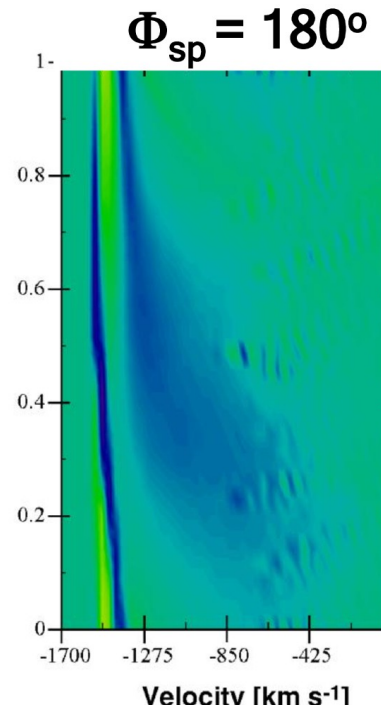
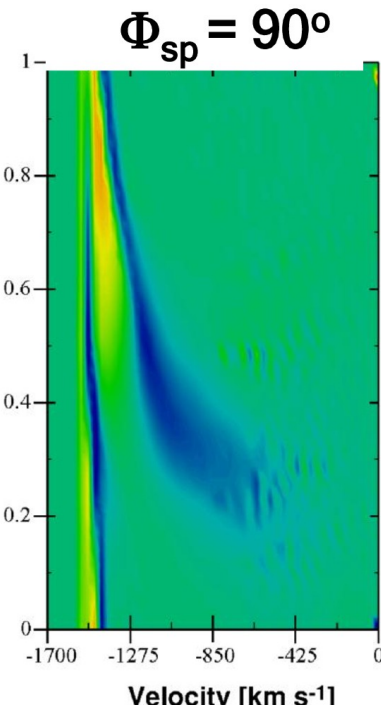
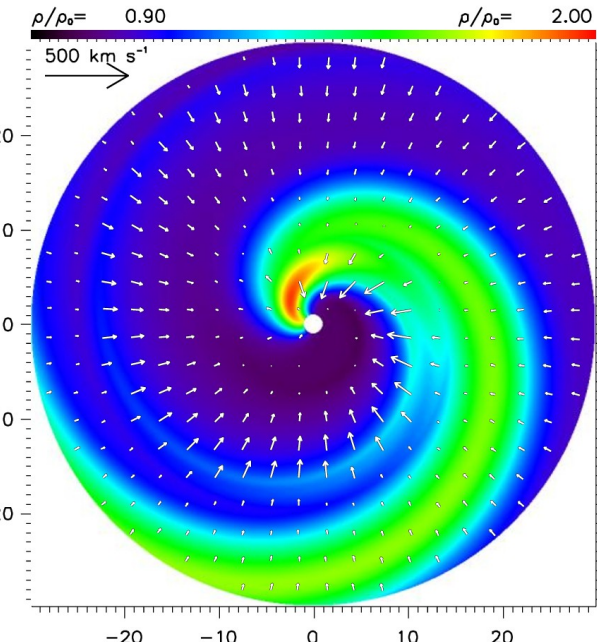
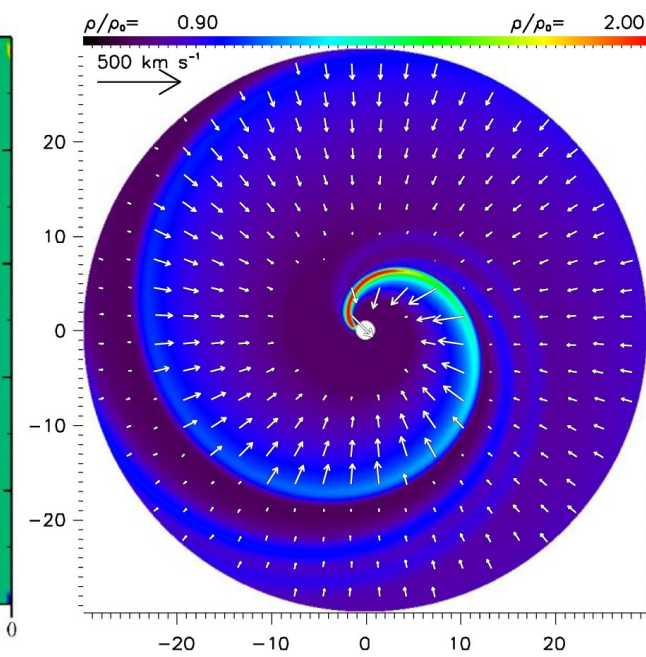
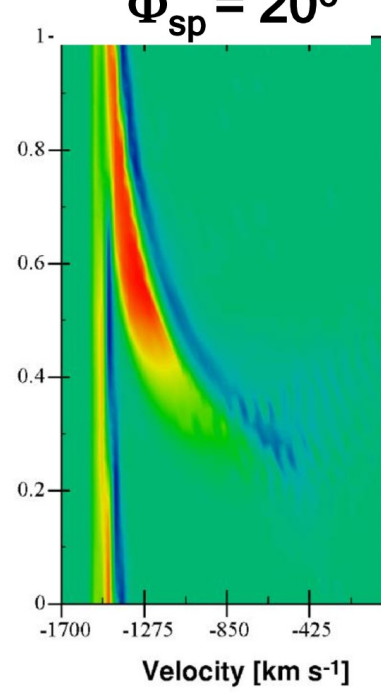
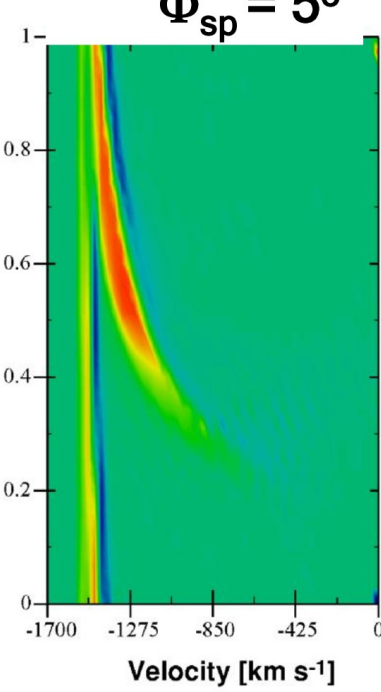
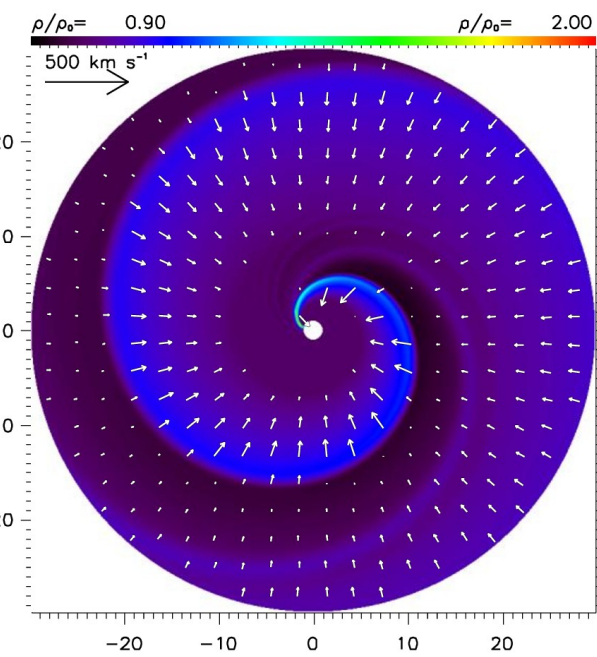
$A_{\text{sp}}=0.1$ $\Phi_{\text{sp}}=50^\circ$ $V_{\text{spot}} < V_{\text{rot}}$

CIR causes DAC because of increased wind density contrasts and velocity plateaus

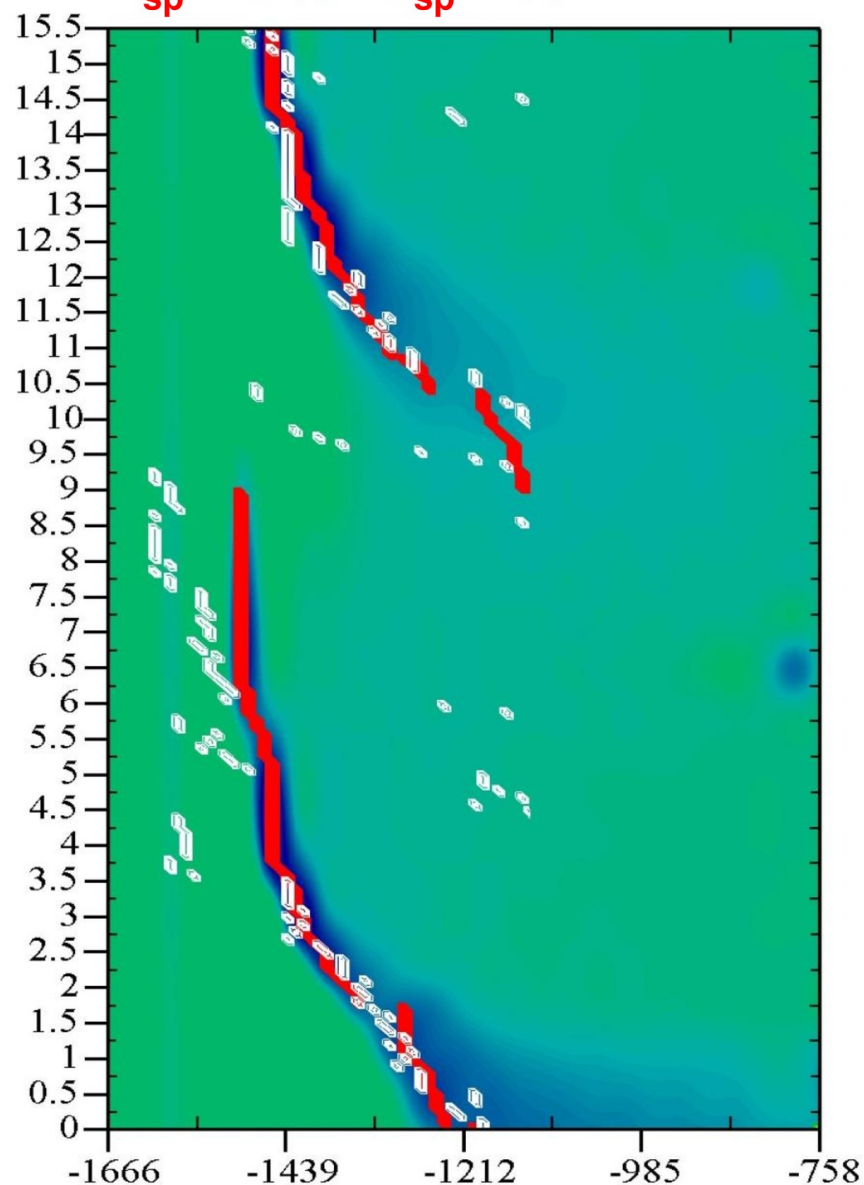
Dynamic Si IV P Cyg lines computed with Wind3D



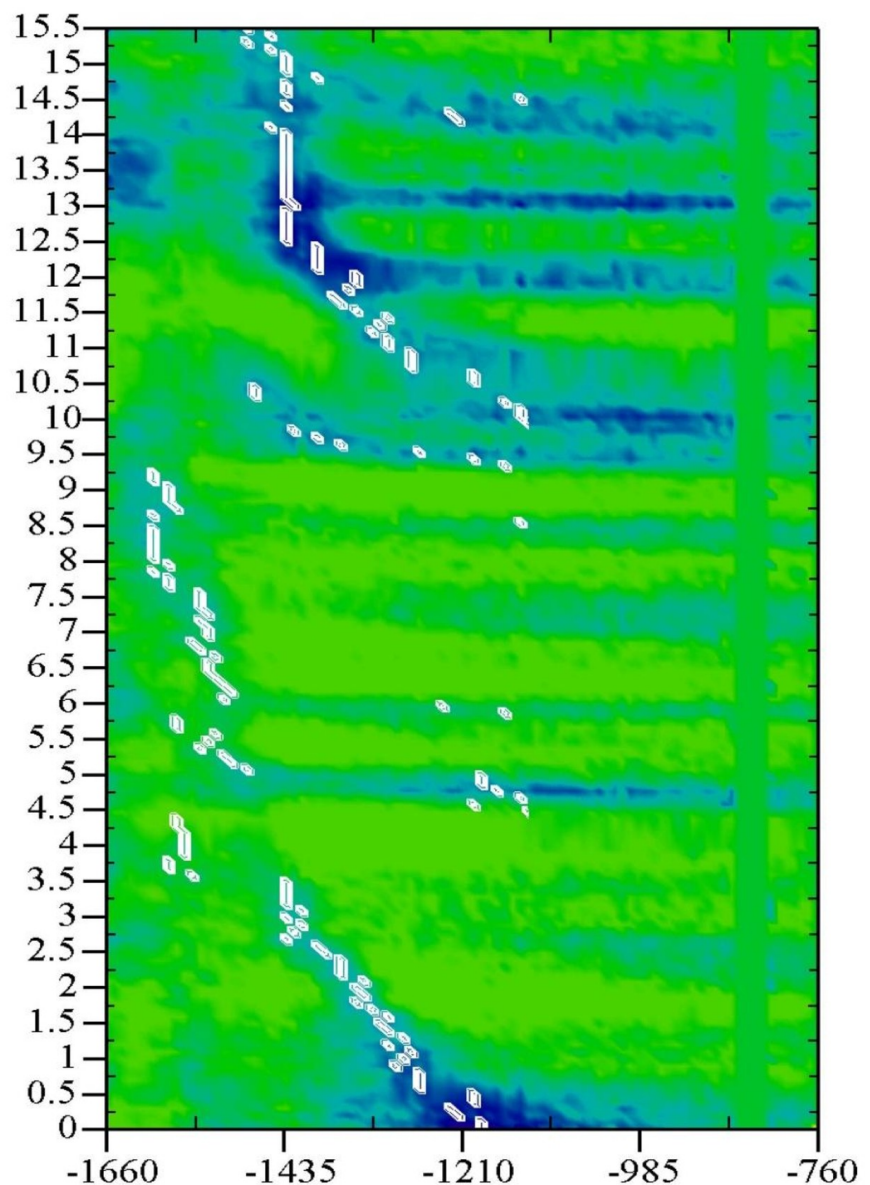
DACs become narrow because the dispersion of projected velocities in the CIRs decreases farther above the stellar surface.

$A_{\text{sp}}=0.5$ $\Phi_{\text{sp}}=5^{\circ}$ $\Phi_{\text{sp}}=20^{\circ}$ 

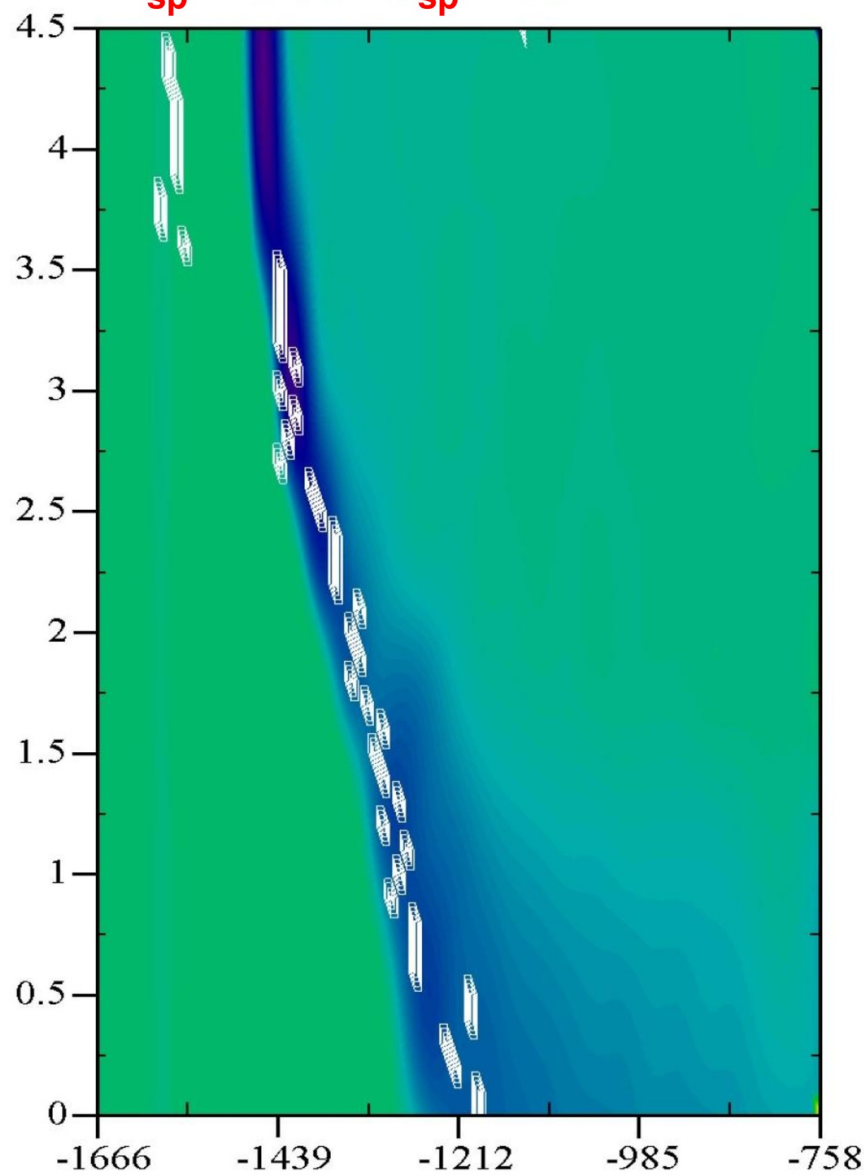
2-spot best fit: $V_{\text{spot}} = V_{\text{rot}} / 5$
 $A_{\text{sp}} = 0.2 \quad \Phi_{\text{sp}} = 20^\circ$
 $A_{\text{sp}} = 0.08 \quad \Phi_{\text{sp}} = 30^\circ$



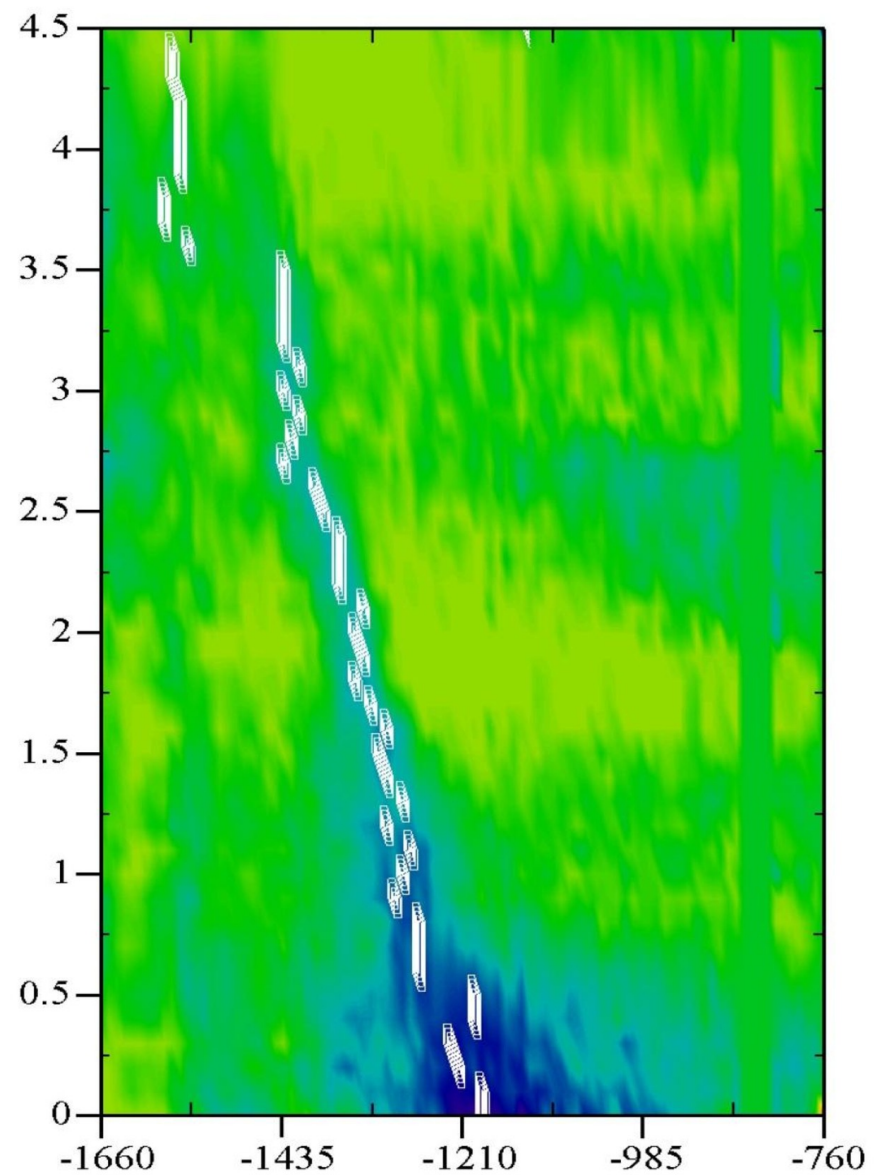
J Pup IUE 1995



2-spot best fit: $V_{\text{spot}} = V_{\text{rot}} / 5$
 $A_{\text{sp}} = 0.2 \quad \Phi_{\text{sp}} = 20^\circ$
 $A_{\text{sp}} = 0.08 \quad \Phi_{\text{sp}} = 30^\circ$



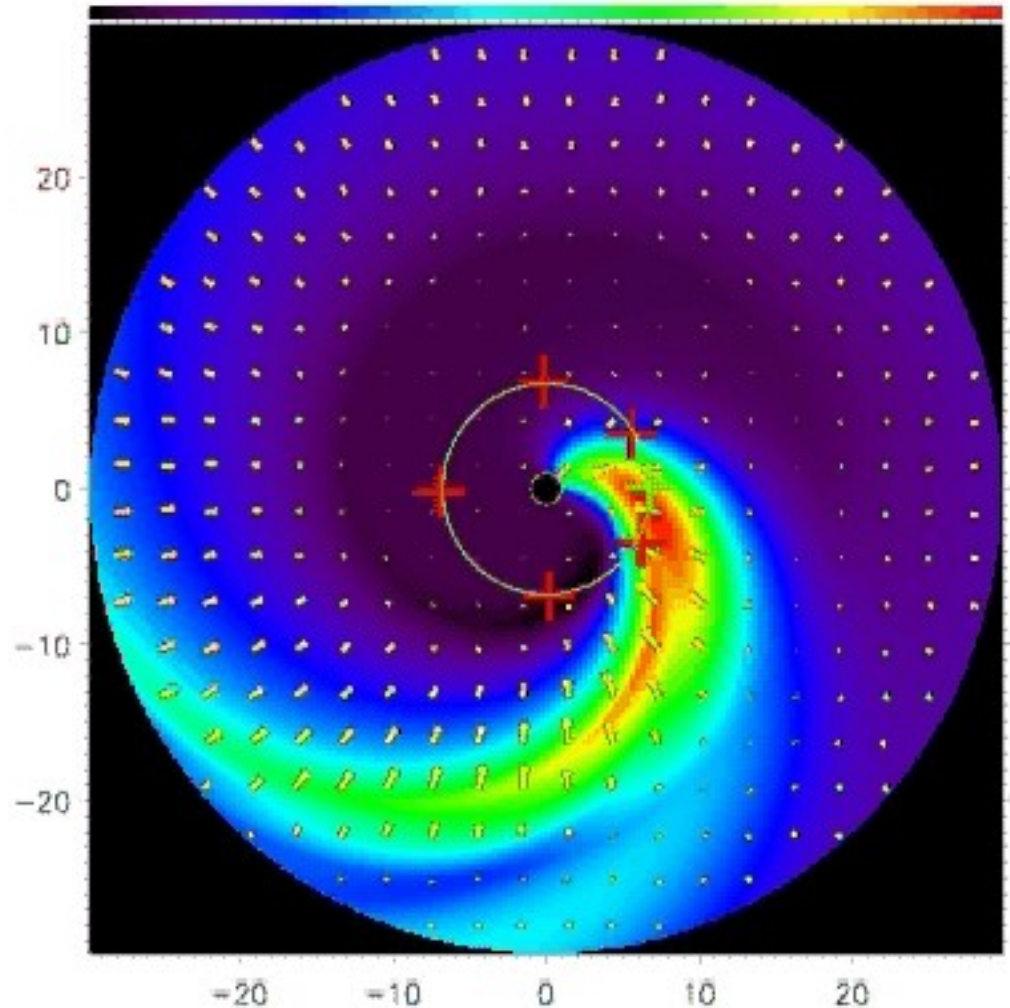
J Pup IUE 1995



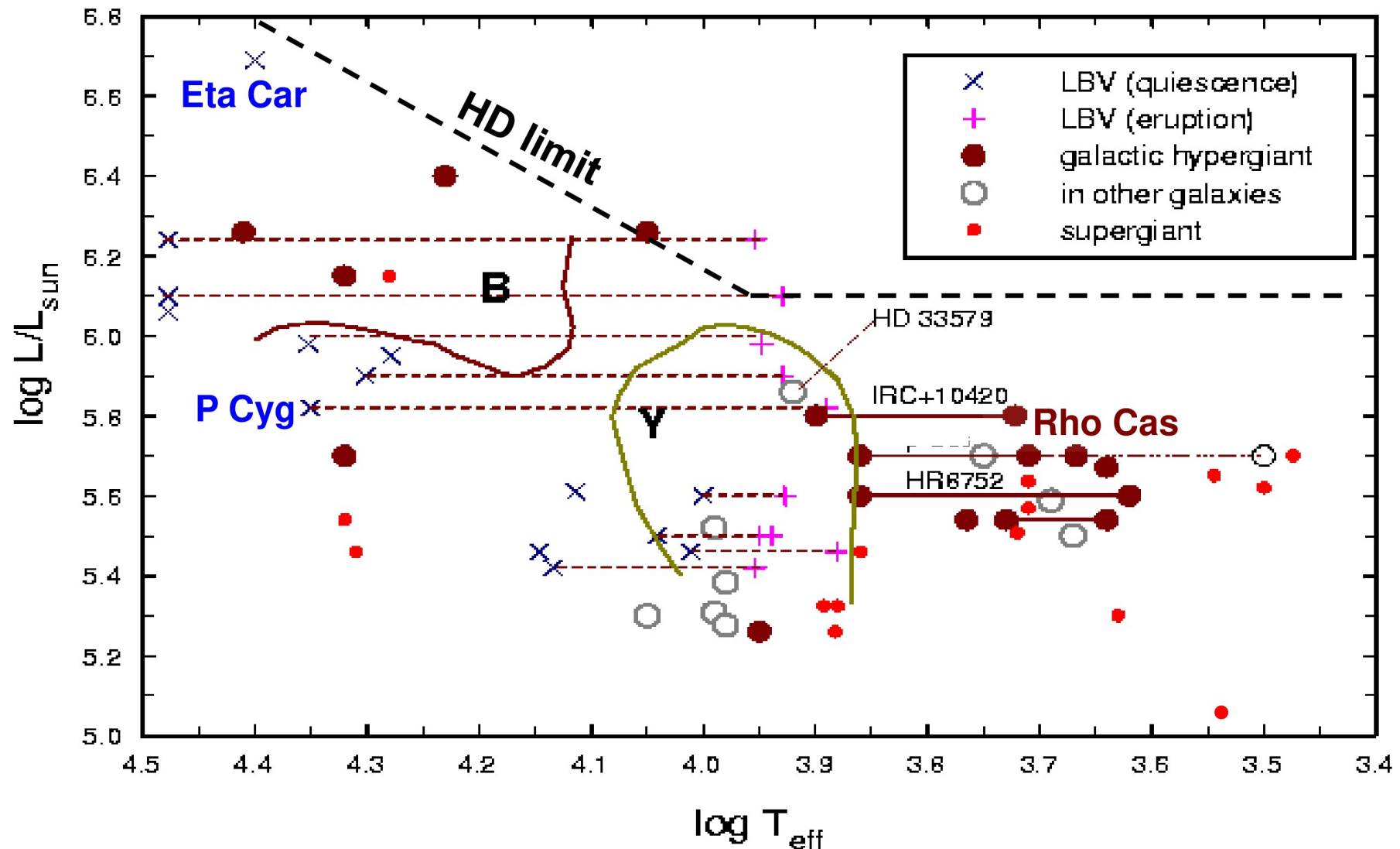
With rotation:

$$A_{sp}=0.1 \quad \Phi_{sp}=50^\circ \quad V_{sp} = V_{rot}/2.5$$

- Spiral shaped density enhancement (CIR)
- changes in velocity in the CIR and in the trailing edge
- CIR is a pattern; particles cross the CIR

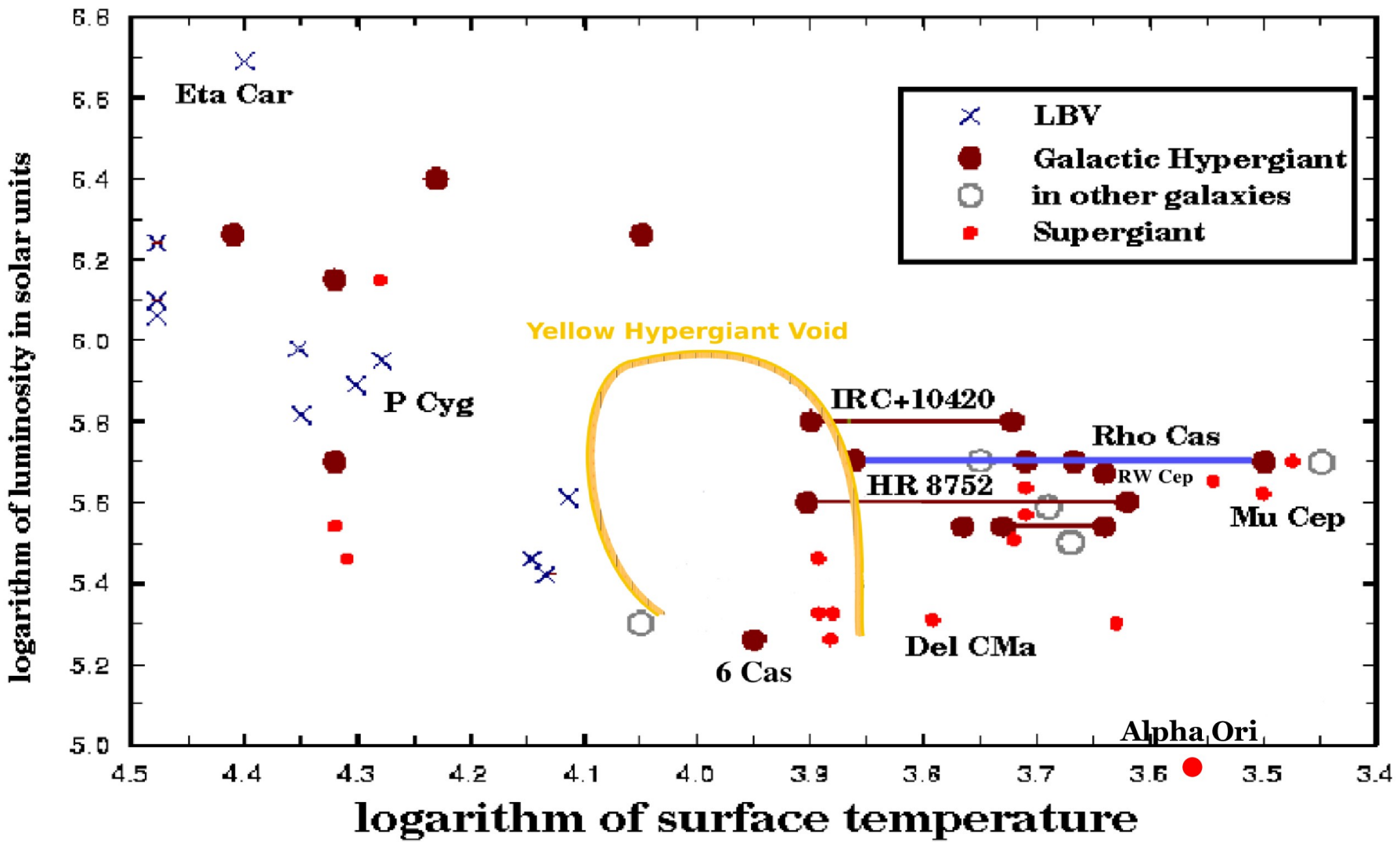


Yellow Hypergiants in the upper H-R diagram



- Most massive and luminous supergiants near upper luminosity limit (F-G Ia⁺).
- Show strong spectral variability and semi-regular V-brightness curves.
- Recurrent eruption events with exceptionally large mass-loss rates to $\sim 10^{-3} M_{\odot}/\text{y}$

The Yellow Hypergiant Void



- Most Yellow Hypergiants cluster near cool border of Yellow Void.
- The Yellow Void is a region devoid of Yellow Hypergiants (evolving blueward).
- Cool Hypergiants thought be on fast blueward evolutionary tracks (de Jager 1998).

LUMINOUS BLUE VARIABLE

P Cygni B1 Ia+

T_{eff} = 19,300 K Log g = 0.0

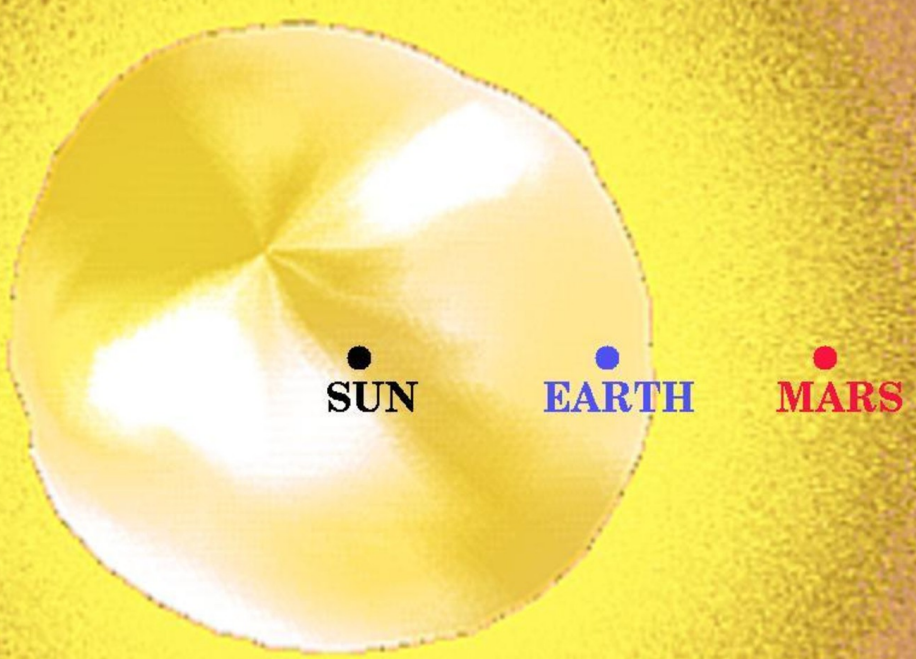
R* = 76 R \odot L* = 630,000 L \odot

YELLOW HYPERGIANT

Rho Cas F - G Ia+

T_{eff} = 7200 K Log g = 0.5

R* = 400 R \odot L* = 100,000 L \odot

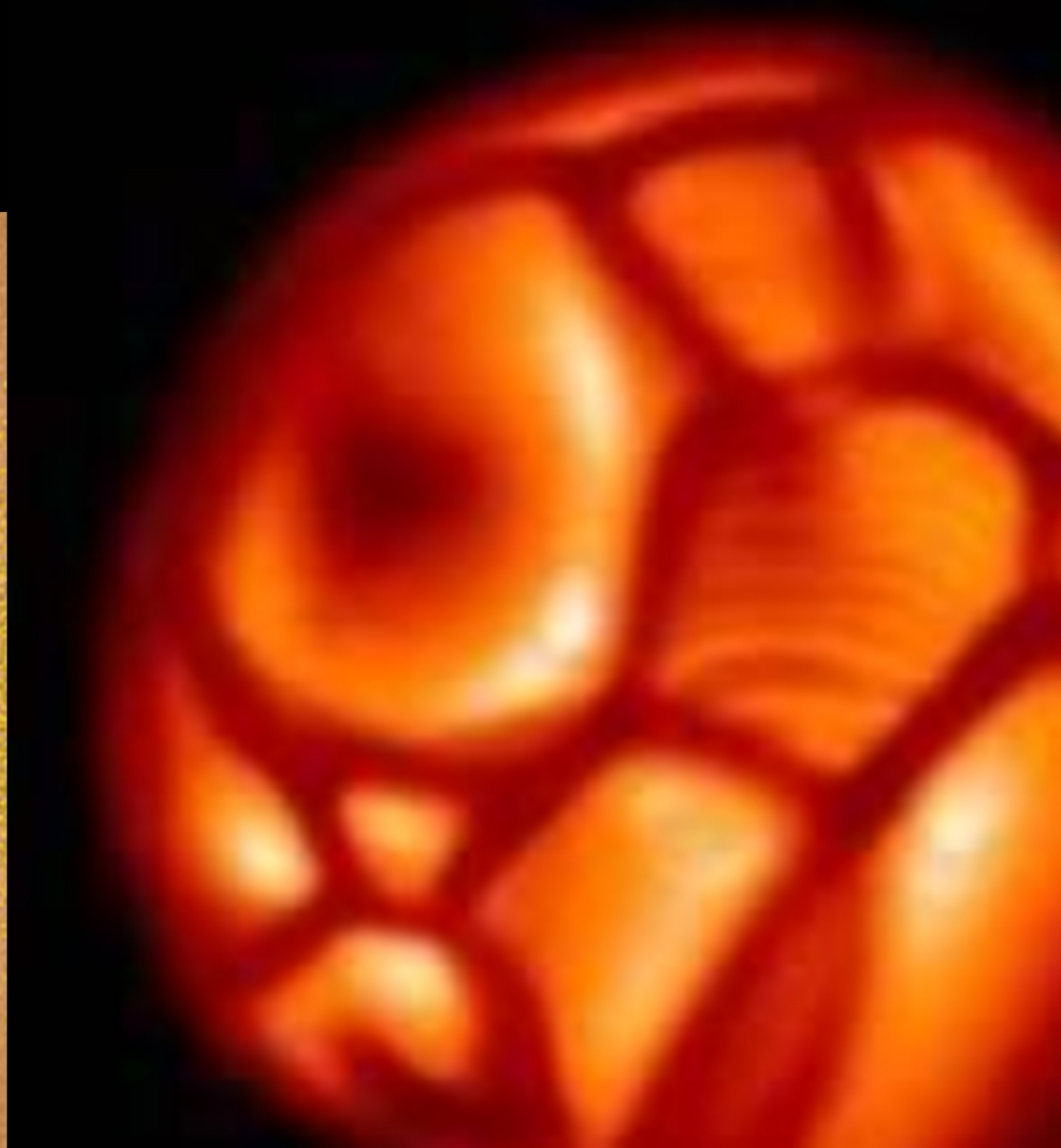


RED SUPERGIANT

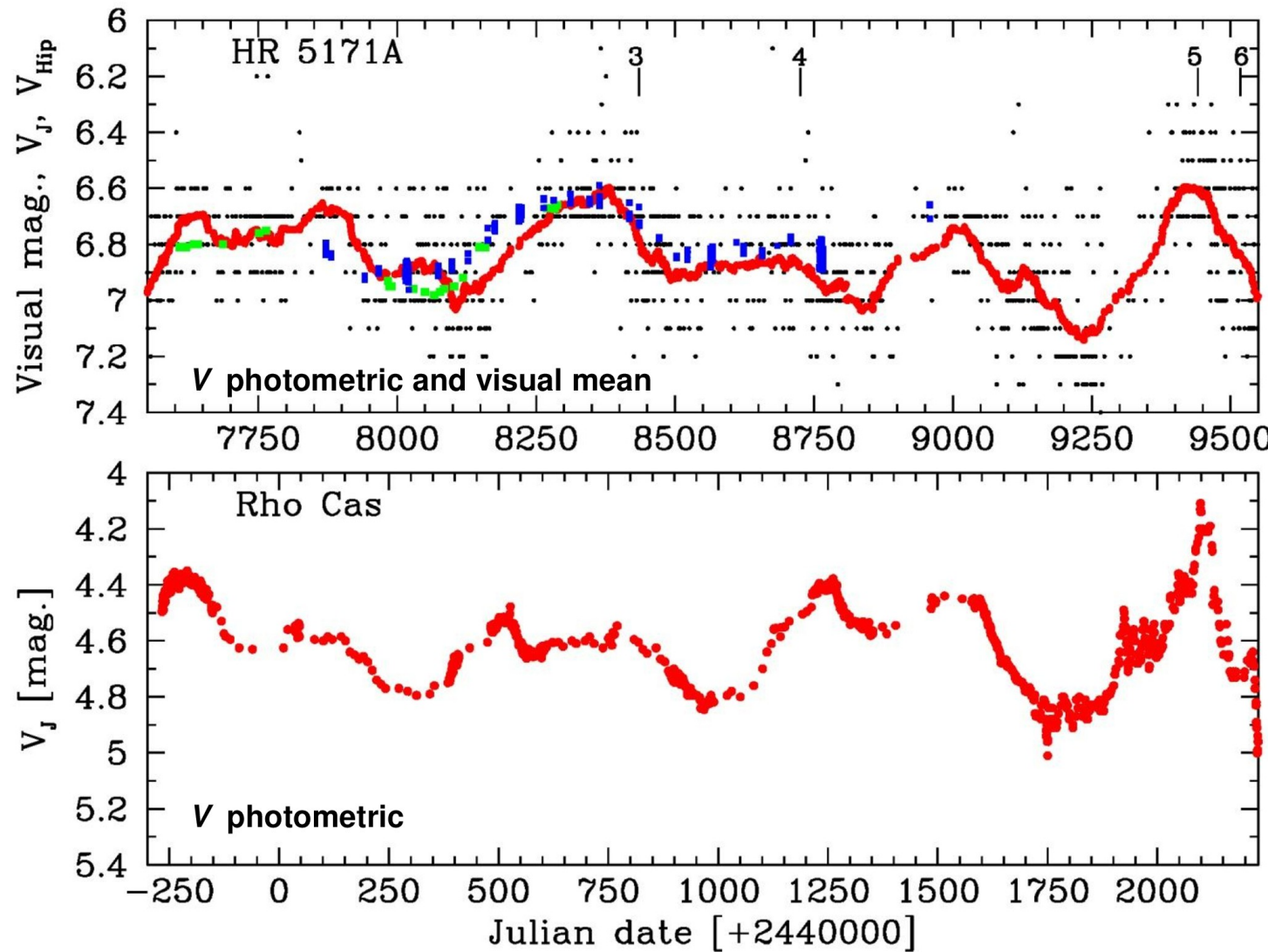
Alpha Ori M2 Iab

T_{eff} = 3500 K Log g = - 0.5

R* = 700 R \odot L* = 40,000 L \odot

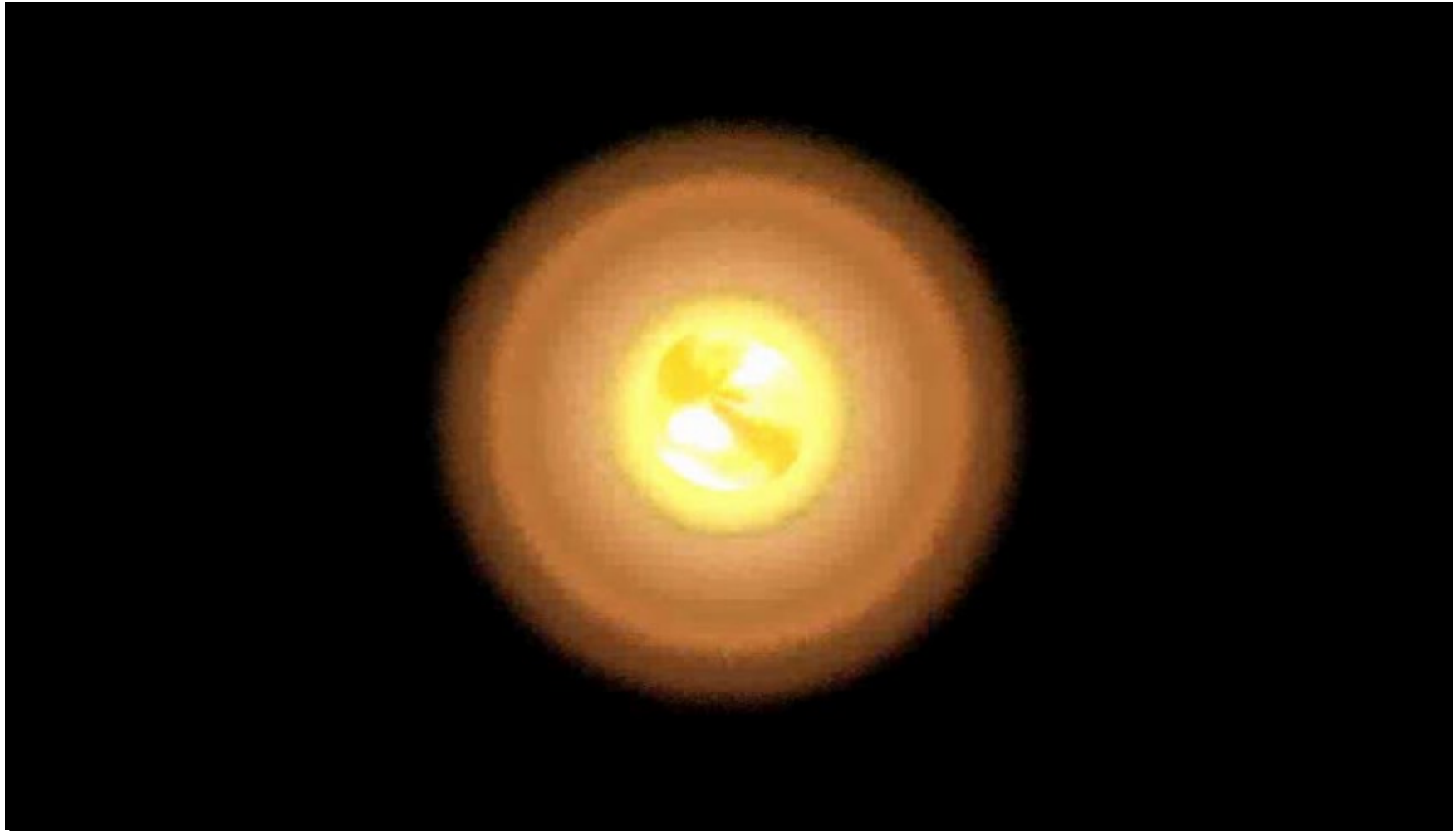


V brightness curves of YHGs Rho Cas and HR 5171



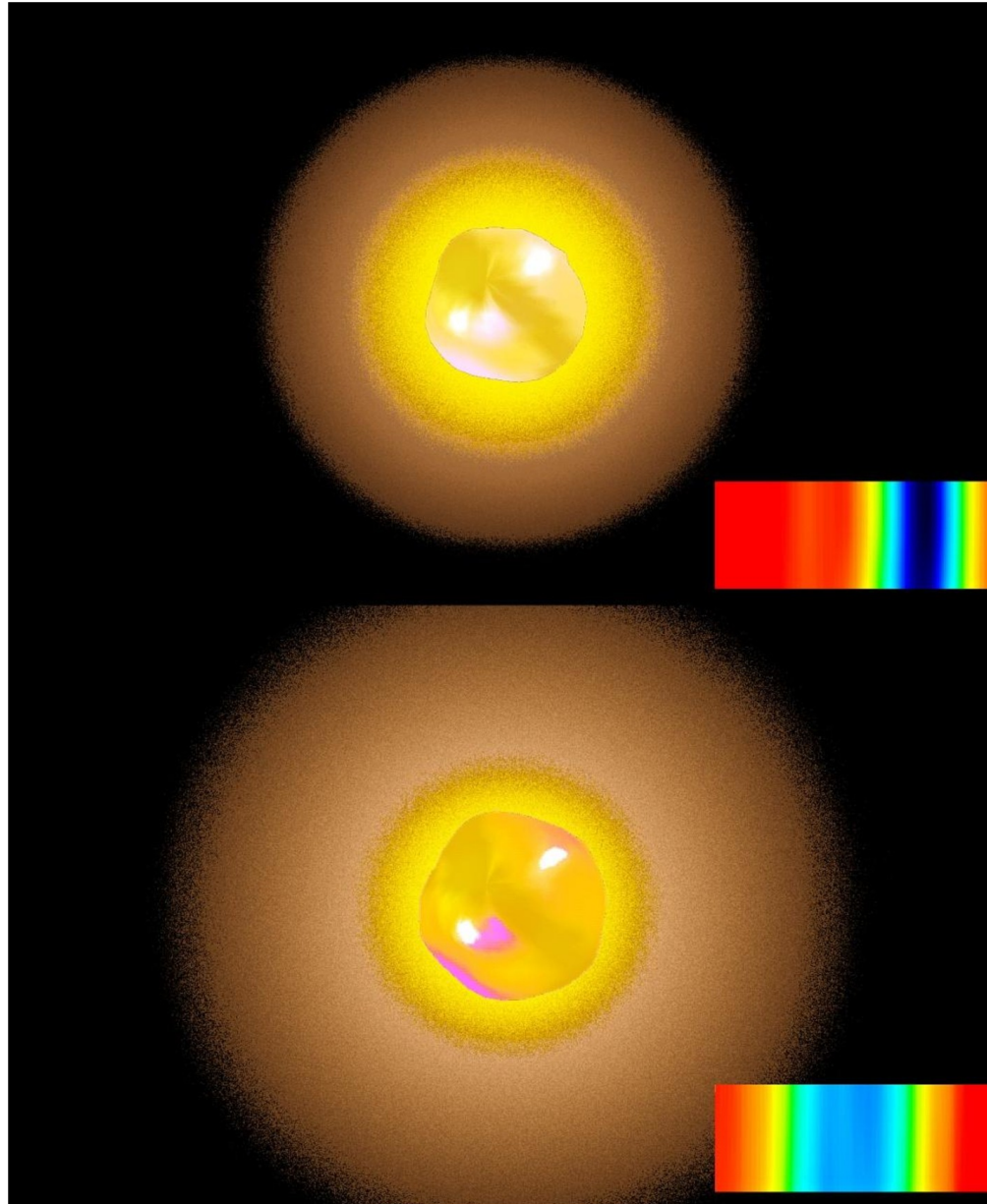
- Quasi-periodic V -variability over several years with $P_q = 240 \text{ d} - 520+\text{ d}$.
- V lightcurve amplitudes of $0^m.2$ to $0^m.5$ due to atmospheric pulsations.
- V lightcurve can occasionally resemble RV Tau stars with double minima.
- V amplitudes can decrease and increase over years and result in ... **outbursts**.

Quiescence Pulsations of Rho Cas



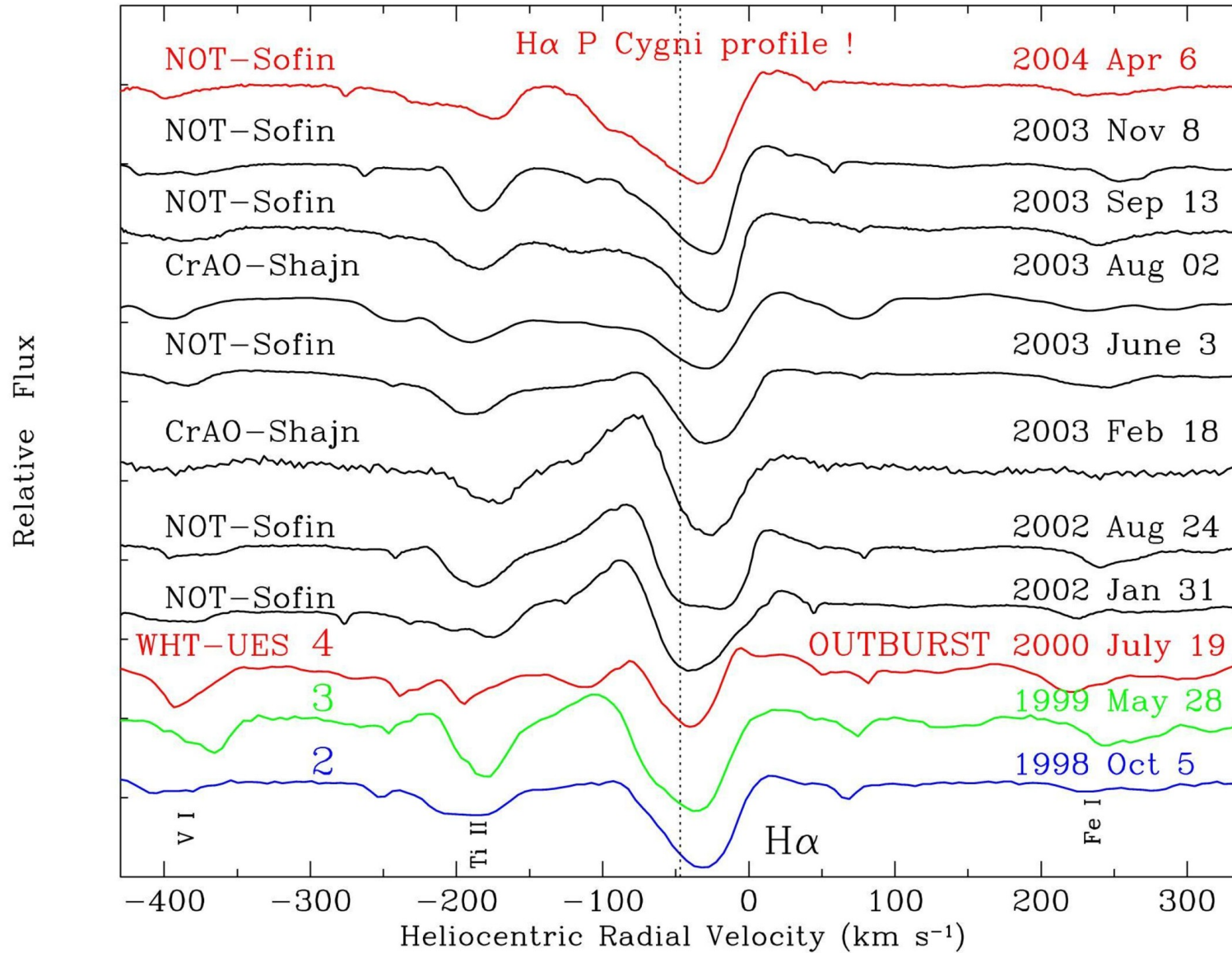
- Atmospheric pulsations show velocity stratification in metal vs. H α lines.
- Pulsations initiate large steady mass-loss rates of $\sim 10^{-5} M_{\odot}/y$.
- Non-radial pulsations in quiescence variability phases.
- Pulsations are linked with strong convective movements and line broadening.

Quiescence Pulsations of Rho Cas



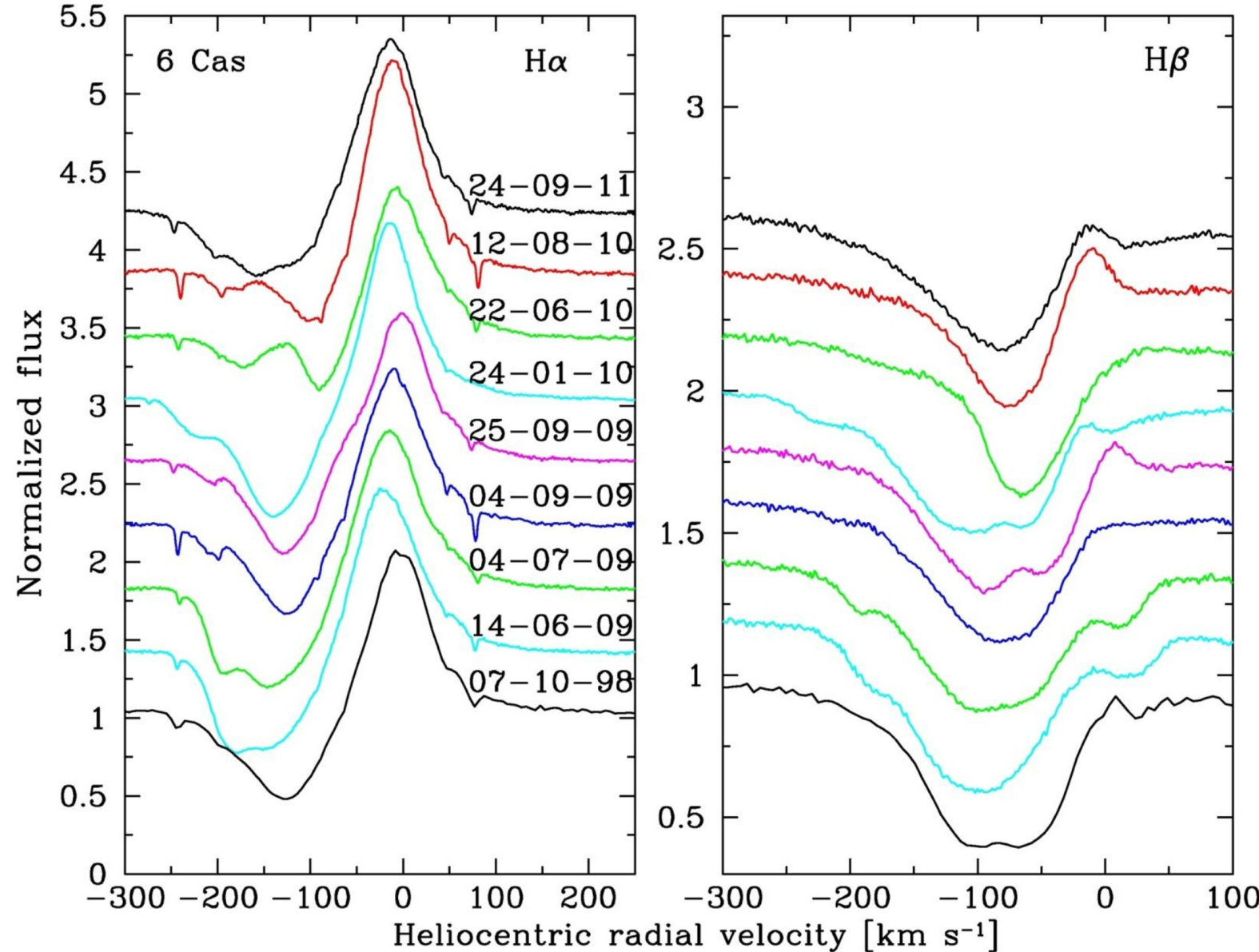
- Photospheric metal lines show strong Doppler shifts in absorption cores.
- V lightcurve follows and lags the radial velocity curve of metal lines.

Long-term H α line variability in Rho Cas



- Strong H α profile variability due to variable mass-loss & extended-wind opacity.
- H α line monitoring reveals P Cyg and inverse P Cyg profiles over years.
- H α absorption very weak during 2000 outburst due to very strong Teff decrease.

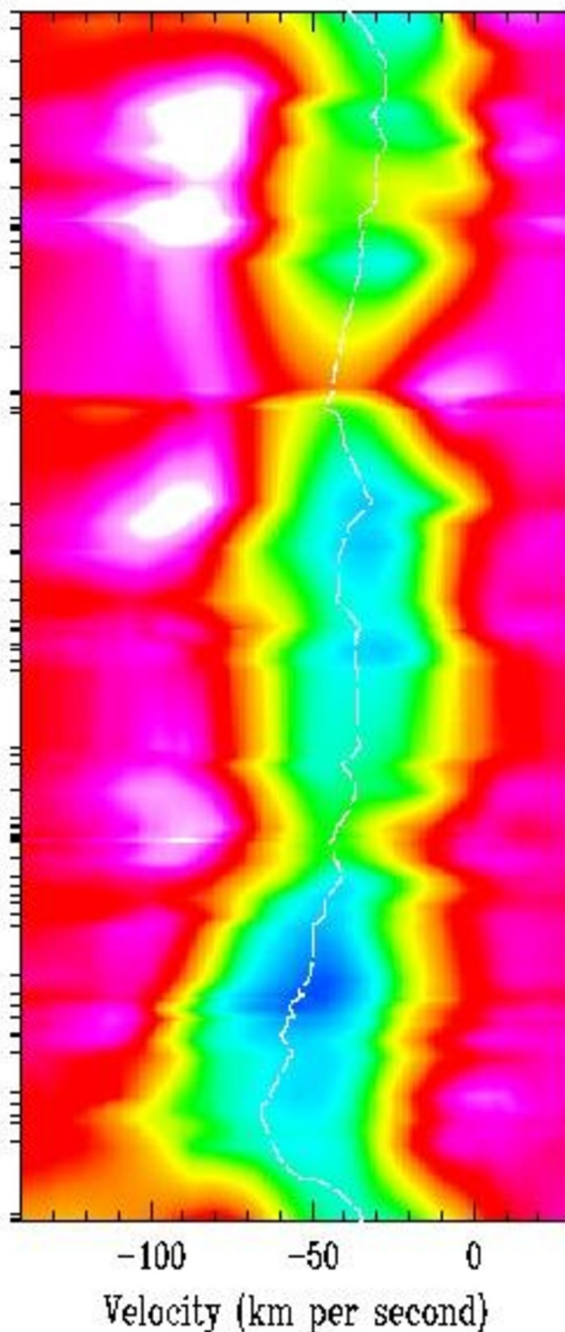
Long-term H Balmer lines variability in YHG 6 Cas



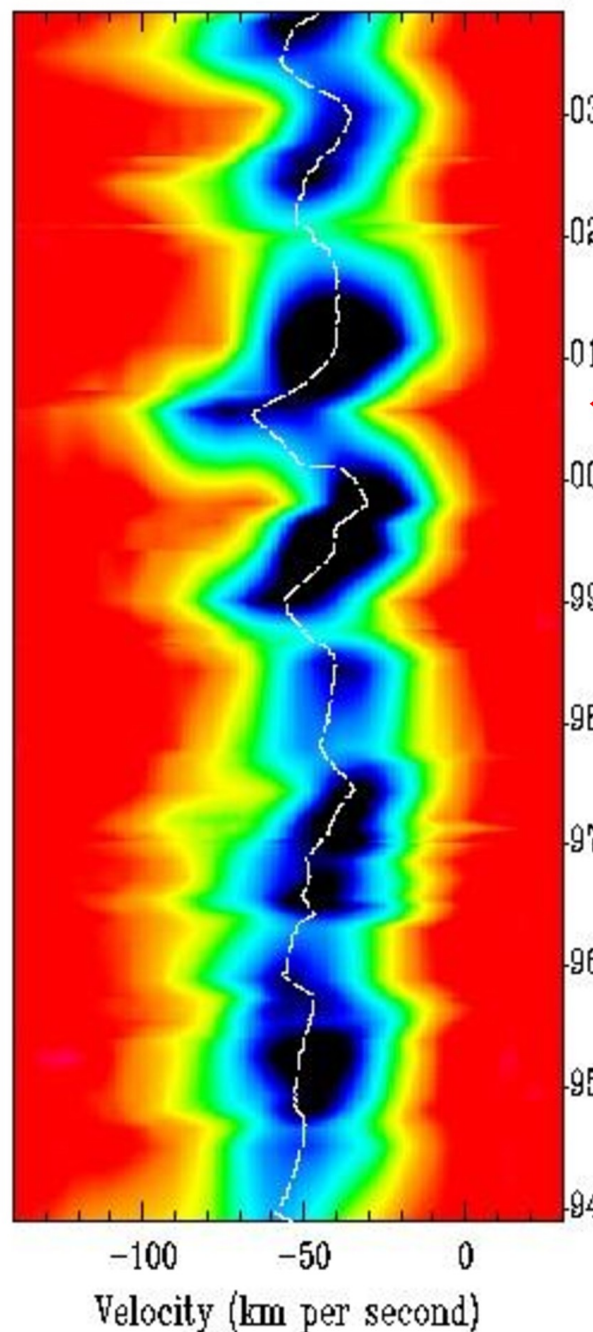
- H α P Cyg and H β profile variability in 6 Cas due to atmospheric pulsations.
- 6 Cas is less luminous than Rho Cas with similarly large wind mass-loss rates.

Long-term Spectroscopic Monitoring of Rho Cas

H α

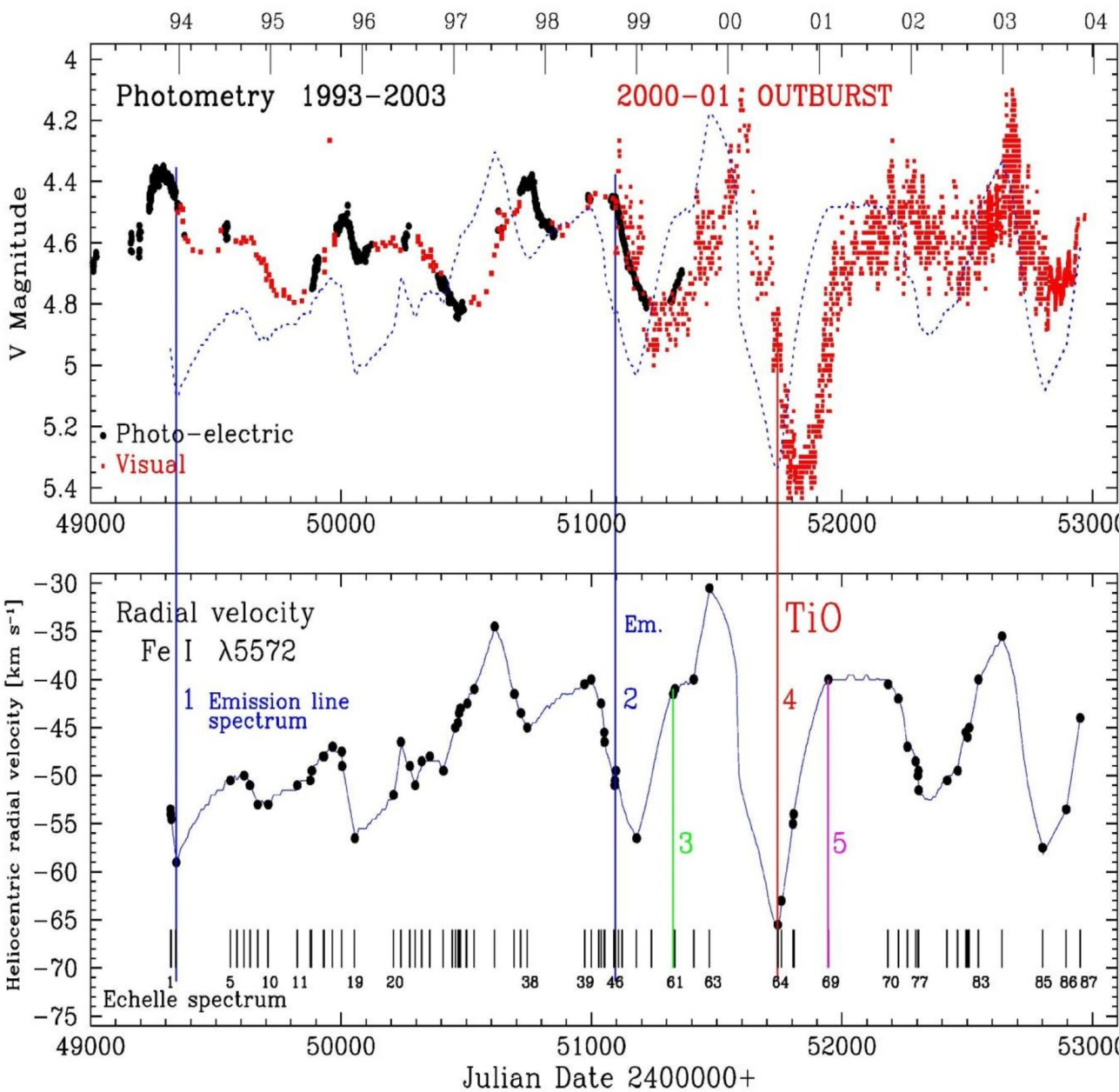


Fe I $\lambda 5572$



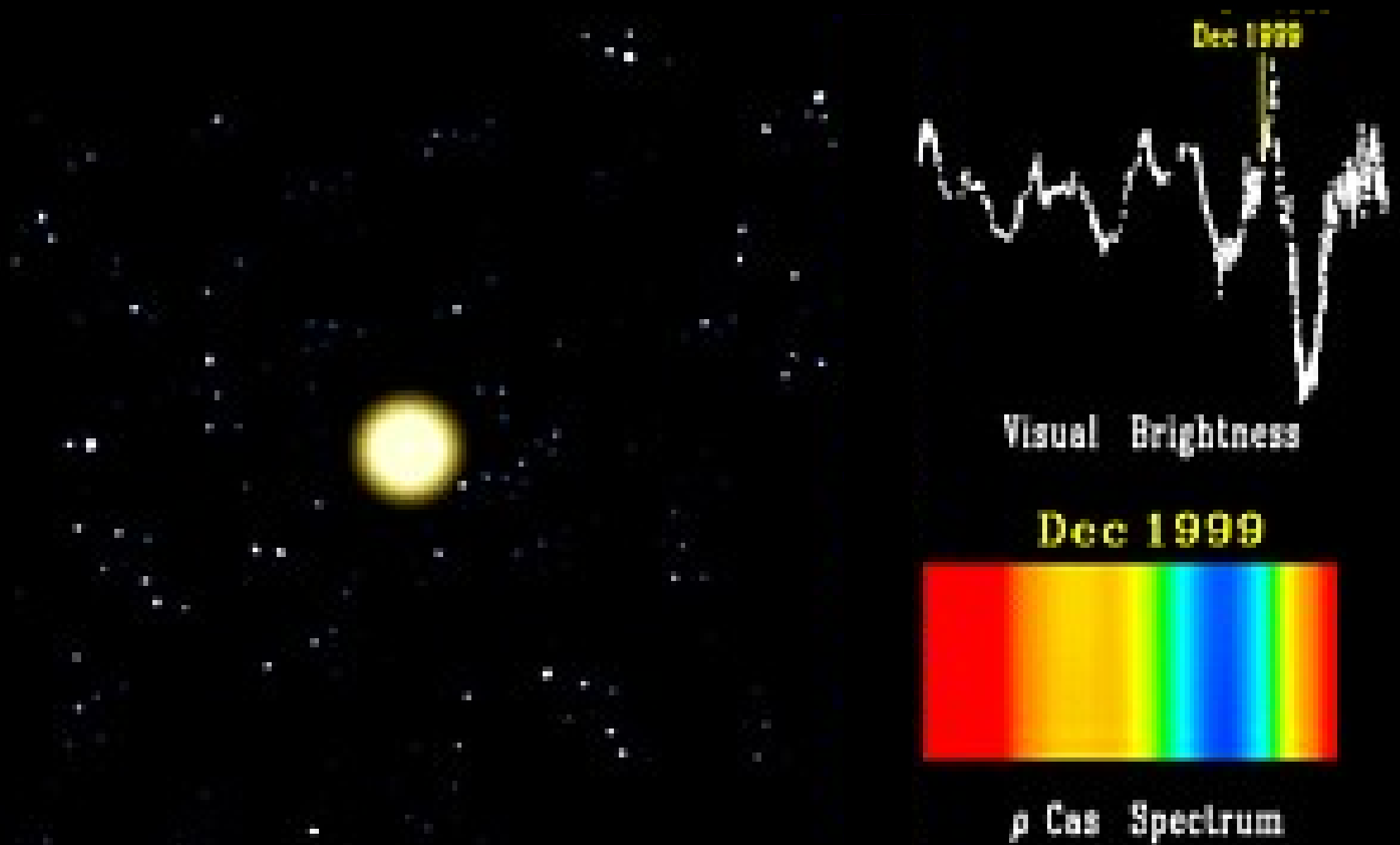
- Striking variability of photospheric lines with $P_q = 300$ to 500 d.
 - H α variability very different from photospheric metal lines.
- Millennium Outburst
ApJ 2003, 583, 923**
- H α line formation region more extended and velocity stratified compared to photospheric lines.
 - Yellow hypergiants have very broad abs. lines due to unusually strong broadening mechanism causing supersonic 'micro'- and 'macro'-turbulence velocity values.
 - Far violet extended wings develop in photospheric lines during outburst events related to strong radial pulsations with global cooling of entire atmosphere.

Millennium Outburst of Rho Cas

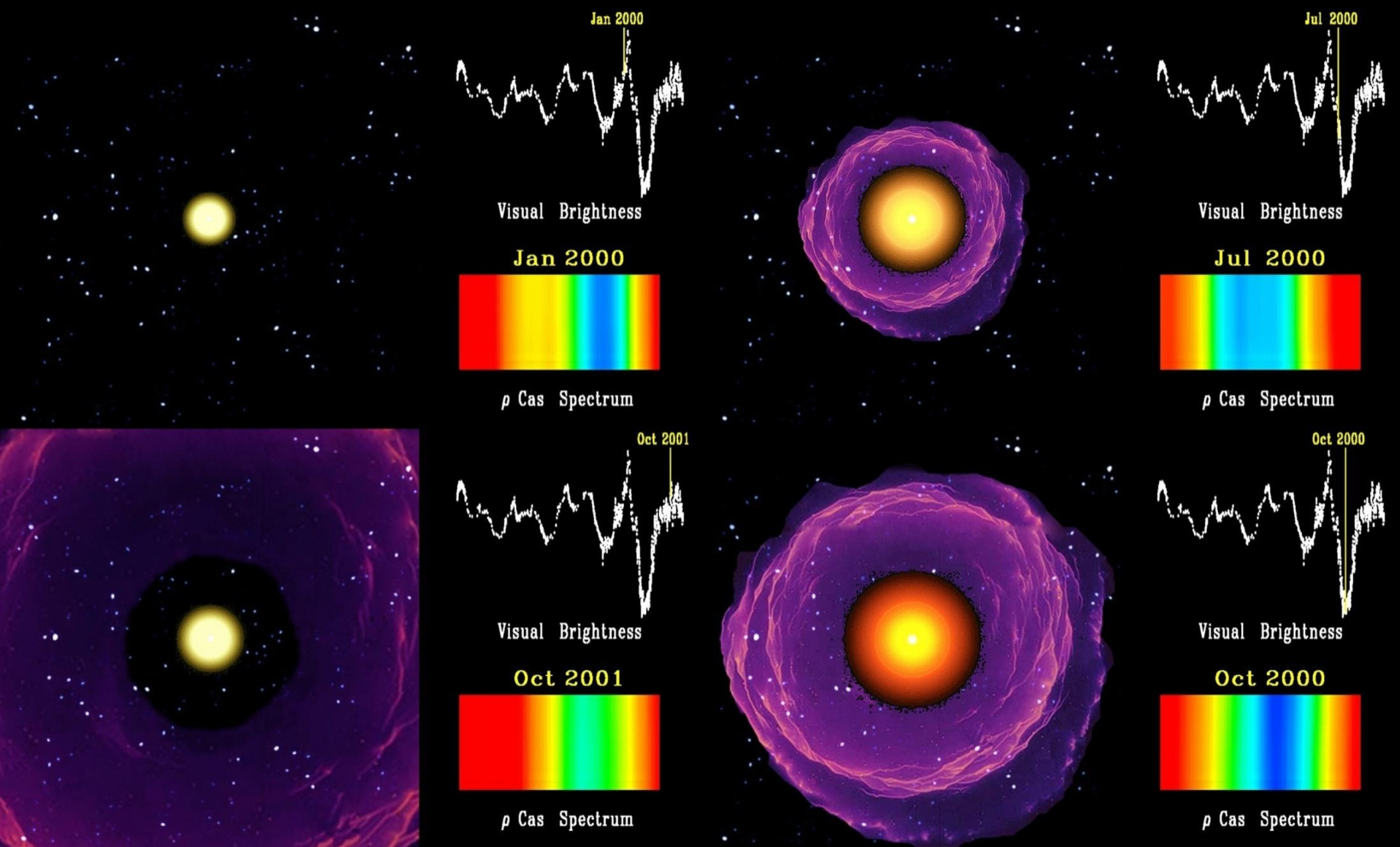


- Outburst related to very large amplitude of phot. V_{rad} curve with strong radial pulsation.
- V dims by 1.5 mag. in 200 d.
- T_{eff} decreases from ~ 7000 K to below 4000 K from RT modeling.
- Shell event with 35 ± 2 km/s observed in new TiO bands.
- \dot{M} increases from $\sim 10^{-5} M_{\odot}/\text{y}$ to $5.4 \cdot 10^{-2} M_{\odot}/\text{y}$.
- Total gas-mass expelled by shell event ~ 5 % of M_{\odot} from TiO bands and violet wings of phot. lines.
- Radiative line driving mechanism too weak and dust driving mechanism not efficient.
- Mechanical wind driving plays important role during outburst events.

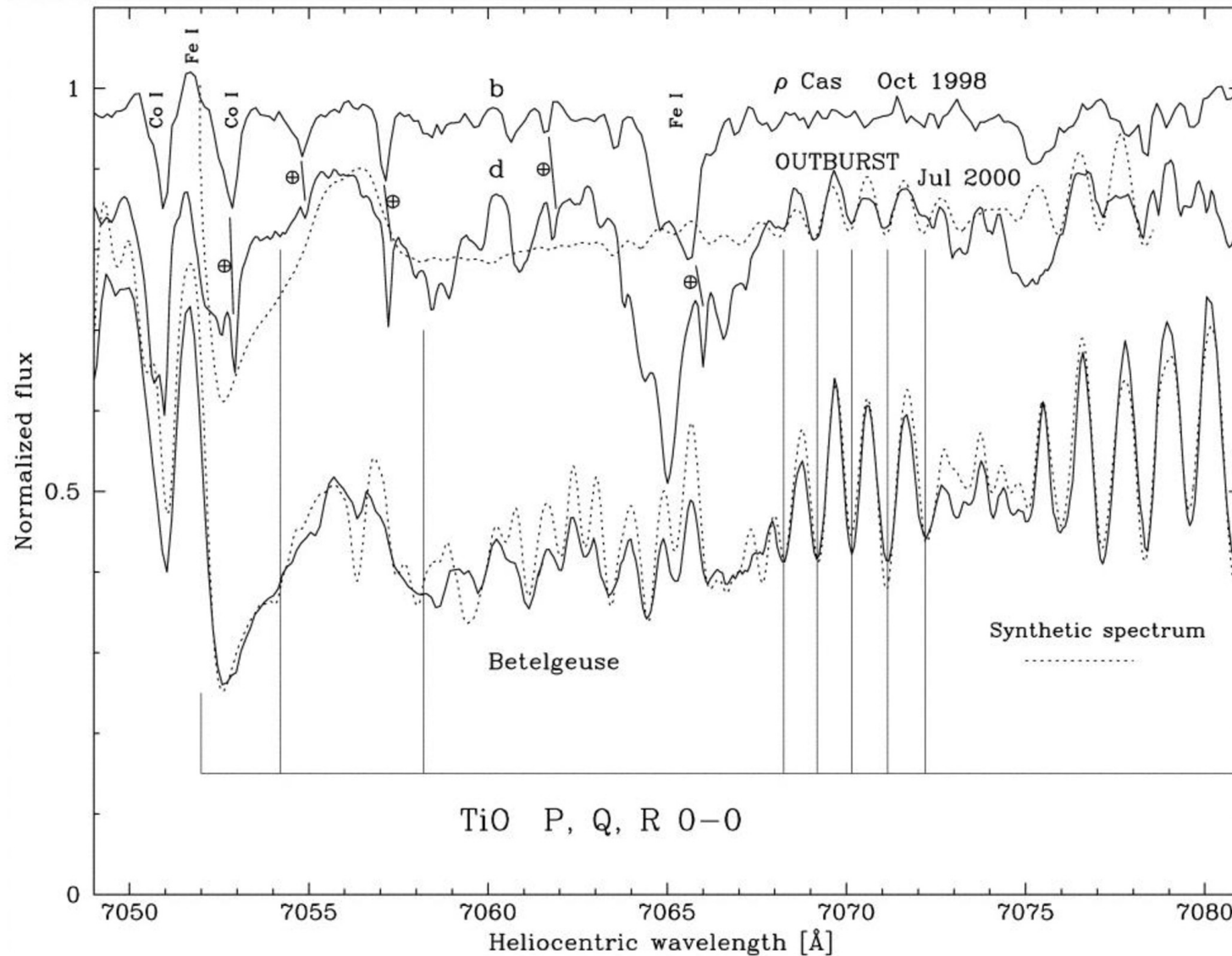
Millennium Outburst of Yellow Hypergiant Rho Cas



Millennium Outburst of Yellow Hypergiant Rho Cas

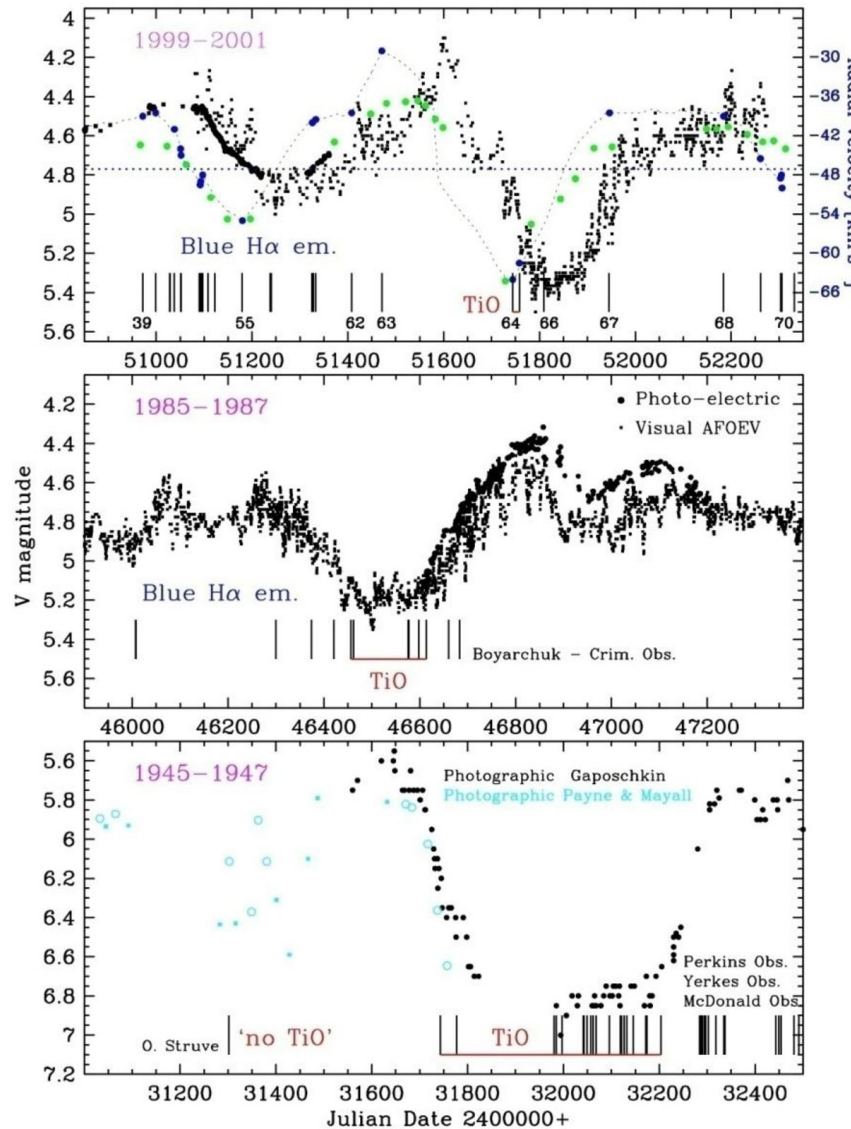


New TiO Bands in Brightness Minimum of Outburst



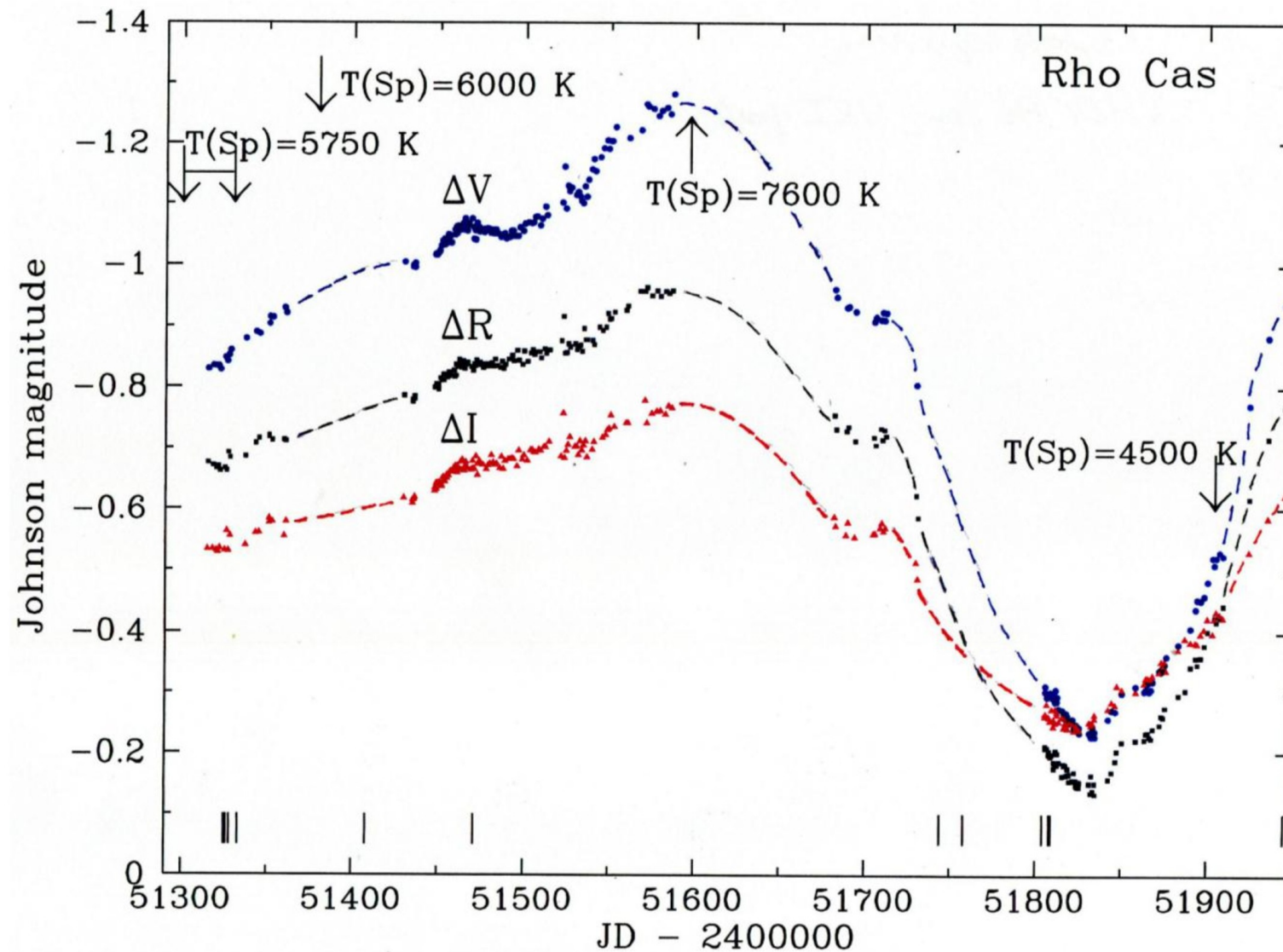
- Near-IR TiO bands appear during deep V brightness minimum, and vanish again.
- TiO bands are observed only in M-type stars (Betelgeuse) with $T_{\text{eff}} < 4000$ K.
- Line blue-shifts yields increase of mass-loss rate by factor >100 .
- Major mass-loss mechanism of YHG is due to punctuated mass-loss events.

Historical Outbursts and TiO in Rho Cas



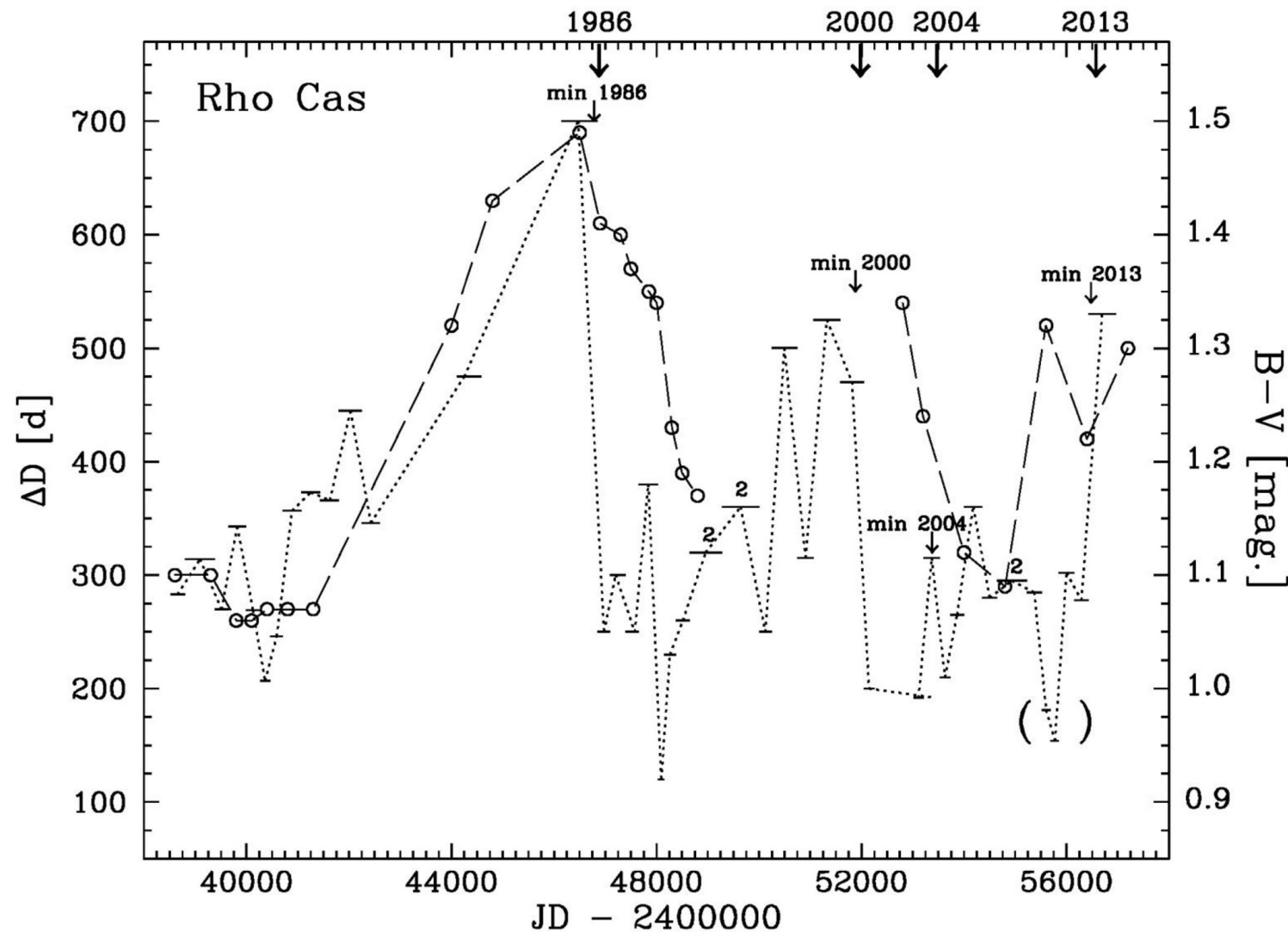
- **3 outbursts on record with spectroscopic observations in 1946, 1986, & 2000.**
- **New TiO bands appearance & disappearance observed in all 3.**
- **Strong blue H α emission (inverse P Cyg) in 1985 and 1999 signaling strong atm. contraction before outburst events.**

VRI Curves of Rho Cas Millennium Outburst



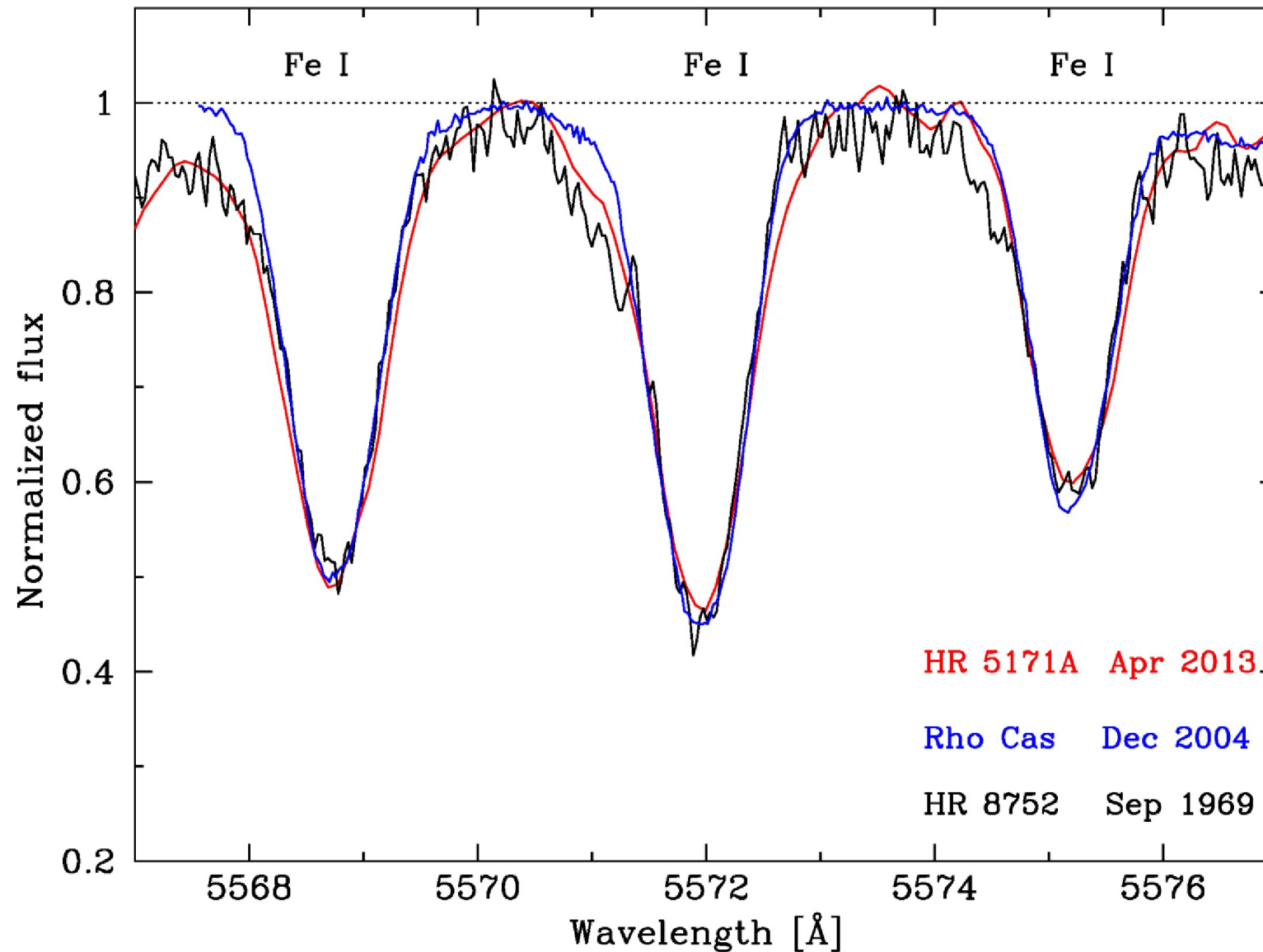
- Spectroscopic monitoring shows Teff decrease from 7600 K to below 4000 K.
- Outburst lasted \sim 1 year, with deep V minimum of \sim 150 d, and $\Delta V \sim 1^m.2$.
- VRI photometry curves show outburst is a global atmospheric cooling event.

Pulsation Period Changes and Outbursts in Rho Cas



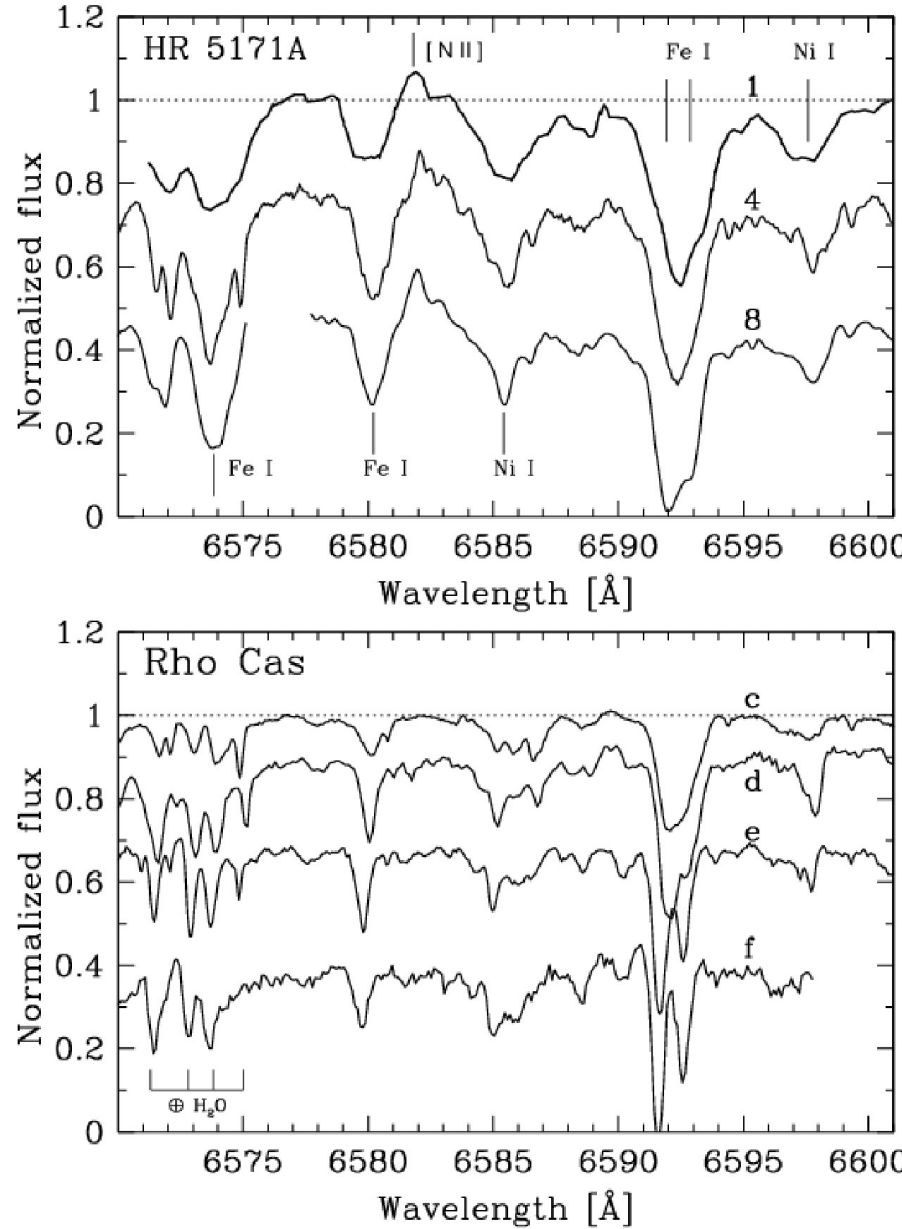
- Strong correlation of photometric variability period ΔD and outburst event.
- ΔD increase over decades until outburst, thereafter suddenly decrease.
- Also observed between 2009 and 2013 before 2013 dimming event.
- Ongoing research with A. van Genderen et al. (in prep.)

Spectroscopic Sisters Rho Cas, HR 5171A, HR 8752



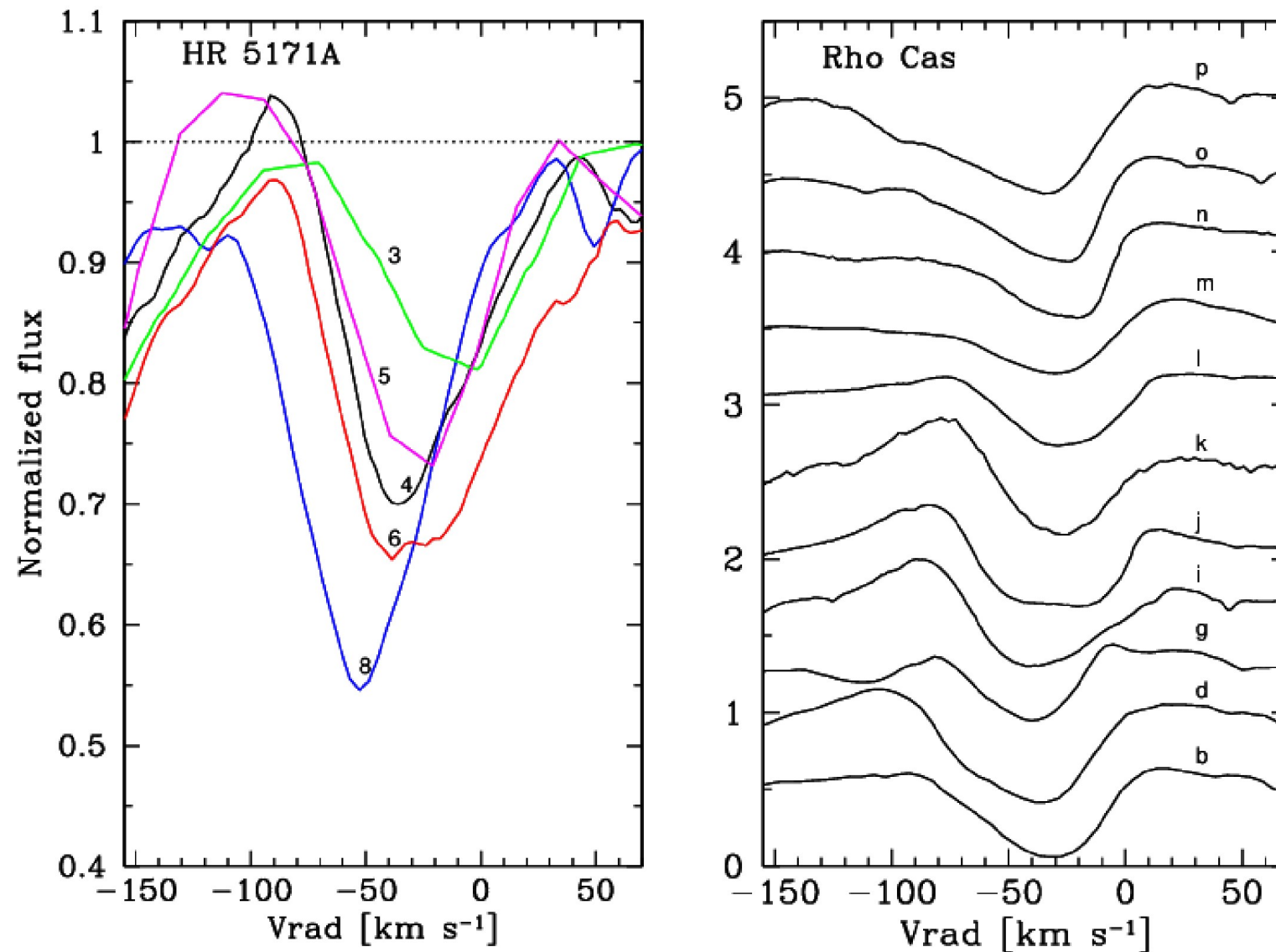
- Photospheric Fe absorption lines show same shapes and widths in 3 YHGs.
- Spectroscopic sister stars during epochs of similar Teff.
- Around AMBER observations HR 5171A spectroscopically identical to Rho Cas.

High-resolution spectra of Rho Cas and HR 5171



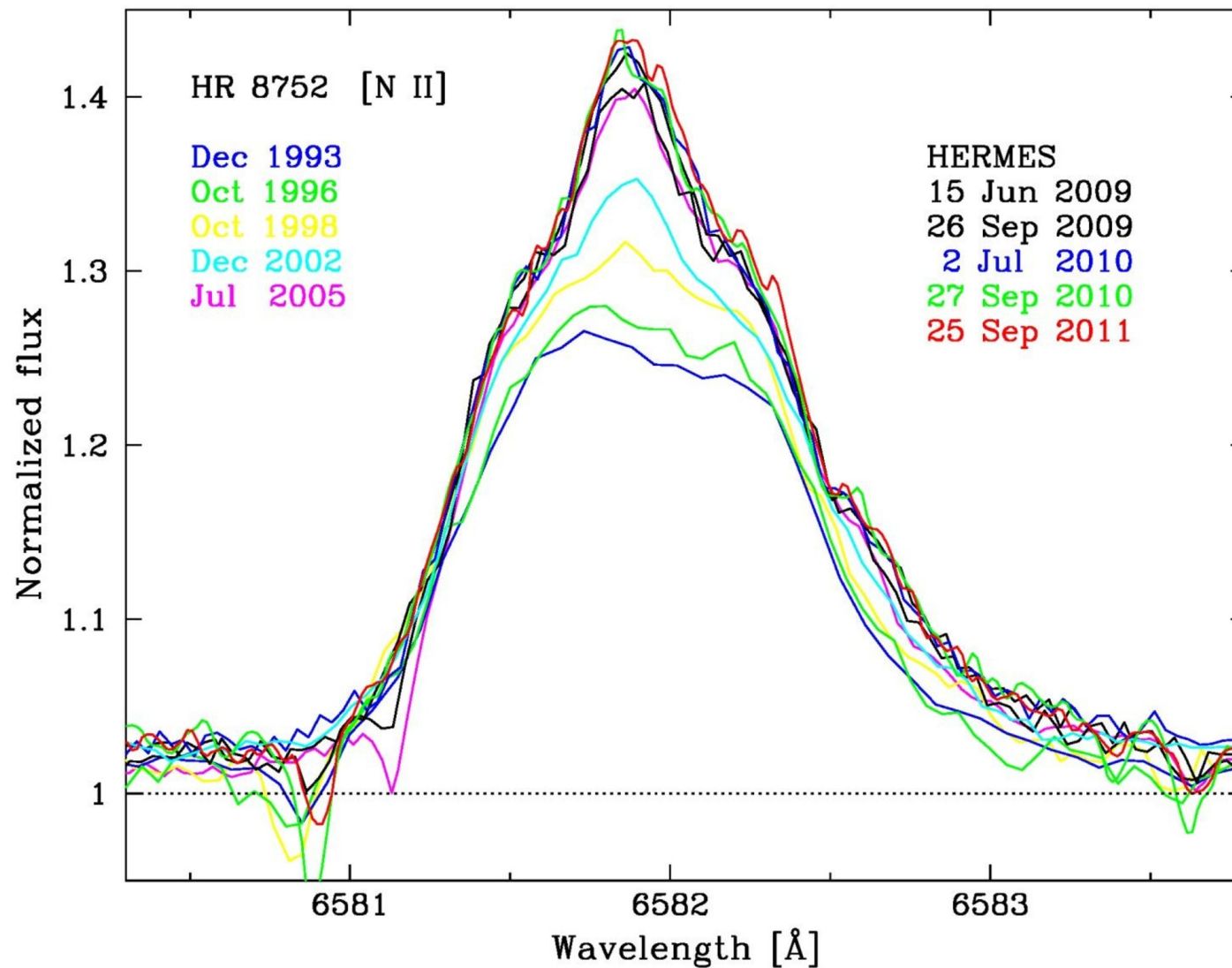
- Yellow Hypergiants show unusually broad photospheric absorption lines.
- Broad absorption lines are due to large microturbulence velocity & convection.
- Recurrent absorption line core splitting and emission line variability in Rho Cas.

Similarity of H α variability in HR 5171A and Rho Cas



- Detailed H α profile variability of HR 5171A is very similar to Rho Cas.
- H α forms in outer regions of extended dynamical atmosphere of YHGs.
- Unobserved H α line formation effects due to close companion in HR 5171A ?

Long-term [N II] emission line variability in HR 8752



- Binary system (YHG + B0) with 40% flux increase in [N II] line over ~20 years.
- Steady Teff increase of > 2000 K in ~40 years.
- HR 8752 currently late A-star (Nieuwenhuijen et al., A&A 2012).
- [Ca II] $\lambda 7323$ in HR 8752 and Rho Cas signal extended gas envelopes in YHGs.

Long-term Teff increase of YHG HR 8752

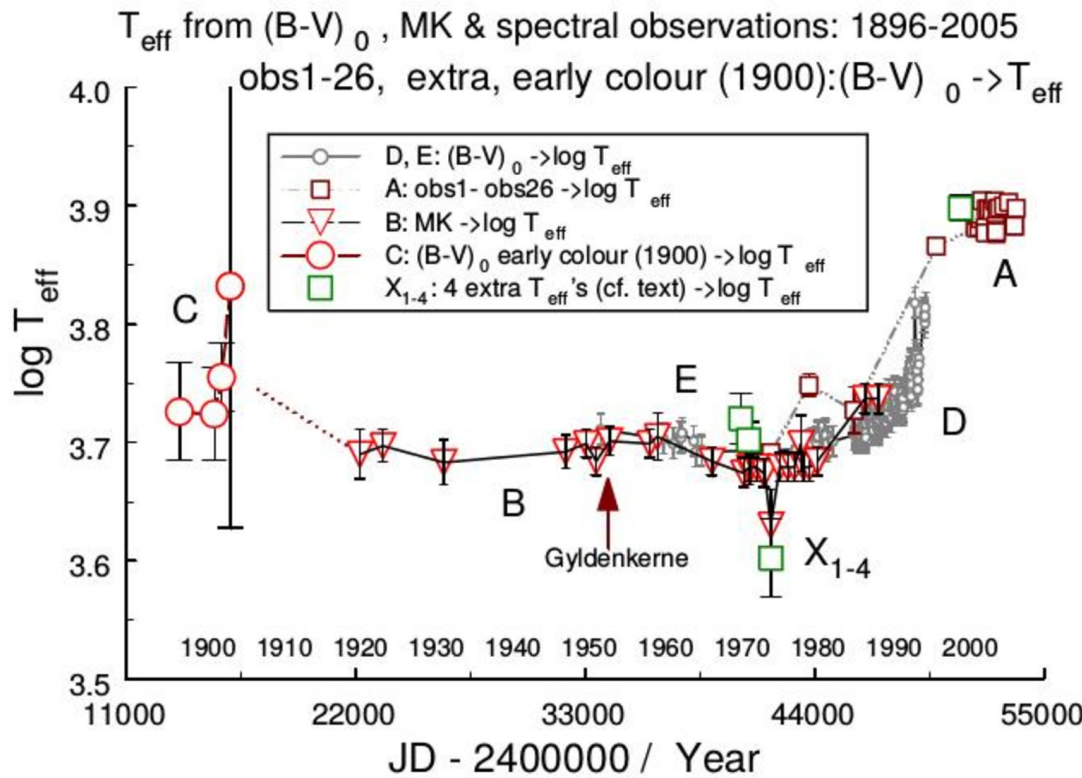
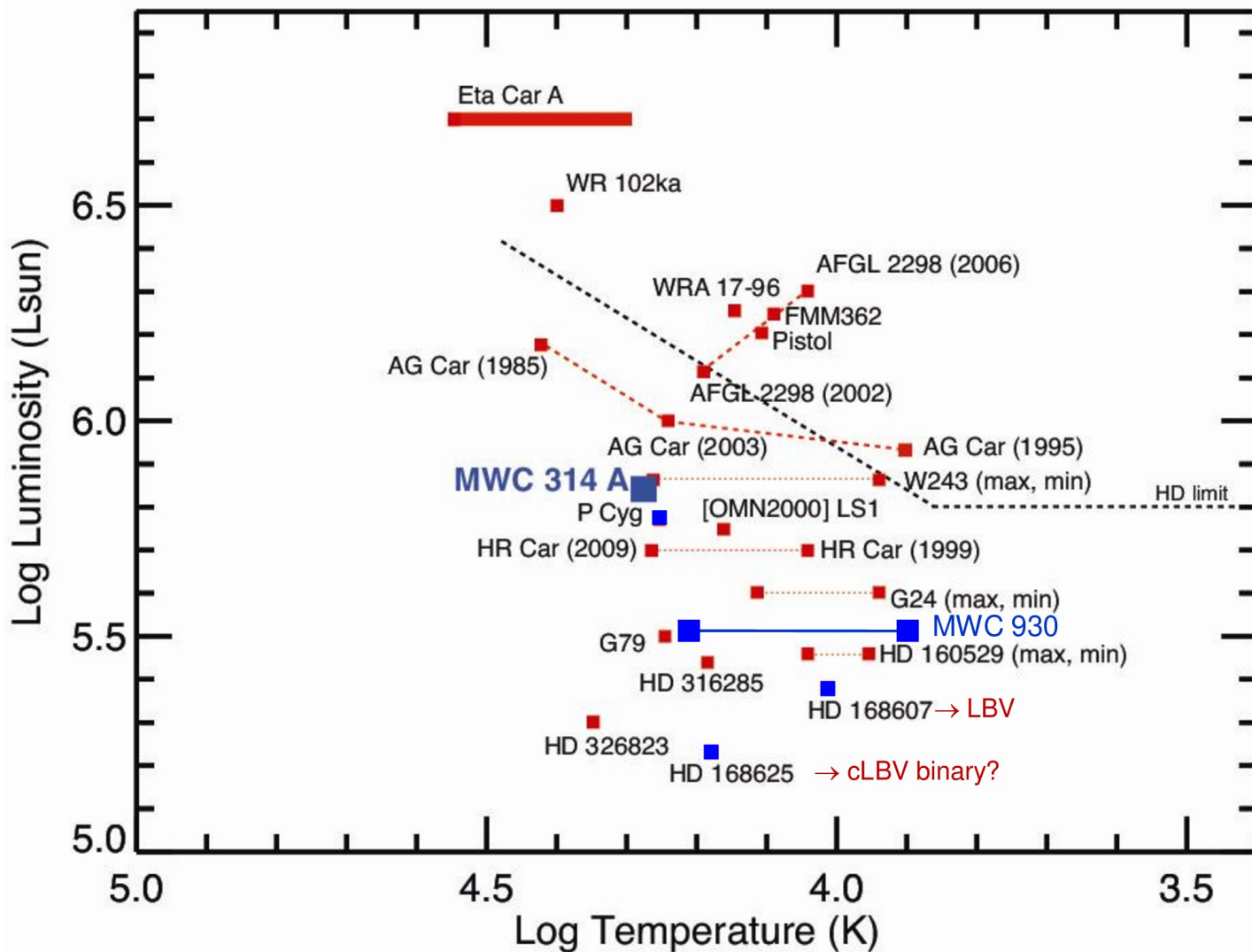


Fig. 10. Combination of the temperatures in one plot: from $B-V$ corrected for interstellar extinction, from $MK \rightarrow T_{\text{eff}}$, from obs1-obs26 (Section 2), and from some extra data (indicated by 'X' (X_{1-4}), cf. text). The temperatures derived from the $B-V$ and MK data combine reasonably well. The temperatures for obs1-obs2, obs4-obs6 also seem to follow the combined data, and the values for obs7-obs26 extend the data. The difference from obs2 is relatively large. This forms step 5.

- Teff increase over last 40 years from photometric and spectroscopic data.
- Superfast evolution of YHG on blueward track ?
- Or new phenomenon due to interaction of YHG atm. with B0-companion?

Modelling the asymmetric wind of LBV binary MWC 314

LBVs and candidate LBVs



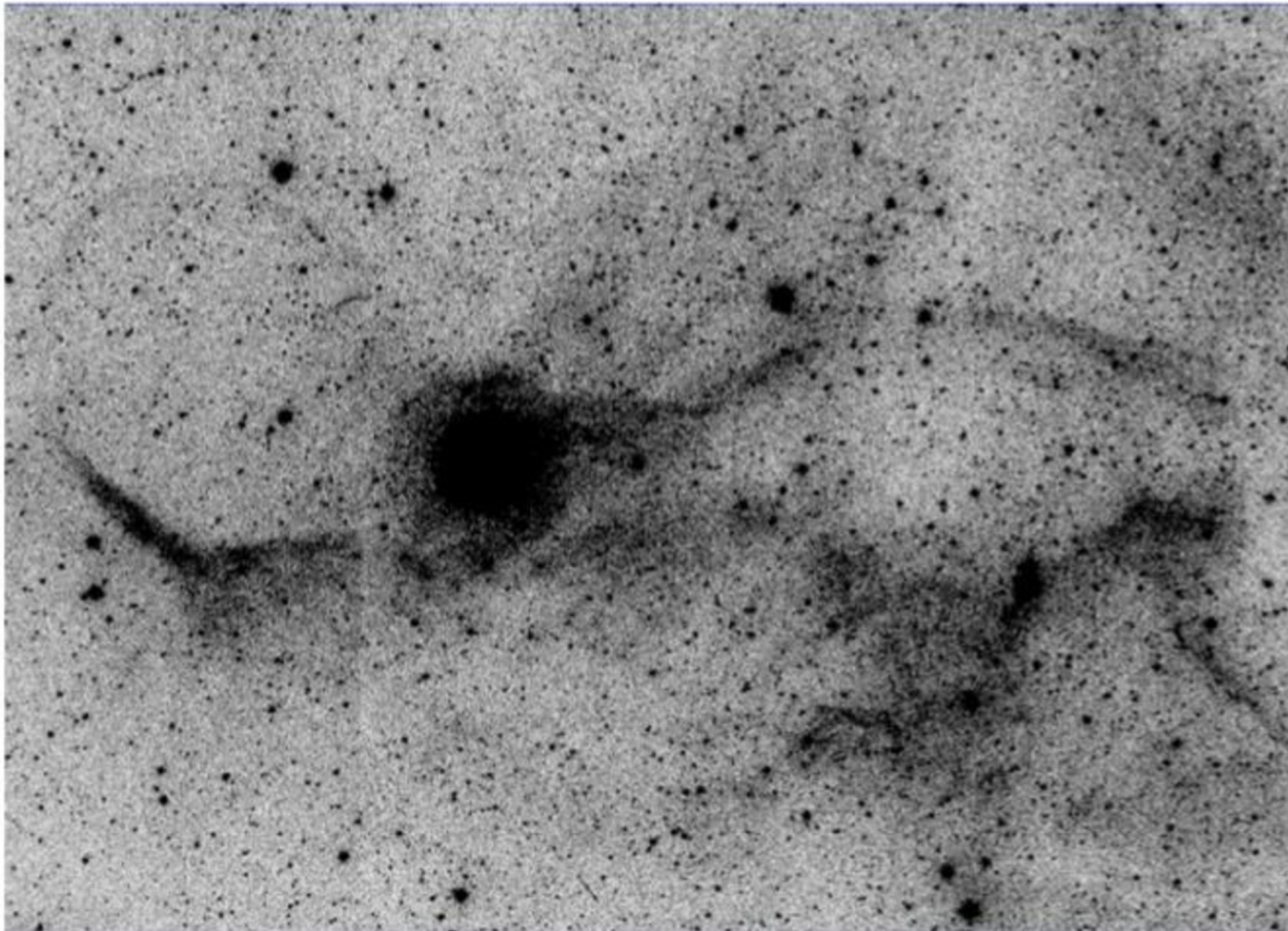
MWC 314 A
 $T_{\text{eff}} = 18000 \text{ K}$
 $\log g = 2.26$
 $\log L_{\star} / L_{\odot} = 5.8$
 $\dot{M} = 3 \cdot 10^{-5} M_{\odot} / \text{yr}$

Mercator-HERMES long-term spectroscopic monitoring 2009-2023

Bi-polar H α nebula of MWC 314

A. P. Marston and B. McCollum: Extended shells around B[e] stars

197



(Marston & McCollum
A&A, 2008)

Very large bi-polar H α
nebula formed 10^5
years ago.

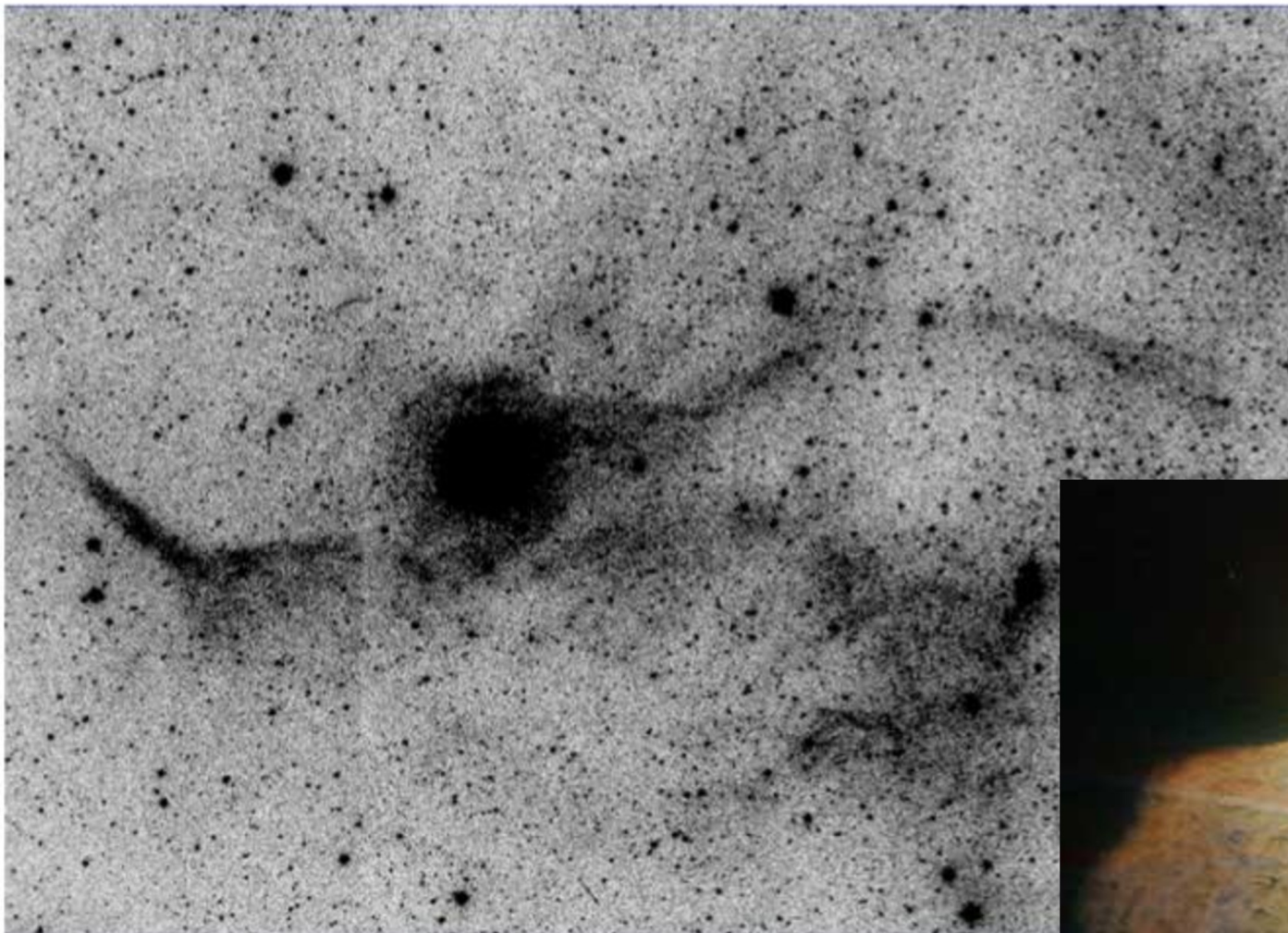
Giant eruption in LBV
phase?

Fig. 1. Narrow band H α image of the environments of MWC314 showing the large east-west bipolar feature around the star. The figure is 12'.5 vertically. For all figures, north is up and east to the left.

Bi-polar H α nebula of MWC 314

A. P. Marston and B. McCollum: Extended shells around B[e] stars

197



(Marston & McCollum
A&A, 2008)

η Carinae
LBV binary $P_{\text{orb}} = 5.5$ yr

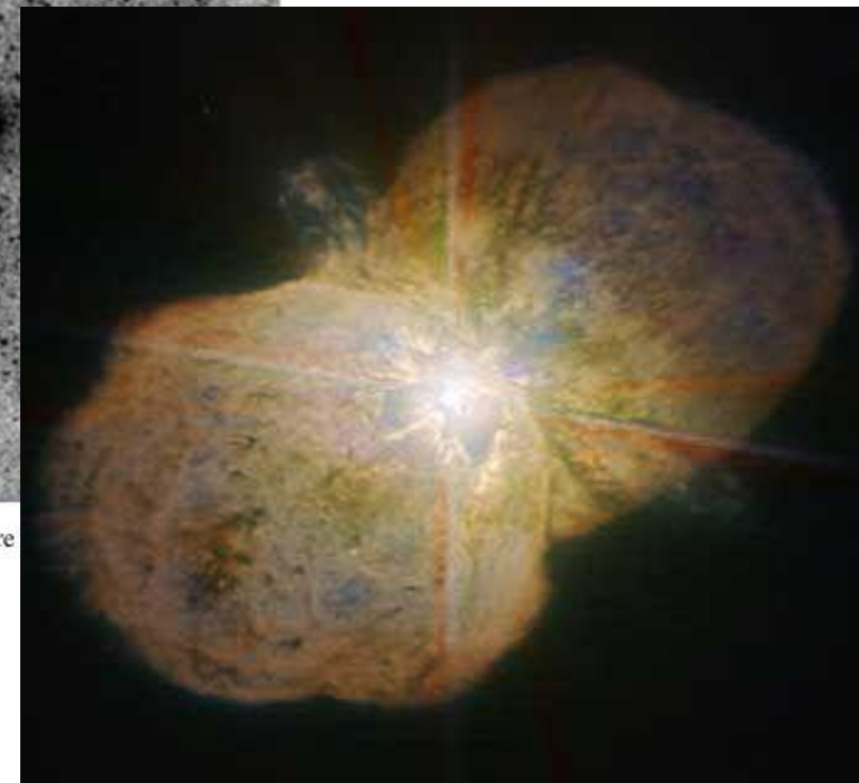
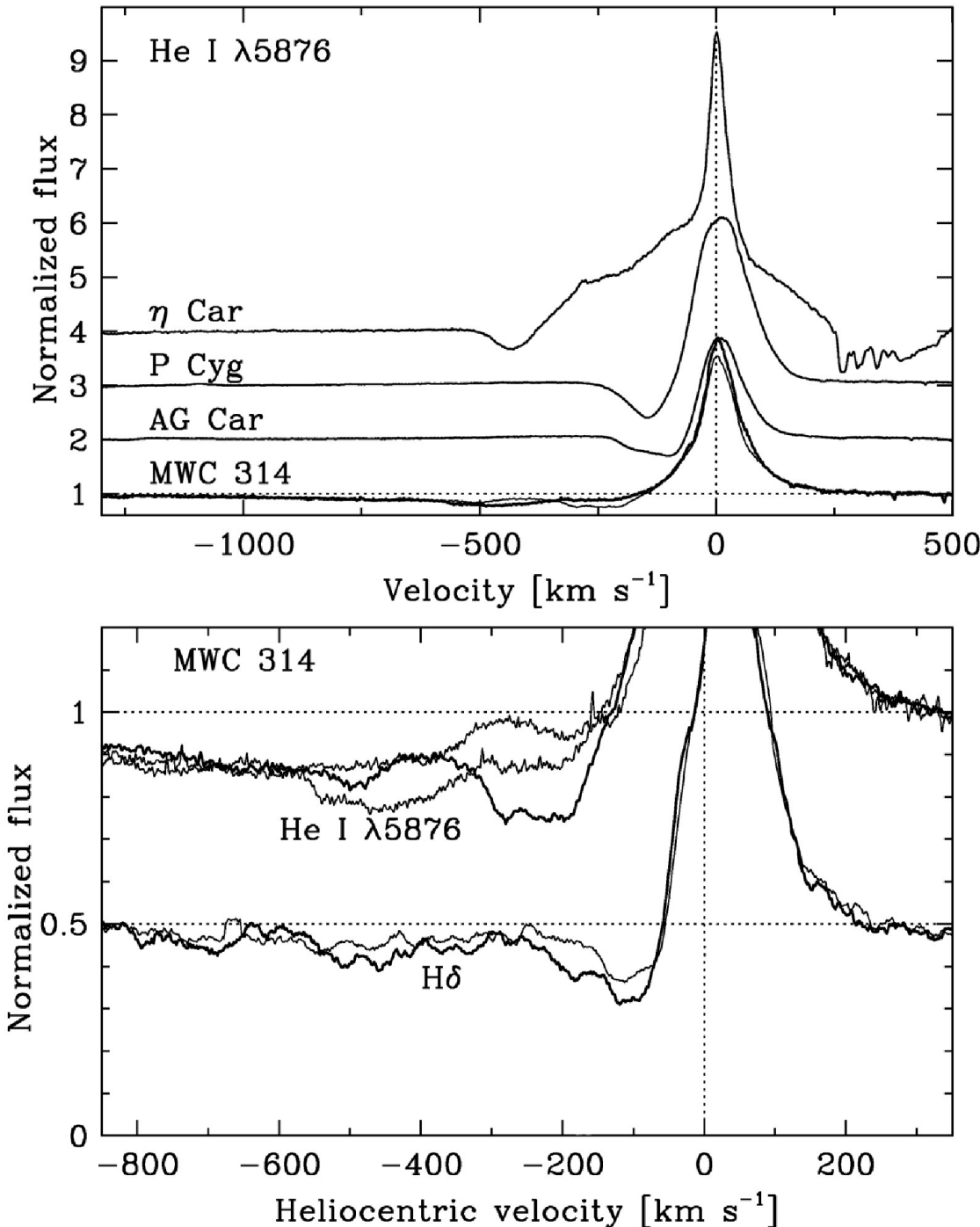


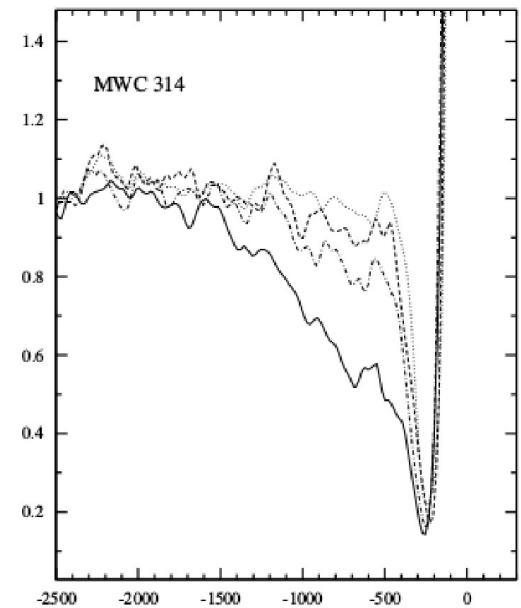
Fig. 1. Narrow band H α image of the environments of MWC314 showing the large east-west bipolar feature 12'.5 vertically. For all figures, north is up and east to the left.

Comparison of He I $\lambda 5876$ in LBVs



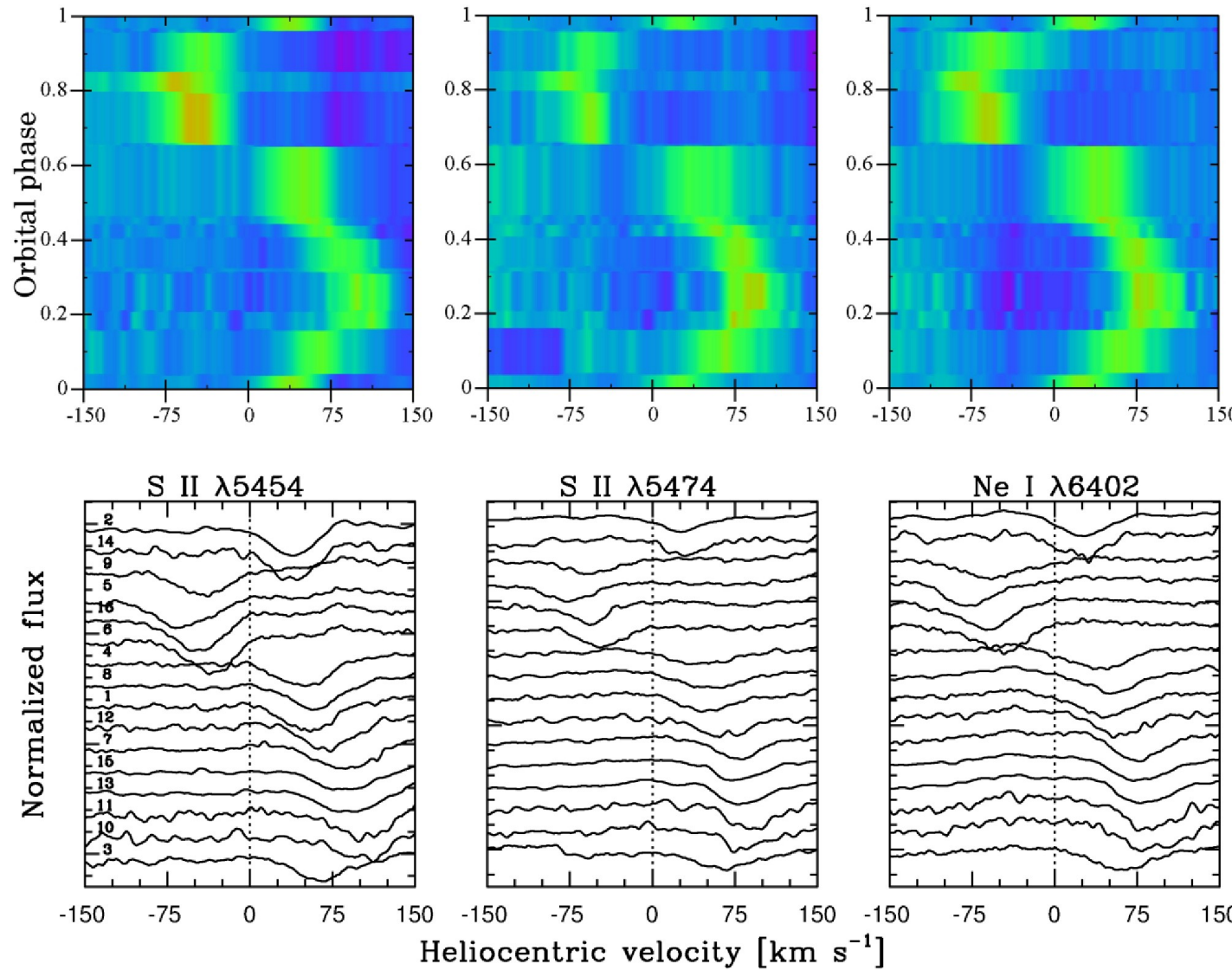
He I P Cyg profiles in
MWC 314 with $v_\infty > 1200$ km/s.

$v_\infty \sim 1500$ km/s in He I $\lambda 10830$
P Cyg line (Groh et al. A&A 2007)



Strong changes in absorption for
 $v_{wind} < 600$ km/s, we also observe
in the higher H lines.

Photospheric absorption lines with orbital phase

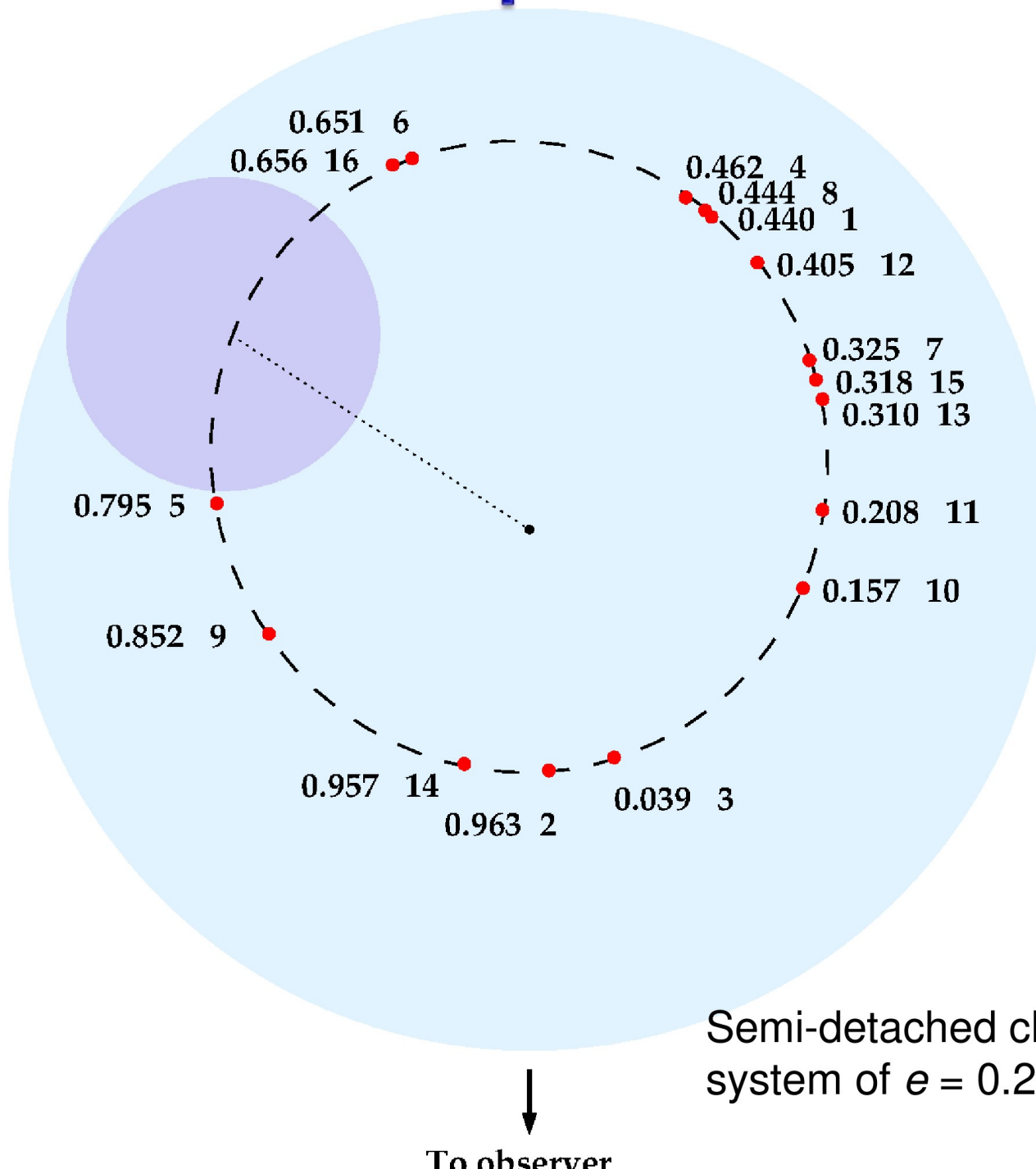


- S-wave observed in high-excitation absorption lines void of emission with amplitude of ~160 km/s. Caused by orbital motion of massive primary.

Observed orbital phases of MWC 314

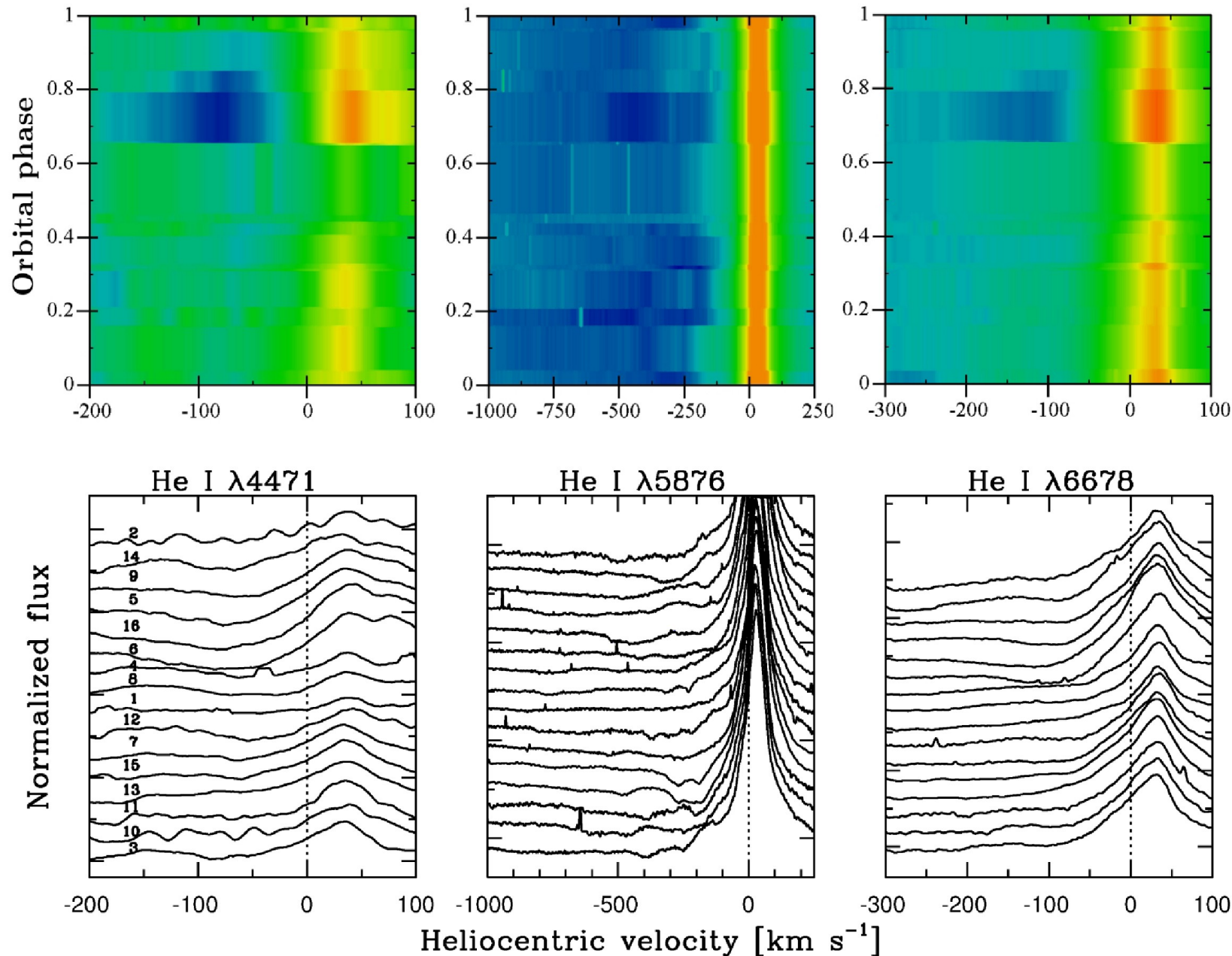
$$R_1 = 86 R_{\odot}$$

$$a = 262 R_{\odot}$$



Semi-detached close binary
system of $e = 0.23$, $P_{\text{orb}} = 2 \text{ m.}$

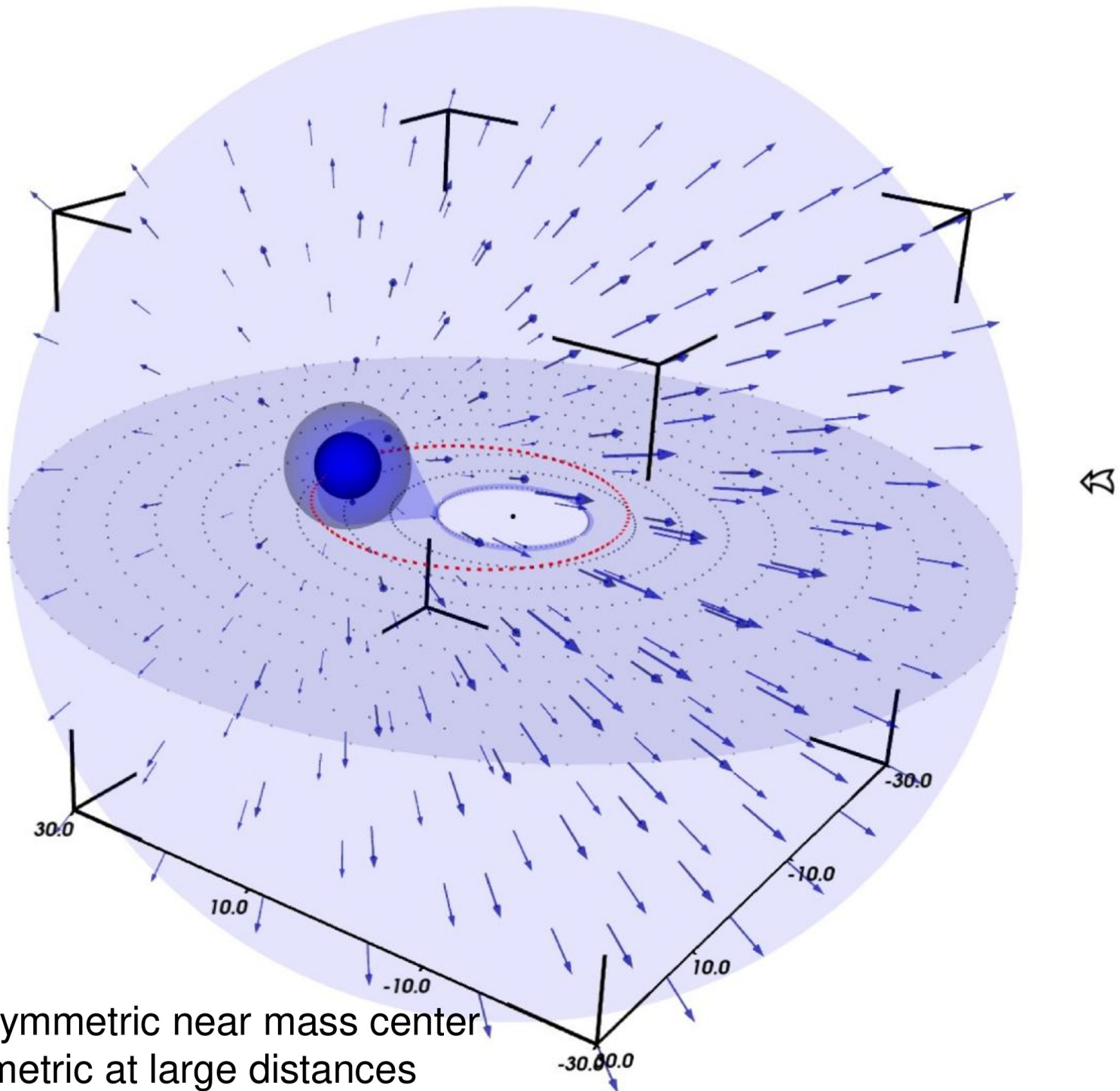
Orbital variability of He I lines in MWC 314



- All He I lines show orbitally modulated wind absorption.
- Maximum wind absorption at $\phi = 0.65 - 0.85$; max RV blueshift of primary

Asymmetric 3-D wind model of MWC 314

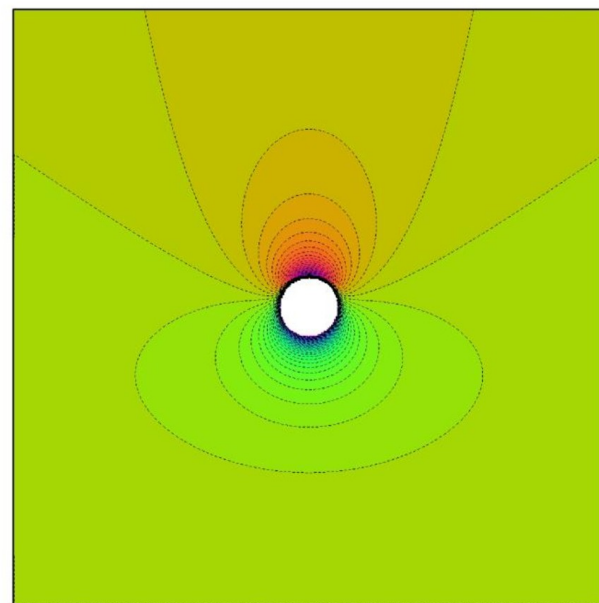
primary at apastron



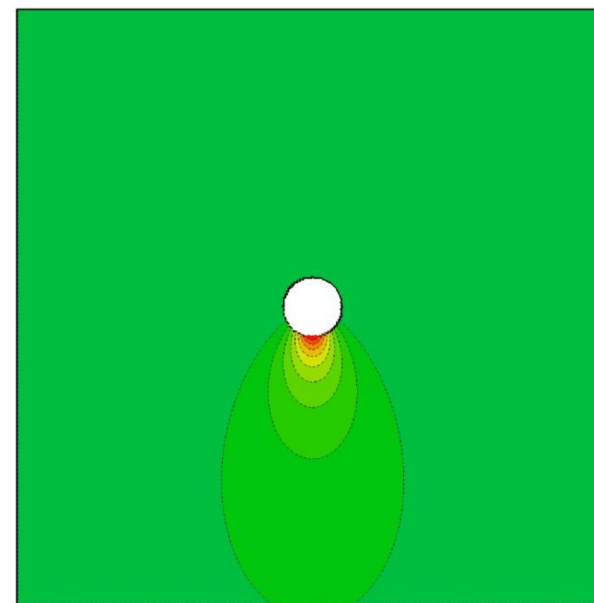
β -law wind model is asymmetric near mass center
and becomes symmetric at large distances

MWC 314 asymmetric expanding wind model

$\mathbf{v}_{\text{wind}} - \mathbf{v}_{\text{sm}}$

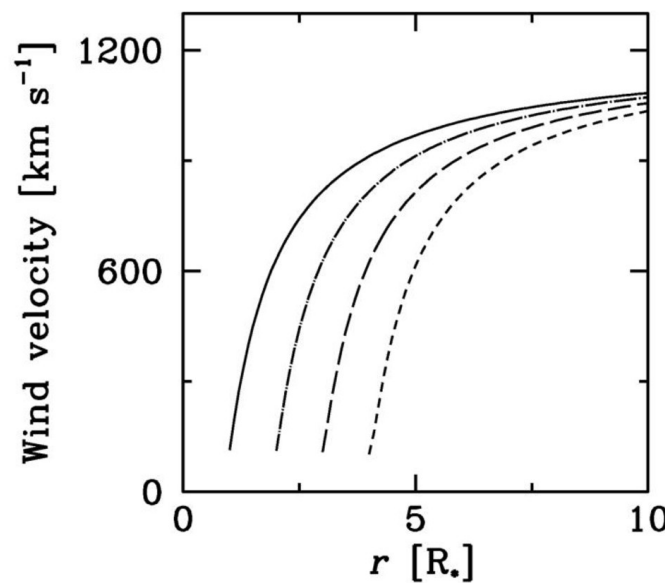


ρ / ρ_{sm}

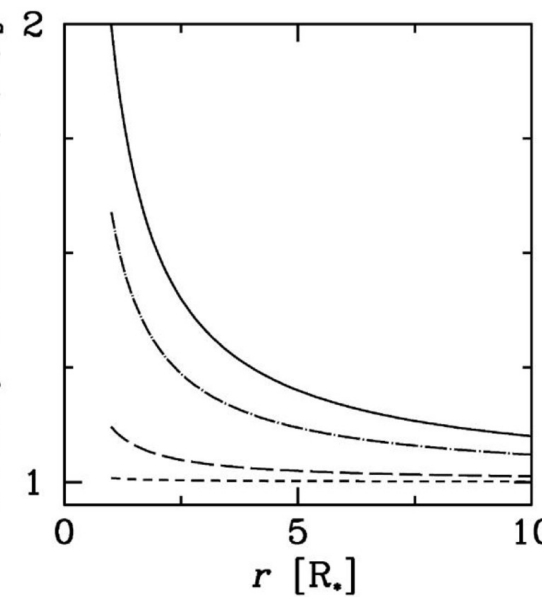


opening angle = $\pi / 4$

\mathbf{v}_{wind}

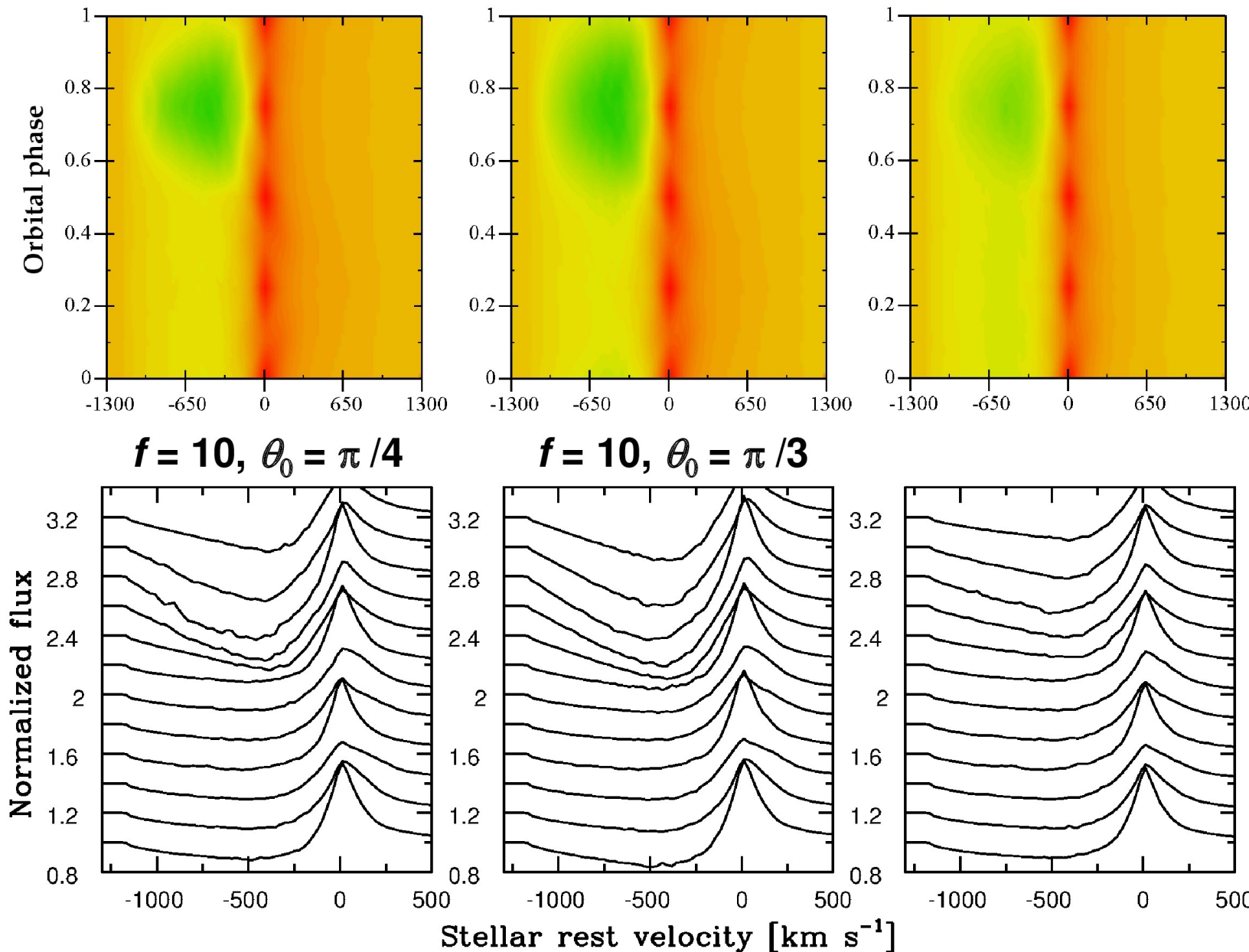


Density contrast ρ / ρ_s



- Parametrized 3-D wind velocity & density model around primary star.
- Wind density enhancement of $\rho / \rho_{\text{sm}} \sim 3.3$ in front of the primary's orbit.

Wind3D RT fit to He I $\lambda 5876$ orbital variability



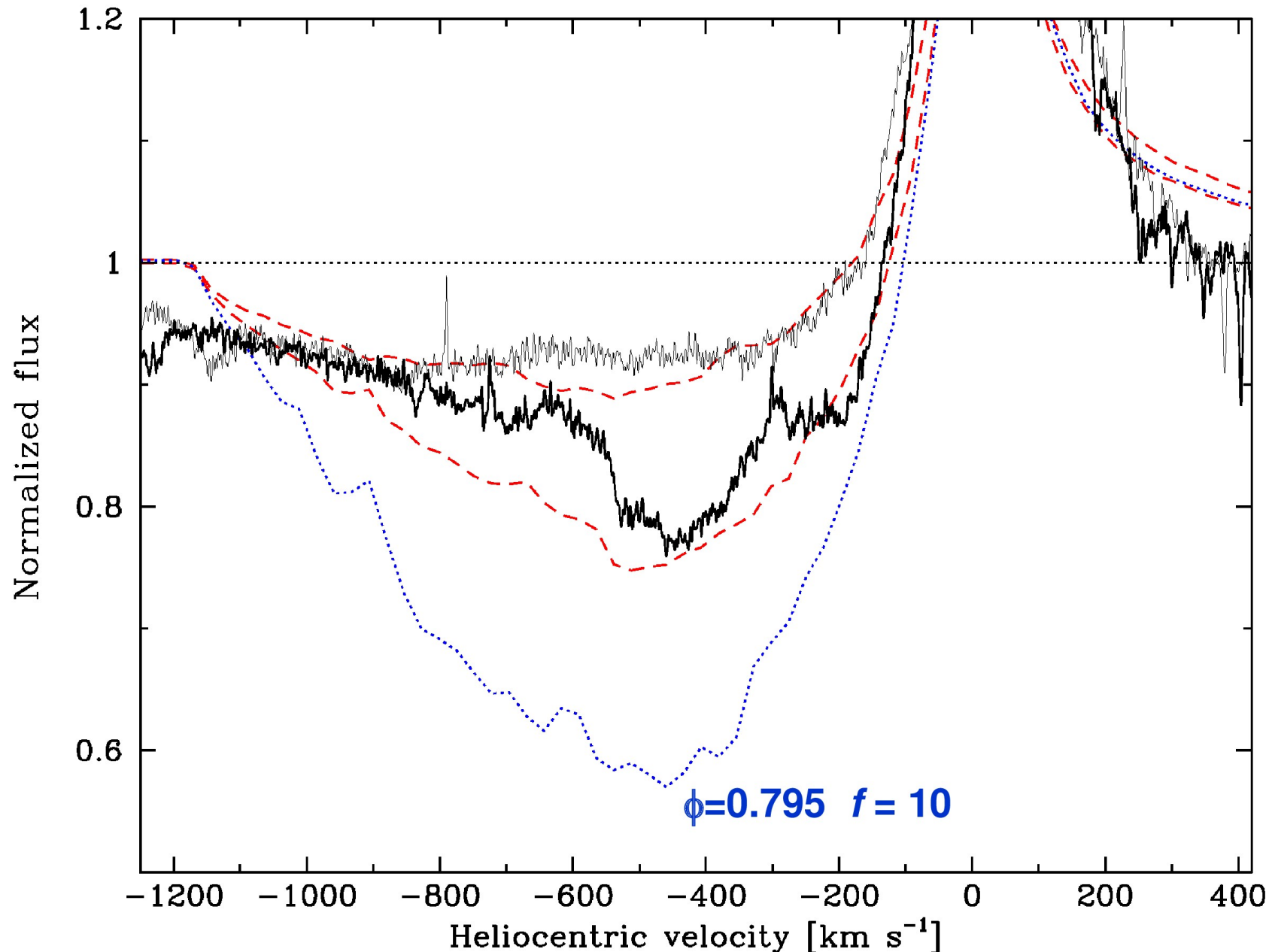
Best fit:
 $f = 3.3$

opening
angle $\theta_0 = \pi/4$

$K_1 = 84.5$ km/s
(obs. Vrad)

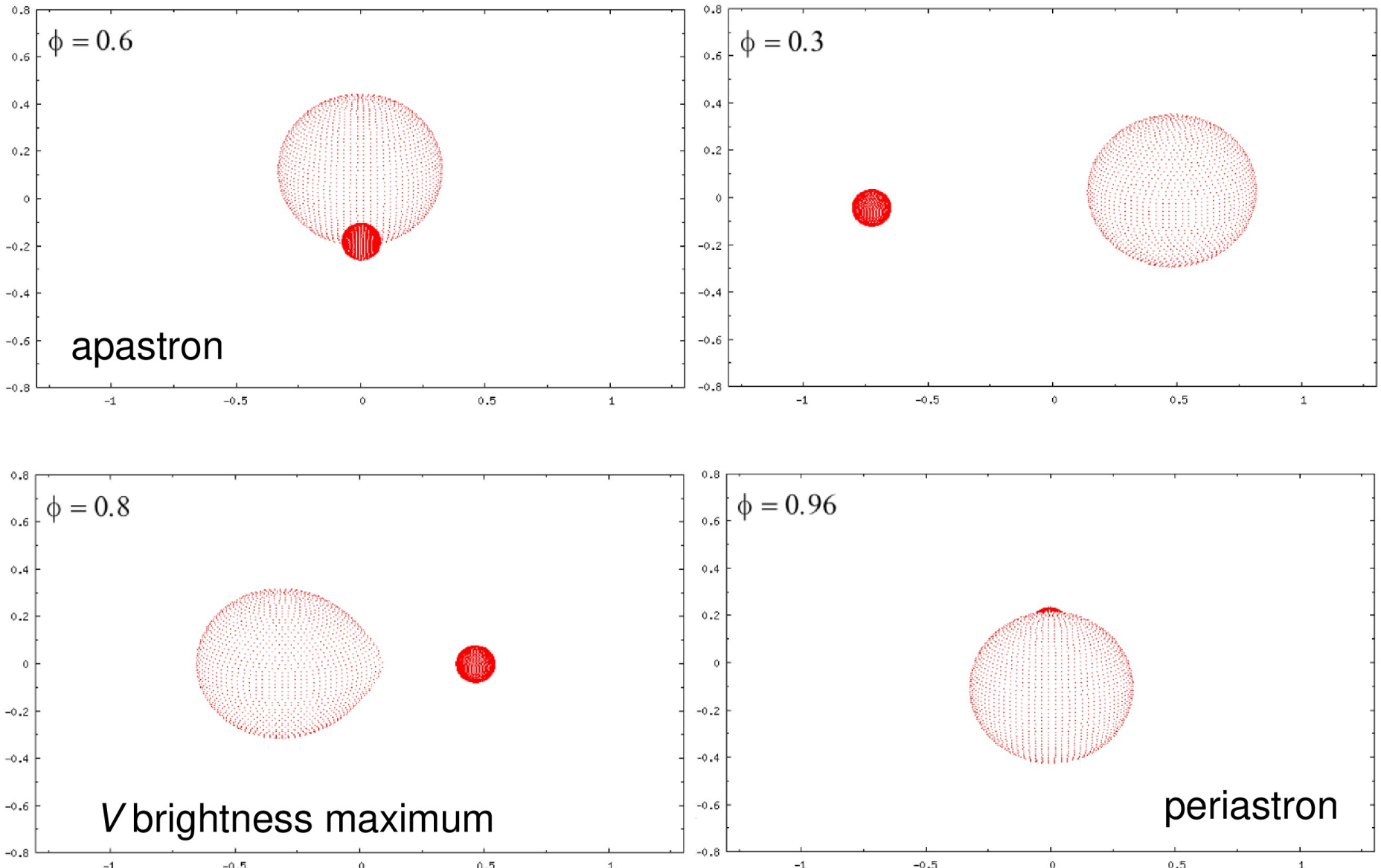
- Parametrized 3-D model reproduces enhanced absorption at $\phi=0.65 - 0.85$.
- 3-D RT Wind3D includes convergence of 3-D line source function with ϕ .

Wind3D RT fit to He I $\lambda 5876$ orbital variability



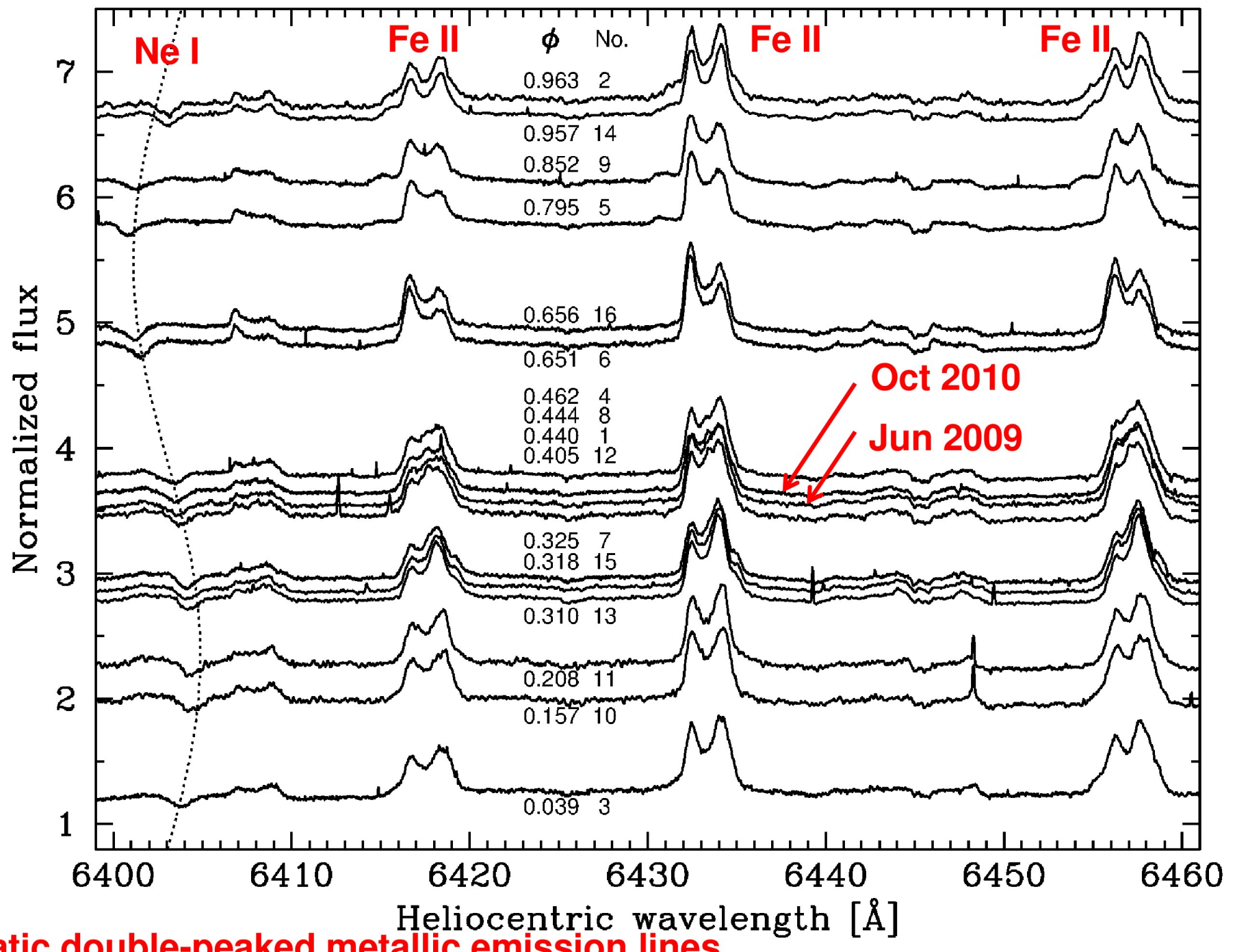
- 3-D best RT fit with Wind3D for wind density enhancement factor $f = 3.3$.

Primary star fills its Roche lobe



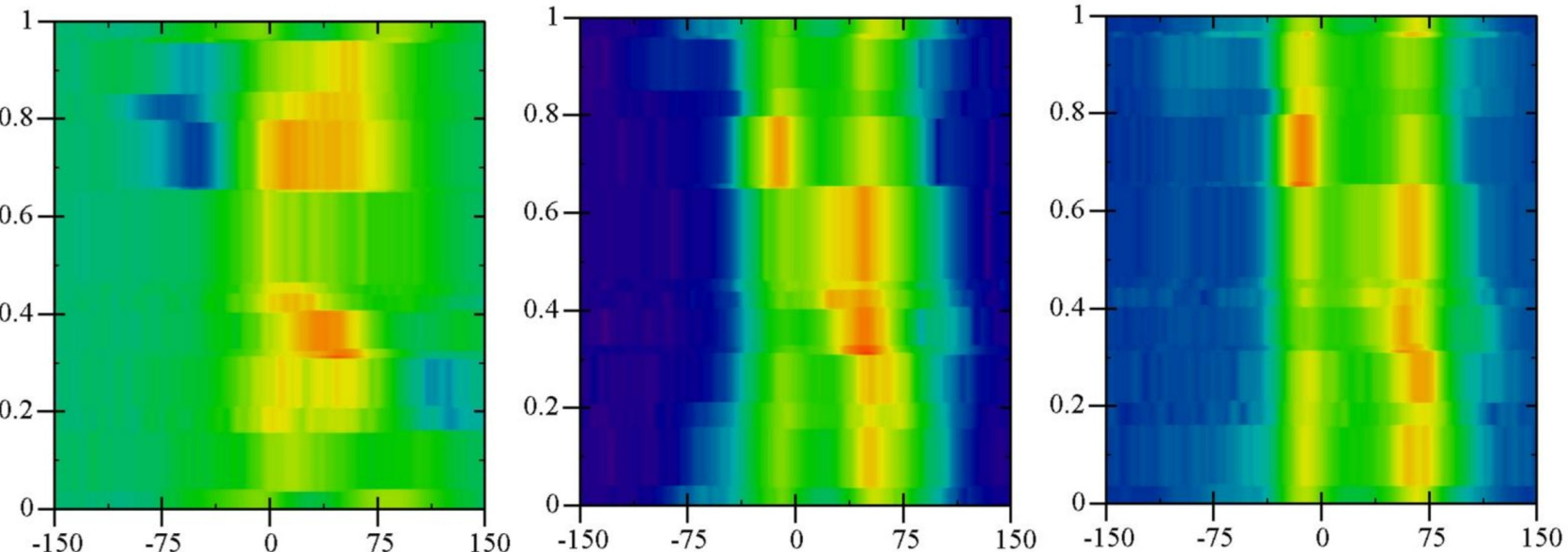
Brightness maximum in quadrature phase when deformation from spherical of primary is largest. Can Roche overflow feed the circumbinary disc of MWC 314?

Orbital modulation of permitted emission lines

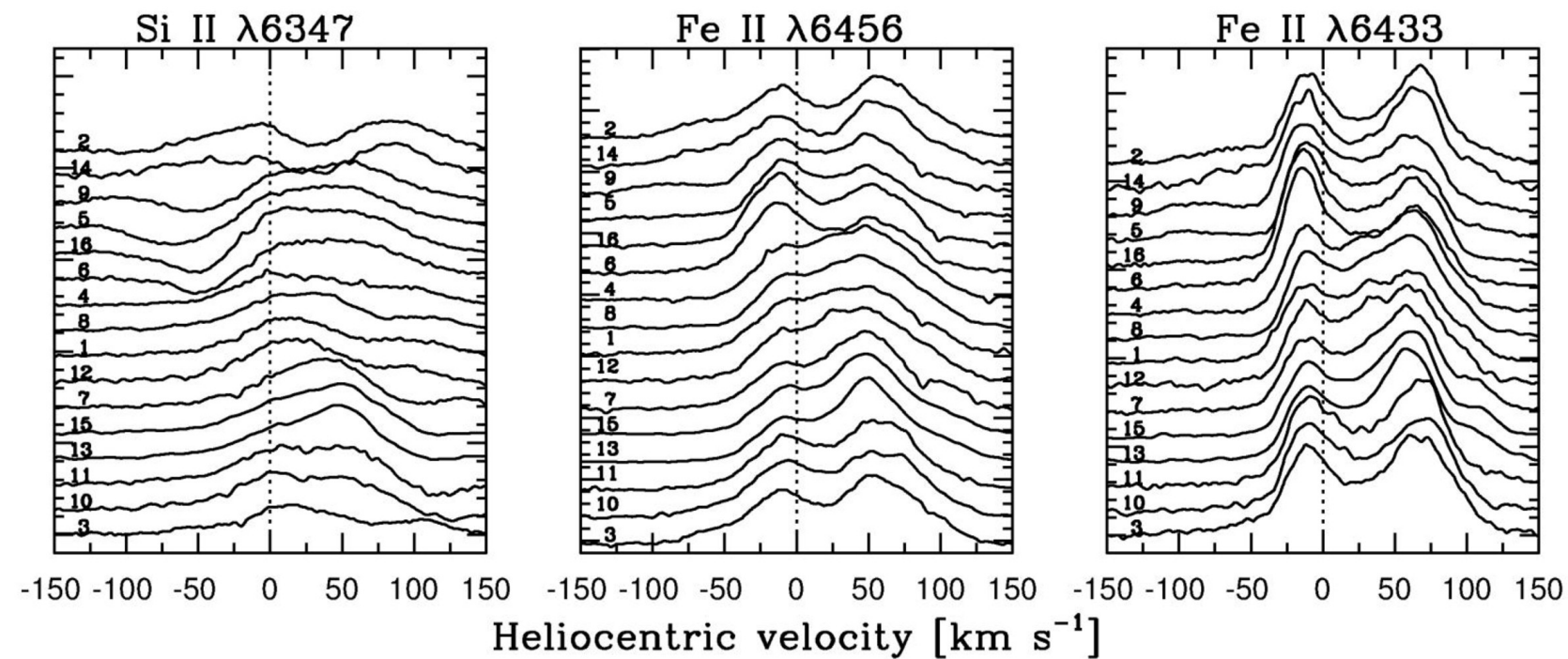


Double-peaked metallic emission lines

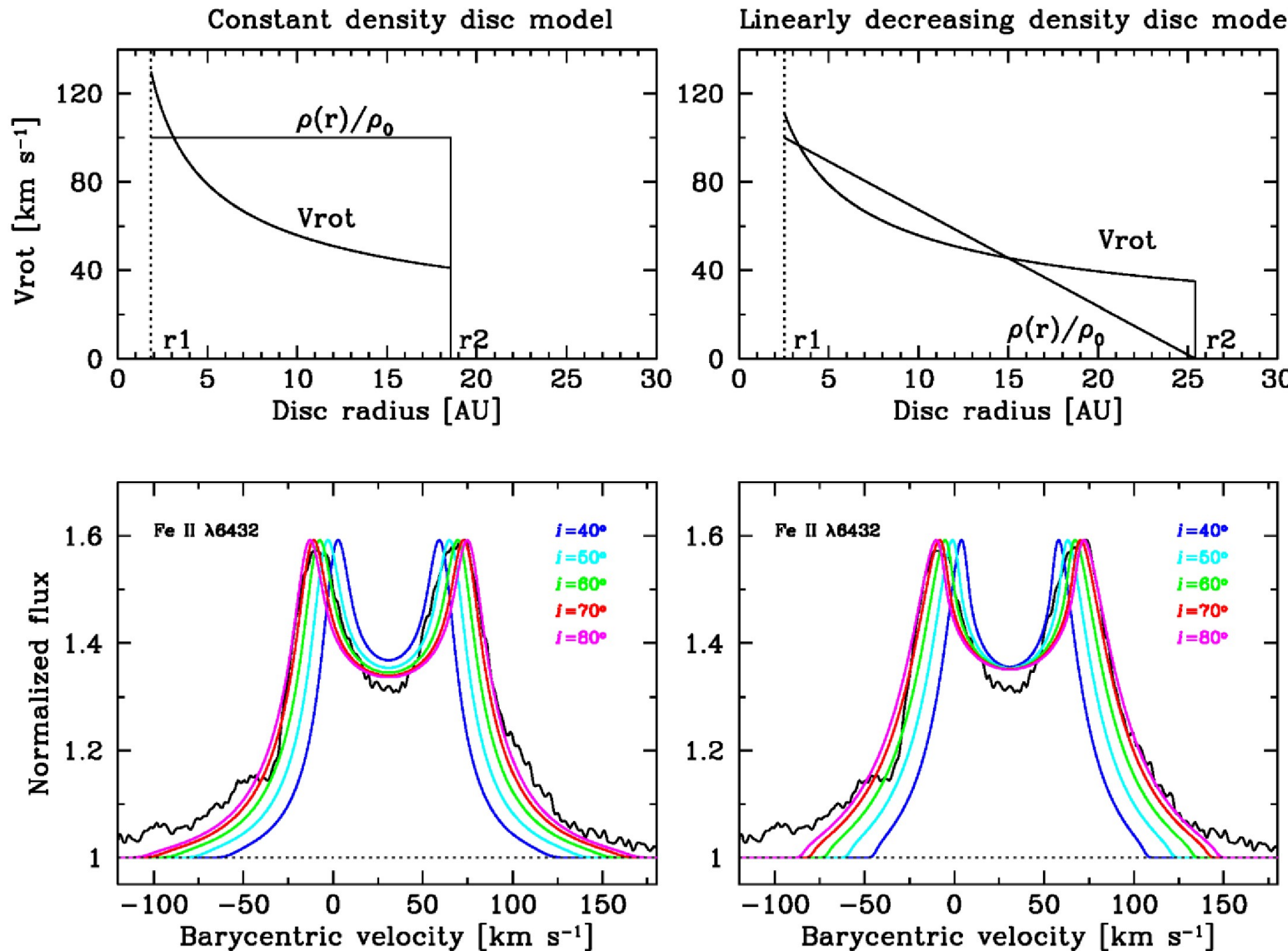
Orbital phase



Normalized flux



Circumbinary disc model of MWC 314



Best fit for isothermal disc model with $40^\circ < i < 80^\circ$ to Fe II line with equal V/R ratio. Keplerian rotating disc model best fits for $i=70^\circ$ with $r_2=25.42$ au, $v_2=41.0$ km s $^{-1}$ (outer disc velocity of line formation) and $r_1/r_2=0.1$.

Questions?

Summary

- Long-term spectroscopic and photometric monitoring of Yellow Hypergiants and Luminous Blue Variables provides essential information about fundamental properties of the atmospheric dynamics and wind physics in these exceptional stars.
- Notorious YHGs such as Rho Cas, HR 5171A , HR 8752 are best suited for long-term monitoring programs since they reveal outburst events, strong Teff variability, and large changes in mass-loss rates.
- More research required for understanding physical origins of the outbursts in terms of pulsation properties, atmospheric velocity fields, and instability mechanisms. Recent new outburst event of Rho Cas in 2013?
- Properties of various YHGs should be compared in detail for finding common aspects. Why is it so hard to detect the (spectral) signatures of the close companion in HR 5171A? More convincing evidence is needed, similar to binarity of MWC 314. Will also clarify the un/importance of binarity for LBVs.
- Long-term spectroscopic observations of YHGs and LBVs reveal possible links between them caused by important effects of atmospheric dynamics due to pulsations. “Outbursts” are observed in hot and cool hypergiants. Can variable emission lines observed for both be excited by propagating shock waves? Advanced theoretical models are needed.